PB83-139493

Engineering Design Manual for Solid Waste Size Reduction Equipment

Cal Recovery, Inc.
Richmond, CA

Prepared for

Municipal Environmental Research Lab.
Cincinnati, OH

Nov 82

U.S. Department of Commerce
National Technical Information Service
NTIS

TYPING GUIDE SHEET
BEGIN FIRST LINE OF TEXT HERE
CENTER OF PAGE
TOP OF IMAGE AREA
DROPPED HEAD, BEGIN SECTIONS HERE

PB83-139493

EPA-600/8-82-028
November 1982

ENGINEERING DESIGN MANUAL FOR SOLID WASTE SIZE REDUCTION EQUIPMENT

by

G. M. Savage
D. J. Lafrenz
D. B. Jones
J. C. Glaub
Cal Recovery Systems, Inc.
Richmond, California 94804

Contract No. 68-03-2972

Project Officer

Carlton C. Wiles
Municipal Environmental Research Laboratory
Solid and Hazardous Waste Research Division
Cincinnati, Ohio 45268

MUNICIPAL ENVIRONMENTAL RESEARCH LABORATORY
OFFICE OF RESEARCH AND DEVELOPMENT
U.S. ENVIRONMENTAL PROTECTION AGENCY
CINCINNATI, OHIO 45268

BEGIN LAST LINE OF TEXT
BOTTOM OF IMAGE AREA OUTSIDE DIMENSION FOR TABLES AND ILLUSTRATIONS
PAGE NUMBER
EPA-287 (Cin.)
(4-76)

REPRODUCED BY
NATIONAL TECHNICAL INFORMATION SERVICE
U.S. DEPARTMENT OF COMMERCE
SPRINGFIELD, VA 22161

TECHNICAL REPORT DATA
(Please read Instructions on the reverse before completing)

1. REPORT NO. EPA-600/8-82-028	**2.**	**3. RECIPIENT'S ACCESSION NO.** PB83 139493
4. TITLE AND SUBTITLE Engineering Design Manual for Solid Waste Size Reduction Equipment		**5. REPORT DATE** November 1982 **6. PERFORMING ORGANIZATION CODE**
7. AUTHOR(S) G. M. Savage, D. J. Lafrenz, D. B. Jones, and J. C. Glaub		**8. PERFORMING ORGANIZATION REPORT NO.**
9. PERFORMING ORGANIZATION NAME AND ADDRESS Cal Recovery Systems, Inc. 160 Broadway, Suite 200 Richmond, CA 94804		**10. PROGRAM ELEMENT NO.** **11. CONTRACT/GRANT NO.** 68-03-2972
12. SPONSORING AGENCY NAME AND ADDRESS Municipal Environmental Research Laboratory--Cin., OH Office of Research and Development U.S. Environmental Protection Agency Cincinnati, OH 45268		**13. TYPE OF REPORT AND PERIOD COVERED** Final Report **14. SPONSORING AGENCY CODE** EPA/600/14

15. SUPPLEMENTARY NOTES

Project Officer: Carlton C. Wiles 513/684-7871

16. ABSTRACT

The design manual provides a collection and an interpretation of information and data that may be used by the solid waste industry for the purpose of designing size reduction equipment for processing municipal solid waste. Inasmuch as the manual is intended for all those involved with solid waste processing, equipment design is addressed in a broad sense from a number of different viewpoints in order to accommodate the needs of the diverse audience. Among the topics discussed in detail in the manual are the following: 1) basic principles and governing parameters; 2) types of refuse size reduction equipment; 3) operation and performance characteristics; 4) performance evaluation; 5) costs; 6) maintenance; 7) safety; and 8) equipment selection and specification.

The design manual also serves as a reference work on size reduction for the industry in that the majority of work published in the field of solid waste size reduction has been compiled and referenced in one volume.

17. KEY WORDS AND DOCUMENT ANALYSIS

a. DESCRIPTORS	b. IDENTIFIERS/OPEN ENDED TERMS	c. COSATI Field/Group

18. DISTRIBUTION STATEMENT RELEASE TO PUBLIC	**19. SECURITY CLASS** *(This Report)* UNCLASSIFIED	**21. NO. OF PAGES** 170
	20. SECURITY CLASS *(This page)* UNCLASSIFIED	**22. PRICE**

EPA Form 2220-1 (Rev. 4-77) PREVIOUS EDITION IS OBSOLETE

NOTICE

This document has been reviewed in accordance with U.S. Environmental Protection Agency policy and approved for publication. Mention of trade names or commercial products does not constitute endorsement or recommendation for use.

FOREWORD

The U.S. Environmental Protection Agency was created because of increasing public and government concern about the dangers of pollution to the health and welfare of the American people. Noxious air, foul water, and spoiled land are tragic testimonies to the deterioration of our natural environment. The complexity of that environment and the interplay of its components require a concentrated and integrated attack on the problem.

Research and development is that necessary first step in problem solution; it involves defining the problem, measuring its impact, and searching for solutions. The Municipal Environmental Research Laboratory develops new and improved technology and systems to prevent, treat, and manage wastewater and solid and hazardous waste pollutant discharges from municipal and community sources, to preserve and treat public drinking water supplies, and to minimize the adverse economic, social, health, and aesthetic effects of pollution. This publication is one of the products of that research and provides a most vital communications link between the researcher and the user community.

The design manual provides the solid waste industry with a reference work on size reduction, which is one of the more prevalent and costly unit processes utilized in solid waste processing. Inasmuch as the manual addresses basic principles, equipment design, and performance evaluation, it should provide the user with a valuable tool for designing efficient size reduction equipment.

Francis T. Mayo, Director
Municipal Environmental Research
Laboratory

ABSTRACT

The design manual provides a collection and an interpretation of information and data that may be used by the solid waste industry for the purpose of designing size reduction equipment for processing municipal solid waste. Inasmuch as the manual is intended for all those involved with solid waste processing, equipment design is addressed in a broad sense from a number of different viewpoints in order to accommodate the needs of the diverse audience. Among the topics discussed in detail in the manual are the following:

- basic principles and governing parameters
- types of refuse size reduction equipment
- operation and performance characteristics
- performance evaluation
- costs
- maintenance
- safety
- equipment selection and specification

The design manual also serves as a reference work on size reduction for the industry in that the majority of work published in the field of solid waste size reduction has been compiled and referenced in one volume.

This report was submitted in fulfillment of Contract No. 68-03-2972 by Cal Recovery Systems, Inc., under the sponsorship of the U.S. Environmental Protection Agency. This report covers the period September 12, 1980, to March 12, 1982, and work was completed as of March 12, 1982.

CONTENTS

Foreword iii
Abstract iv
Figures vii
Tables ix
Acknowledgment xi

1. Introduction 1

2. Use of the Manual 6

3. Description of Available Shredding Equipment 8
  Low RPM/Shear-Type Shredders 8
  Pulpers 10
  Hammermills 10
  Vertical Ring Shredder 15
  MSW Shredding Facilities 15
  Shredder Manufacturers 18

4. Design of Refuse Size Reduction Systems 19
  Principles of Refuse Size Reduction 19
    Introduction 19
    Elementary Forces 20
    Early Energy Theories 21
    Representation of Particle Size Distribution 23
    Degree of Size Reduction 24
    Matrix Modeling of Breakage 25
    Internal Shredder Configuration 29
  Shredder Operation and Performance 33
    Particle Size Distribution 33
    Effect of Multiple Size Reduction 34
    Rotational Velocity 35
    Moisture Content 35
    Condition of Hammers 36
    Specific Energy Requirement 36
    Power and Throughput Relationship 38
    Hammer Wear 39
    Operational Problems 44
  Mill Holdup 44
  The Motor and Shredder as a System 48
    Shredder Motors 48
    Mass Moment of Inertia 52
    Motor Torque, Inertial Torque, and Load Torque 53
    System Analysis and Design 56

5. Maintenance Considerations 63

6. Health and Safety 66
  Noise 66
  Nuisance Dust 66
  Explosions 69
  Projectiles 72

7. Economics of Size Reduction 74
  Costs of Size Reduction 74
  Hammer Maintenance 77
  Cost Estimation 80

8. Selecting A Shredder 82
  Type of Machine 82
  Vertical-Shaft versus Horizontal-Shaft Shredders 83
  Machine Components 83
    Motor 83
    Hammer 83
  Operational Alternatives 84
    Multiple-Stage Size Reduction 84
    Shredding of Homogeneous Feedstocks 84
    Fine Grinding 85
  Establishments of Equipment Specifications 85
  Hammer Tip Velocity 86
  Desired Particle Size 86
  Power and Energy Requirements 87
  Maintenance 91
  Manufacturers' Reputation 93

9. Performance Evaluation in the Field 94
  Comparison Between Size Reduction Alternatives 95
  Test Methods for Shredder Performance Evaluation 99
    Method 1: Performance Documentation According to Manufacturer Specifications 99
    Method 2: Determination of the Effect of Changing Throughput on Shredder Maintenance 99
    Procedures 99

References 110

Appendices

A. Refuse Size Reduction Literature Reviews 114
B. Size Reduction Devices Used in Solid Waste Processing Facilities 122
C. Partial Listing of MSW Shredder Manufacturers 129
D. Utilization of Selection and Breakage Functions in Shredder Analysis 131
E. Shredder Rotor Mass Moment of Inertia 140
F. Derivation of Governing Equations for Motor Power in Terms of Motor Characteristics 154

FIGURES

Number Page

1 Composition of municipal solid waste and selected fractions derived therefrom 2

2 Particle size distributions of municipal solid waste 3

3 Low-rpm/shear-type shredder 9

4 Pulper 11

5 Horizontal swing hammermill (cross-sectional view) 13

6 Horizontal swing hammermill 14

7 Vertical hammermill 16

8 Vertical ring shredder 17

9 Energy requirements for selected solid waste fractions using a 187 kW horizontal swing hammermill 26

10 Effect of moisture on specific energy consumption 37

11 Hammer wear associated with MSW size reduction as a function of alloy hardness and degree of size reduction 45

12 Hammer wear associated with MSW size reduction as a function of alloy hardness 46

13 Relation of holdup to power requirement 47

14 Torque-slip diagram for polyphase induction motor 50

15 Load diagram developed from shredder power measurements and motor performance data 57

16 Power recording for a refuse shredder located at the University of California 58

17a Load torque and motor torque for a 150 kW shredder motor with slip = 1.7 percent and I = 90 kg-m^2 60

17b Load torque and motor torque for a 150 kW shredder motor with slip = 1.7 percent and I = 140 $kg\text{-}m^2$ 60

17c Load torque and motor torque for a 150 kW shredder motor with slip = 1.7 percent and I = 190 $kg\text{-}m^2$ 61

17d Load torque and motor torque for a 150 kW shredder motor with slip = 1.7 percent and I = 430 $kg\text{-}m^2$ 61

18 Motor torque and load torque for the Tinton Falls vertical ring shredder 62

19 Time requirements for hammer and grate change in primary shredders as a function of throughput capacities 64

20 Estimated gross power requirements for size reduction of MSW as a function of throughput and nominal size of product given $P_{fw}/P_g = 0.10$ 89

21 Observed and derived flow rate-size relationships 98

22 Flow diagram for Method 1 100

23 Flow diagram for Method 2 101

24 Example of a size distribution data sheet 104

25 Example of wear measurement data sheet 107

26 Example of data sheet for hammer change time 109

D.1 The feed and product size distributions for selection and breakage function sample calculations 135

E.1 Typical hammermill rotor assembly 143

F.1 Equivalent circuit of one phase of a polyphase induction motor . . 155

F.2 Equivalent circuit of one phase of a polyphase induction motor with no load 155

TABLES

Number		Page
1	Particle Size of Municipal Solid Waste	4
2	Emperical Relations Among Throughput, Holdup, Power, Specific Energy, and Product Size in Terms of Machine Parameters for Horizontal Hammermills	31
3	Applicable Range of Physical Parameters of Horizontal Hammermills for the Empirical Relations Given in Table 2	33
4	Range of Coefficient Values Showing Effect of Flow Rate and Moisture Content in Full-Scale Operations	40
5	Observed Rates of Hammer Wear in Refuse Shredding	41
6	Principal Groups of Hardfacing Alloys	43
7	Noise Levels Around Size Reduction Equipment	67
8	Total and Respirable Dust Levels Reported Around Refuse Size Reduction Equipment	68
9	Estimated Capital Costs in 1981 Dollars for MSW Shredders	75
10	Breakdown of Maintenance Costs (1981 Dollars) for MSW Shredders	76
11	Typical Costs for Hammer Maintenance	78
12	Estimated Cost Elements for a 60 Mg/h Primary Shredder Designed to Produce a Nominal Product Size of 10 cm	81
13	Average Product Size at Various Grate Openings and Refuse Throughputs	87
14	Calculation of Shredder Power Requirements	92
15	Hammermill Specifications	97
D.1	Assumed Feed Size Distribution for Selection and Breakage Function Analysis	134

D.2 Calculated Product Size Distribution from Selection and Breakage Function Analysis 136

E.1 Description of Rotor Elements 147

E.2 Contribution of Rotor Elements to Mass Moment of Inertia 153

ACKNOWLEDGEMENT

Cal Recovery Systems wishes to acknowledge the cooperation of the following plant managers for information supplied by them regarding the operation and performance of their size reduction equipment:

Name/Title	Facility/Location
Edward R. Maloney Shredder Manager	Outagamie County Shredder Appleton, Wisconsin
Carl Albert Chief Operator	Harrisburg Steam Plant Harrisburg, Pennsylvania
W.J. Larson Chief, Refuse Utility	Tacoma, Washington
Craig Starr Superintendent, Solid Waste Div.	Lane County Eugene, Oregon
Emil Nigro Coordinating Engineer	Chicago Southwest Supplementary Fuel Processing Facility Chicago, Illinois
A.O. Chantland, P.E. Director of Public Works	Ames Solid Waste Recovery System Ames, Iowa
Gary Baker Process Superintendent	Western Lake Superior Sanitary District Duluth, Minnesota
Ken Brunner Plant Manager	Madison Energy Recovery Madison, Wisconsin
Gerald E. Donavan Plant Manager	Bridgeport Resource Recovery Facility Bridgeport, Connecticut
Kenneth L. Cramer Plant Manager	Baltimore County Resource Recovery Facility Baltimore County, Maryland
Howard A. Schmidt Manager	Solid Waste Reduction Center Ft. Louderdale, Florida

John L. Gray Superintendent	Monmouth County Reclamation Center Tinton Falls, New Jersey
Anthony R. Nollet President, Aenco, Inc.	Albany ANSWERS Albany, New York
David S. Hedlund Manager, Market Development	Americology Milwaukee, Wisconsin
Edward May Plant Manager	Baltimore City Pyrolysis Plant Baltimore, Maryland
Floyd Chaney Sanitation Superintendent	City of Odessa Odessa, Texas

As of March, 1981, approximately three million tons of MSW had been size reduced in the plants listed above.

SECTION 1

INTRODUCTION

Size reduction is the single most used and one of the costlier of the unit processes in refuse processing, and as such, its characterization and control are of significant interest to the solid waste industry. Over the past fifteen years, the use of size reduction equipment in waste processing has expanded from a shred-and-landfill mode to a position in which the shredder is the dominant piece of processing equipment in full-scale resource recovery systems. The recovery systems often include a myriad of size reduction units intended for a diversity of purposes, among which are the size reduction of raw solid waste, of the air-classified light fraction, of recovered ferrous scrap, of oversize bulky waste, and of recovered glass fractions.

An idea of the position of the shredder in a resource recovery operation and of the material that must be processed by the machine may be gained from the flow diagram and other information given in Figure 1. Lists shown in the figure indicate the diversity of the components of MSW to be size reduced. Obviously, the variety of the components is reflected by a correspondingly wide variation in the physical and mechanical properties of the components. Furthermore, the data listed in Table 1 and plotted in Figure 2 demonstrate that this wide variation extends to the particle size and particle size distribution of the components.

The number of shredders used by the solid waste industry expanded from 27 in 1971, to 87 in 1974, to 137 in 1981. Indeed, in the past decade the average rate of growth in number of shredder installations was approximately 18 percent per annum. Coupled with the growth rate of shredder usage has been a significant increase both in the understanding of refuse size reduction and in the innovations in the design of commercial equipment. The latter directly followed from the efforts of manufacturers to meet the growing need of the solid waste industry for an ample supply of reliable and competitively priced units. Consequently, amenities such as hydraulic systems for opening and closing the shredder enclosures and electrical systems to sense the load during shredding and to provide control of refuse flow, while virtually absent fifteen years ago, are now the state-of-the-art.

The growth in the public domain with respect to the understanding of solid waste size reduction is largely attributable to the efforts and sponsorship of the U.S. EPA and of its predecessor, the U.S. Public Health Service. During the past fifteen years (1966-1981) these two agencies funded the majority of research and development work in the size reduction of refuse. Over the years, the work has included evaluations of refuse shredders

BEGIN FIRST LINE OF TEXT HERE
CENTER OF PAGE
TOP OF IMAGE AREA
DROP HEAD BEGIN SECTION HERE

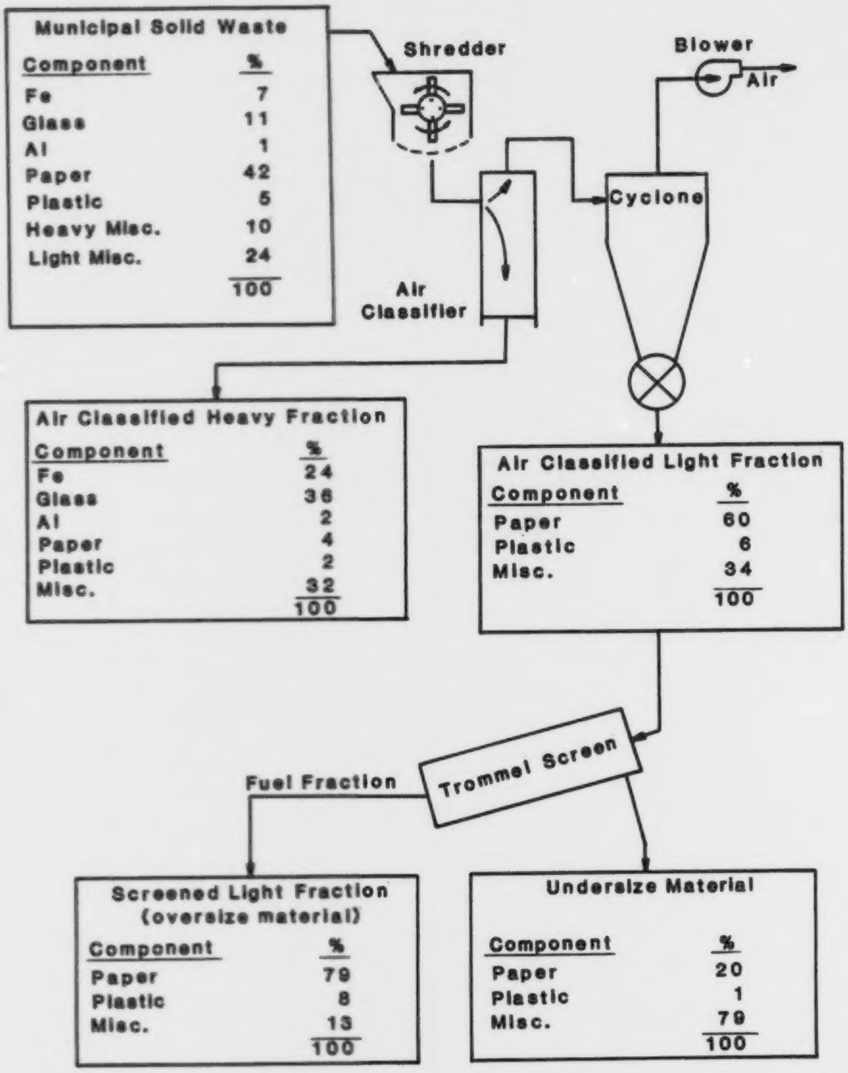

Municipal Solid Waste

Component	%
Fe	7
Glass	11
Al	1
Paper	42
Plastic	5
Heavy Misc.	10
Light Misc.	24
	100

Air Classified Heavy Fraction

Component	%
Fe	24
Glass	36
Al	2
Paper	4
Plastic	2
Misc.	32
	100

Air Classified Light Fraction

Component	%
Paper	60
Plastic	6
Misc.	34
	100

Screened Light Fraction (oversize material)

Component	%
Paper	79
Plastic	8
Misc.	13
	100

Undersize Material

Component	%
Paper	20
Plastic	1
Misc.	79
	100

Figure 1. Composition of municipal solid waste and selected fractions derived therefrom.

BEGIN LAST LINE OF TEXT
3/8"
BOTTOM OF IMAGE AREA, OUTSIDE DIMENSION FOR TABLES AND ILLUSTRATIONS

PAGE NUMBER
EPA Form 2350-4 (4-80)
(PREVIOUSLY 2IN, EPA FORM 287)
TYPING GUIDE SHEET

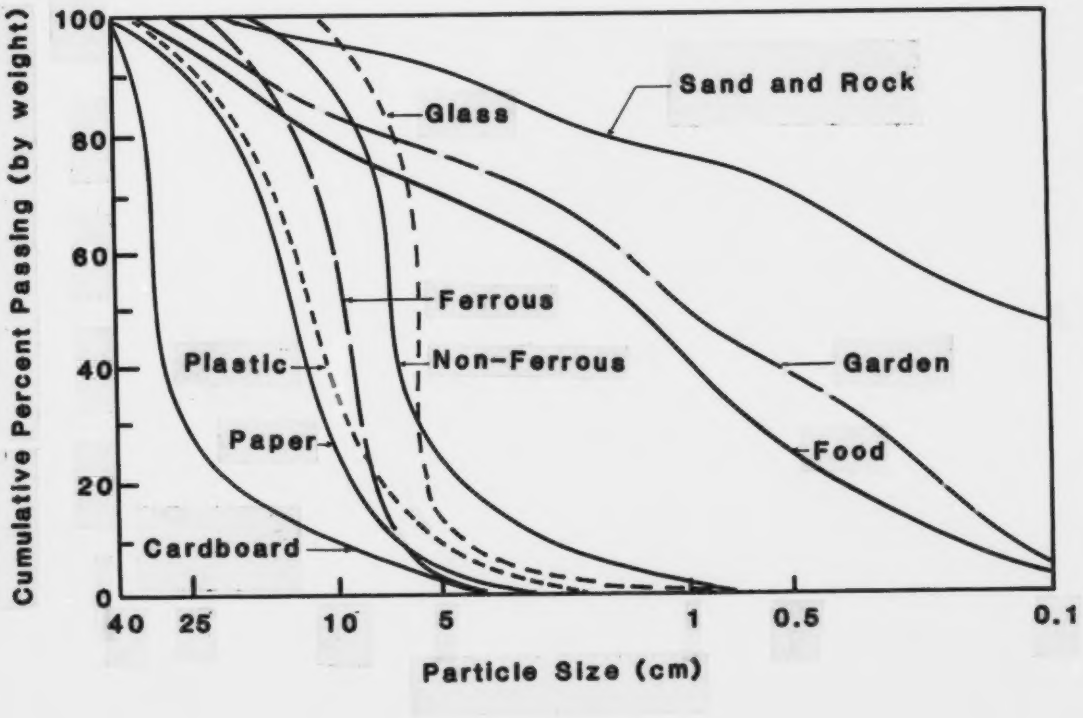

Figure 2. Particle size distributions of municipal solid waste.

BEGIN FIRST LINE OF TEXT HERE
CENTER OF PAGE
TOP OF IMAGE AREA
DROPPED HEAD; BEGIN SECTIONS HERE
BEGIN LAST LINE OF TEXT
3/8"
PAGE NUMBER
BOTTOM OF IMAGE AREA; OUTSIDE DIMENSION FOR TABLES AND ILLUSTRATIONS
EPA Form 2350-4 (4-80)
(PREVIOUSLY CIN, EPA FORM 287)
TYPING GUIDE SHEET

TABLE 1. PARTICLE SIZE OF MUNICIPAL SOLID WASTE

	Characteristic 63.2 Percent Passing (cm)	Nominal 90.0 Percent Passing (cm)	Reference
Richmond, CA (1976-78)	10.9	18.3	A
"	15.5	30.5	
" (1980)	12.2	--	
" (1980)	16.8	--	
" (1980)	18.5	--	
" (1981)	11.9	--	
Average	14.3	24.4	
Northeastern City	8.6	24.7	B
Cambridge, MA (1973)	16.0	29.5	C
Middlebury, VT (1973)	28.7	49.3	C
Western City (1977)	13.0	21.3	B
Gainesville, FL (1971)	10.9	23.4	D

References

A. Unpublished University of California (Berkeley) data.
B. Data courtesy of Cal Recovery Systems, Inc.
C. Data derived from "Characterization of Municipal Solid Waste," Winkler, P.F. and Wilson, D.G., Compost Science, Volume 14, No. 5, 1973.
D. Data derived from "Particle Size Spectrum and Compressibility of Raw and Shredded Municipal Solid Waste," Ruf, J.A., Ph.D Thesis, University of Florida, 1974.

and of the shredded product. In studies begun by the U.S. Public Health Service and continued by the U.S. Environmental Protection Agency (EPA) during the mid- and late-1960's, an investigation was made of the composting of shredded solid waste [1]. These studies were followed in the late 1960's and early 1970's by investigations regarding the utility of refuse shredding as a means of eliminating the need for cover material in landfill disposal [2]. Fundamental research was initiated in the early 1970's under EPA sponsorship, the goals of which were to identify and describe basic parameters that govern and characterize the process of refuse size reduction, and the integration of size reduction processes with other resource recovery unit processes [3,4]. During the late 1970's and early 1980's, the EPA programs in refuse size reduction were expanded to include the testing of shredders located in the field [5]. The results of the field tests subsequently were used to enlarge the existing data base for refuse size reduction and to verify findings and conclusions reached in fundamental research efforts conducted previously. The present design/user manual may be regarded as being the culmination of the EPA activities in solid waste size reduction, in that it constitutes the single reference in which the knowledge gained to date has been collected, interpreted, and coalesced.

The purpose of this manual is to supply the solid waste industry with a state-of-the-art reference in which is not only reported available information but also are presented methods and means for the practical application of the information. Although the emphasis is on design considerations for refuse size reduction equipment, the manual includes sections on the specification, selection, and testing of size reduction hardware; aspects of maintenance and safety applicable to refuse size reduction; and the economics associated with refuse shredding.

SECTION 2

USE OF THE MANUAL

The design manual was formulated for use by the broad collection of individuals associated with refuse processing and resource recovery in one way or another. The collection includes public works and sanitation officials, equipment manufacturers, system designers, plant operators, and researchers. To meet the needs of such a diverse group, the scope of the manual was made to extend from fundamental concepts to empirical data on solid waste size reduction.

The primary emphasis of the manual, as the title emplies, is on the aspects of design, i.e., the theoretical and empirical knowledge that may be applied to the design of a size reduction system. By its nature, design implies a greater depth of coverage and broader base than that required solely for shredder selection, i.e., the selection of a piece of equipment based upon a set of given criteria. In particular, the coverage of the design aspects for solid waste processing, is especially broad, due to the relative newness of the industry and the lack of design theories supported by many years of confirmation in the field. In contrast to the coal and mineral processing industries for which design theories and explanation of physical phenomena have been developed and confirmed for over a century, the solid waste processing industry is a neophyte and as such, design theories pertinent to it have not been adequately confirmed by the test of time. With this qualification in mind, it is pointed out that the design theories and empirical information presented in this manual are the latest and best documented of the theories and information reported to date.

In keeping with the theme of producing a manual of significant utility to the solid waste industry, considerable effort was spent in describing the application of available information on refuse size reduction and the incorporation of the experience of equipment operators. Plant-oriented information such as man-hour estimates for maintenance operations and the influence of operational variables on shredder performance, is primarily intended for the individuals most closely associated with equipment operation (e.g., system designers and plant operators). Economic data are presented in a form that enables less technically-oriented decision makers to estimate the costs associated with size reduction.

A detailed section on performance testing was prepared as a means of supplying rational test methods for the evaluation of size reduction equipment, and of serving as an interim standard pending the development and consensus approval of formal test standards. The latter are exemplified by the standards being developed by the E38.08 Committee of the American Society for Testing and Materials (ASTM). The test methods not only will allow the evaluation of the performance of installed equipment, and therefore be of practical use to plant owners, operators, and equipment vendors; they will also provide a guideline for individuals concerned with shredder design, e.g., researchers and developers.

A major part of the manual is addressed specifically to the design of refuse size reduction equipment. It includes discussions of the relationship of operating variables to shredder performance and the analysis of size reduction from the standpoint of an electro-mechanical system. It is anticipated that this information will be of particular interest to individuals who have the responsibility of supplying and selecting equipment, and of those who are concerned with the design and development of size reduction equipment for solid waste.

Finally, the design manual is intended to provide a source of information on topics that are germane to refuse size reduction. In keeping with this intent, a review of pertinent literature is included in the manual (Appendix A).

Inasmuch as the principal purpose of the manual is to provide information and guidelines for shredder design, a set of equipment selection criteria is not given in detail. However, to the degree that design and selection overlap, and the overlap is significant, the selection of equipment is addressed. However, if additional information regarding shredder selection is desired, it can be found in the EPA report, Solid Waste and Shredder Selection (reference [6]).

SECTION 3

DESCRIPTION OF AVAILABLE SHREDDING EQUIPMENT

The Waste Management Equipment Manufacturers Institute divides various types of size reduction devices into crushers, cage disintegrators, shears, shredders, cutters, clippers, hammermills, and grinders. However, for practical purposes the units commonly employed for refuse size reduction are designated collectively as "shredders," and are taken to include hammermills and grinders. The comminution characteristic common to shredders, hammermills, and grinders is one that entails a combination of shearing, tearing, and impact phenomena.

Size reduction equipment for shredding MSW and its components can be differentiated according to rotational velocity into low-rpm and high-rpm devices. In the former, shearing and tearing serve as the primary means of achieving size reduction of the material; and in the latter, impact and tearing are the primary means of accomplishing the disintegration of the particles.

LOW RPM/SHEAR-TYPE SHREDDER

One of the more recent innovations in MSW size reduction equipment is the low-rpm, high torque shredder, sometimes known as a "shear-type" shredder. The design of the low-rpm shredder is indicated by the illustration in Figure 3. It can be described as a unit that contains two horizontal counter-rotating shafts, each equipped with fixed protuberances ("cutters"), to shear and tear the material. In low-rpm shredders, shear and deformation rather than impact are the primary mechanisms of particle size reduction. The counter-rotating cutters in low-rpm shredders typically operate within a range of 20 to 70 rpm at tip speeds on the order of 0.5 to 4 m/s, whereas the typical hammermill is designed to operate within a range of 600 to 1200 rpm at hammer tip speeds of 30 to 70 m/s. The intermediate ranges of rpm and tip speeds (i.e., 100 to 600 rpm, and tip speed at 45 to 30 m/s) apparently have not as yet been investigated or used to any great extent in MSW shredder applications. Low-rpm shredders are driven through a gear reducer with an electric motor or a hydraulic drive system.

Low-rpm shredders are commonly employed for shredding tires, because the shearing action and high torque availability are conducive to efficient size reduction of such difficult-to-shred items when only modest throughputs are required. With respect to size reducing MSW, only a relatively few low-rpm shredders are in use at present. Consequently, there is a dearth of available information and test data regarding their performance and operation.

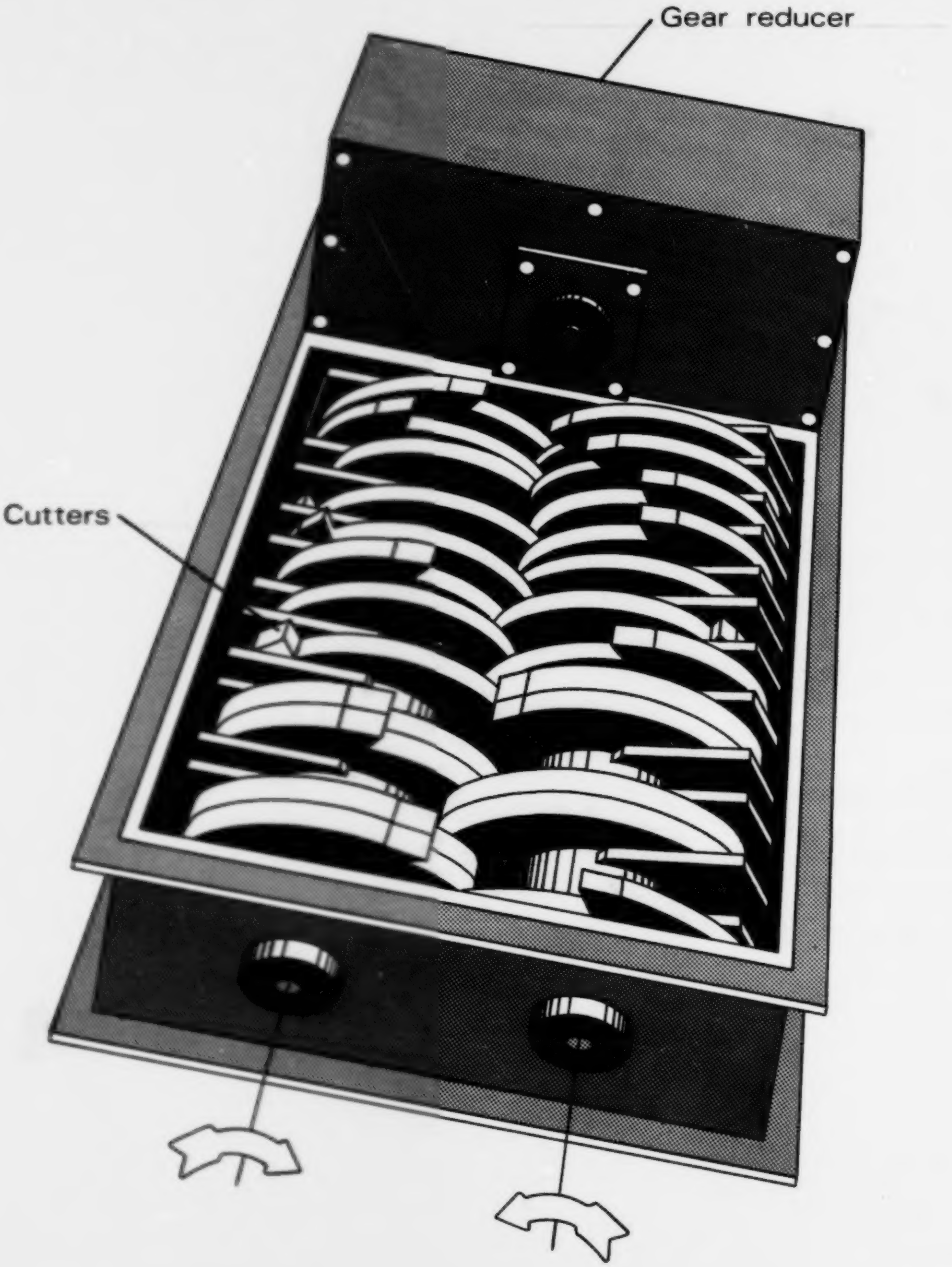

Figure 3. Low-rpm/shear-type shredder.

PULPERS

With the exception of a few instances, most shredders are designed to operate in the dry processing mode, i.e., no moisture other than that needed for dust control is added. As a result, the only moisture usually available for the process of size reduction is the inherent, and free moisture in the waste materials. Normally, the free moisture content of MSW is on the order of 25 to 45 percent on an oven-dry weight basis. Size reduction through the application of wet processing methods ("pulping") has been developed, but has had only a limited use in resource recovery. (In wet processing, the waste is slurried and the slurry is passed through a comminutor.) Presently, only one manufacturer in the United States, Black Clawson, supplies a solid waste pulping system.

The water and waste slurry formed in the pulping of solid waste usually has two to eight percent solids content (oven-dry weight basis), depending upon the composition of the waste and the particular pulping system. In waste pulping systems, water serves to weaken the bonds of the cellulosic components and hence to promote size reduction. In addition, after pulping is accomplished, the water serves as the conveying medium. A pulper is illustrated in Figure 4. It consists of: 1) a tank into which the water and waste are introduced; 2) a rotating impeller, usually positioned at the bottom of the tank, for agitating and comminuting the wetted waste; and 3) an extraction plate or grating that covers the discharge opening on the bottom of the tank. Pulpers may have additional components such as "raggers" and reject openings. "Raggers" are used to remove textiles and membranous material (e.g., plastic bags) that cannot be size reduced to the degree necessary to pass the extraction openings. Reject (or tramp metal) openings are installed to permit the discharge of difficult-to-shred objects (e.g., heavy metal objects) from the pulper other than by way of the extraction openings. Waste pulping may be accomplished in either a continuous or a batch processing mode.

Because of the dearth of available published literature on solid waste pulping, it is difficult to supply and to develop design criteria for the process. However, reference materials have been and are published by the pulp and paper industry, which has long studied the pulping of wastepaper.

HAMMERMILLS

Of the many types of size reduction devices, the hammermill shredder (both vertical-shaft and horizontal-shaft machines) is the one most widely used in refuse processing. The hammermill is a high-rpm impact shredder in which size reduction is accomplished through a combination of tensile, compressive, and shear forces applied to the feedstock as a consequence of particle-particle collisions and collisions between the particles and the internal elements (e.g., hammers, grate bars) of the machine.

The shaft (rotor) of a hammermill can be oriented in the horizontal ("horizontal hammermill") or in the vertical direction ("vertical hammermill"). Regardless of the orientation of their rotors, the mills can be equipped either with fixed hammers or with hammers that swing or pivot about

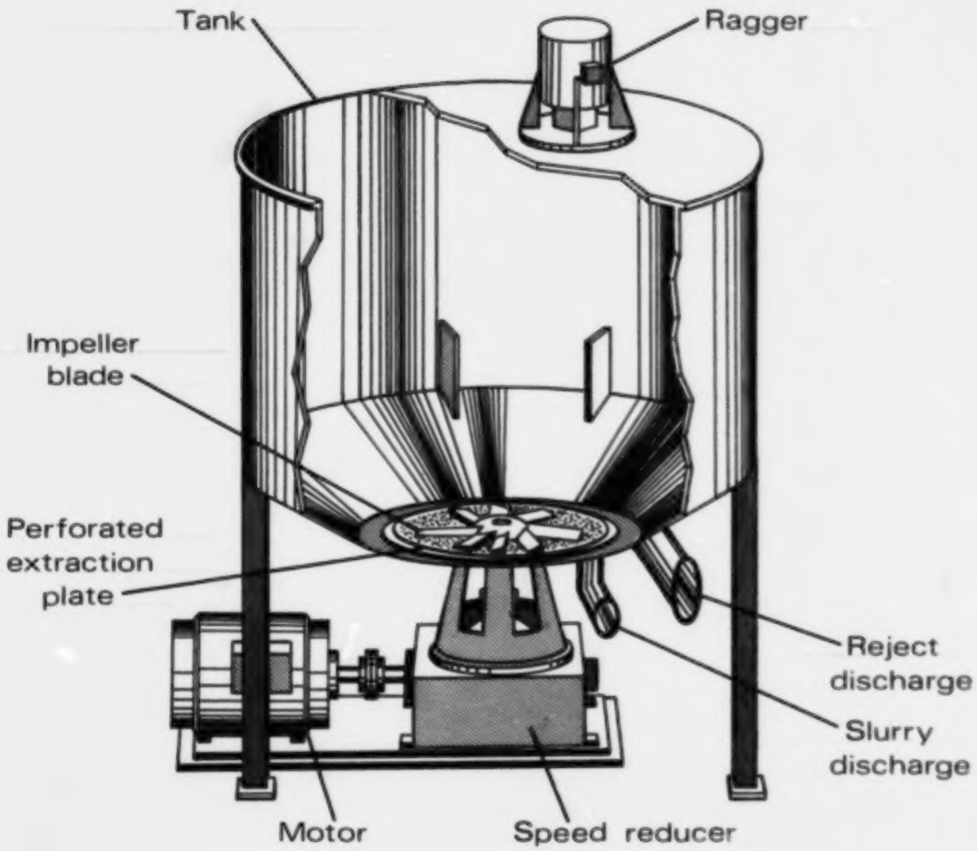

Figure 4. Pulper.

an axis (usually a set of pins) parallel to but offset from the axis of rotation of the rotor. The horizontal swing hammermill is the type most commonly used for size reduction of refuse. Its principal parts are the rotor, hammers, hammer pins, grates, the enclosure or frame, and the flywheel. Its rotor and flywheel are mounted horizontally on bearings attached to the frame. The bottom portion of the hammermill enclosure contains the grate bars or cage sections. A cross-sectional view of a horizontal hammermill is shown in Figure 5.

Hammermill grate bars are bars of metal provided with evenly spaced integral protuberances that establish the clear opening ("grate spacing") through which the shredded feedstock must pass. Several grate bars (e.g., 10 to 20) typically are required. Grate cages, on the other hand, consist of curved, perforated plates. The perforations function as grate openings. Usually, the grate cage is formed of two to six curved sections. The use of grate bars or perforated plates generally depends upon the required grate opening or spacing requirements, and upon the type of material to be size reduced. Typically, the use of grate cages is limited to fractions of MSW that have no steel components. Therefore, hammermills used in the processing of raw MSW are not equipped with grate cages. On the other hand, grate cages are used in the size reduction of the cellulosic fractions of refuse (e.g., wastepaper, air classified light fraction), and in the secondary size reduction of refuse fractions that have been processed to remove ferrous scrap. The maximum diameter of the perforations of a grate cage generally is on the order of 5 to 7 cm.

Regardless of the manner of providing the grate openings, the hardware containing the openings typically occupies the bottom 150° to 180° of the hammermill enclosure.

Hammers in a hammermill may have one of a variety of configurations. The configuration depends upon the one favored by the manufacturer of the machine. During the rotation of the rotor-hammer assembly (usually at 900 to 1200 rpm), the hammers fly in a circumferential pattern about the axis of rotation. Each hammer is free to move within a limited arc between the plates ("disks") of the rotor assembly upon impact with articles in the refuse. The arc of the hammer-swing generally is constrained by pins in the adjacent rows of the rotor assembly. Material to be size reduced is introduced into the machine through an in-feed chute. In the machine, particles that make up the material collide with the hammers and with each other until at least one dimension of the particle becomes small enough to permit passage through the openings in the bottom of the machine.

Most large horizontal hammermills (i.e., greater than 30 Mg/h) are equipped with an articulated section which is operated hydraulically, in order to facilitate the performance of maintenence on the machine, primarily replacement or resurfacing of the hammers, as shown in the illustration in Figure 6.

Grate spacing geometry, i.e., size of the openings and open area percentage, determine to a large extent the residence time of the material in

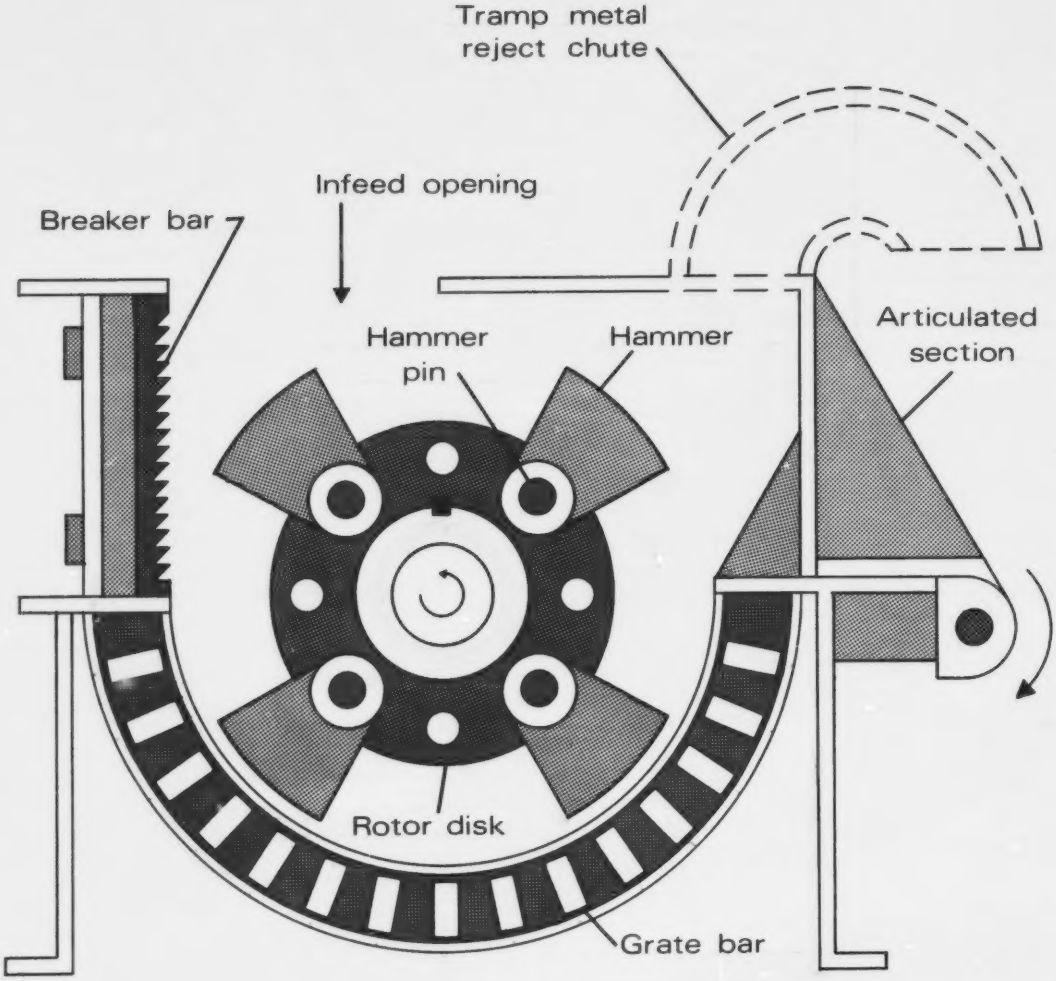

Figure 5. Horizontal swing hammermill (cross-sectional view)

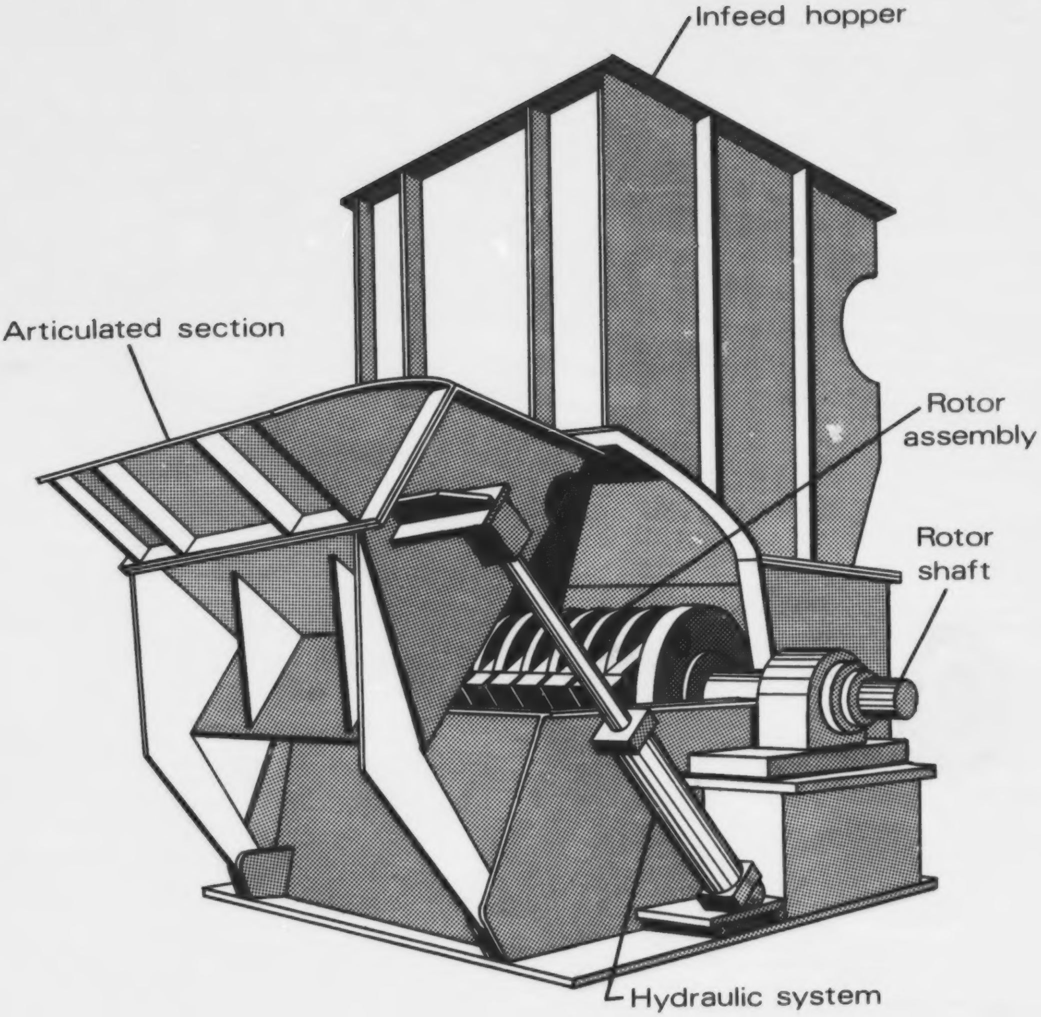

Figure 6. Horizontal swing hammermill.

the mill and the size distribution of the size reduced product. Size distribution also is influenced by feedrate, moisture content, and rotor speed.

As the name implies, the rotor is oriented in a vertical position in a vertical hammermill. The arrangement is shown in Figure 7. The feedstock is introduced into the throat of the machine and then drops parallel to the axis of the rotor. It is discharged peripherally through an opening located in the side and near the bottom of the enclosure, shown in Figure 7. The hammers in a vertical hammermill are free to rotate in a constrained arc, as are the hammers in a horizontal swing hammermill.

VERTICAL RING SHREDDER

The principal physical difference between the design of a vertical hammermill and that of a ring shredder is the use of hammers to accomplish size reduction in the former, and the use of a set of gear-like teeth in the latter. The gear-like grinders, termed "grinders," are free to rotate 360° about axes that are offset from but parallel to the axis of rotation of rotor shaft. The "ring grinders" and the rotor to which they are attached, fit in a stationary housing equipped with replaceable liners. Upon introduction into the upper part of the machine, input material falls directly onto a set of breaker bars designed to break apart large-size objects. Thereafter, the material drops into the space between the teeth and the housing liner. In this part of the machine, size reduction is accomplished through induced shear and the self-comminution interaction between the particles undergoing size reduction. Comminuted material is discharged from a vertical ring shredder through an opening in the side of the shredder enclosure located near the bottom of the unit. An illustration of a vertical ring shredder is presented in Figure 8.

In addition to the principal physical difference noted above (i.e., ring grinders versus hammers), vertical ring shredders also exhibit a key operational difference in relation to both vertical and horizontal hammermills. The difference is manifested in the use of a lower rpm and concomitant tip speed in the design of the vertical ring mill. Due primarily to the difference in the tip speed, vertical ring shredders tend to tear and shear materials in contrast to hammermills where the primary breakage occurs through impact and tearing.

The vertical ring shredder and the size reduction devices described in the preceding paragraphs are all designed to provide sufficient inertia to absorb transient loadings due to throughput surges and the introduction of difficult-to-shred materials. The inertia may be incorporated into the rotor assembly, or it may be provided through a combination of the inertia inherent in the rotor and that in a flywheel located outside of the shredder enclosure.

MSW SHREDDING FACILITIES

According to a survey of shredding facilities [7], 97 shredder installations were in existence in 1981. This number represents an increase of approximately 28 percent over the previous year. However, due to a variety

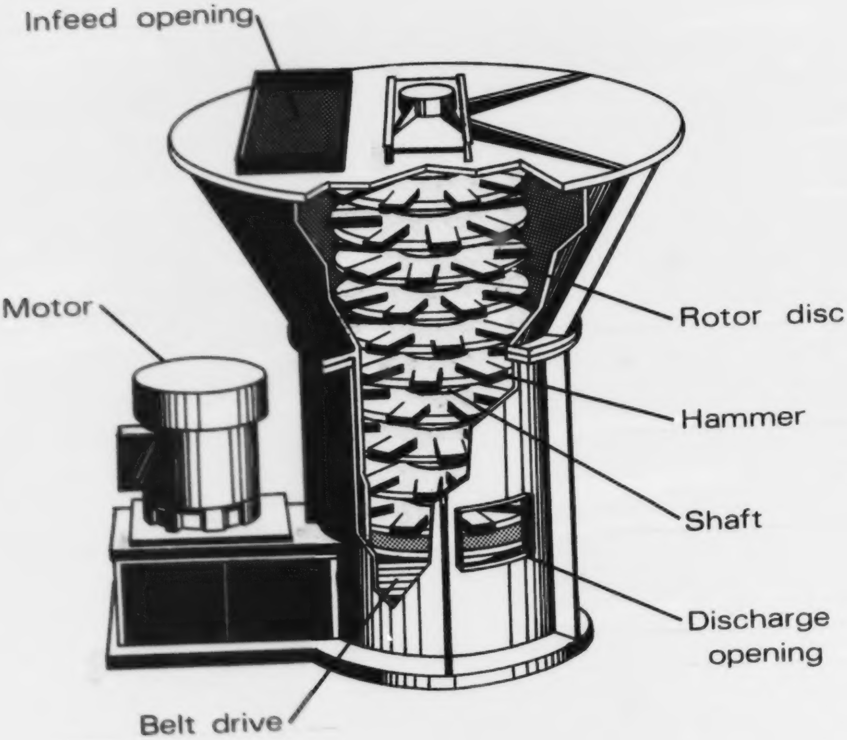

Figure 7. Vertical hammermill.

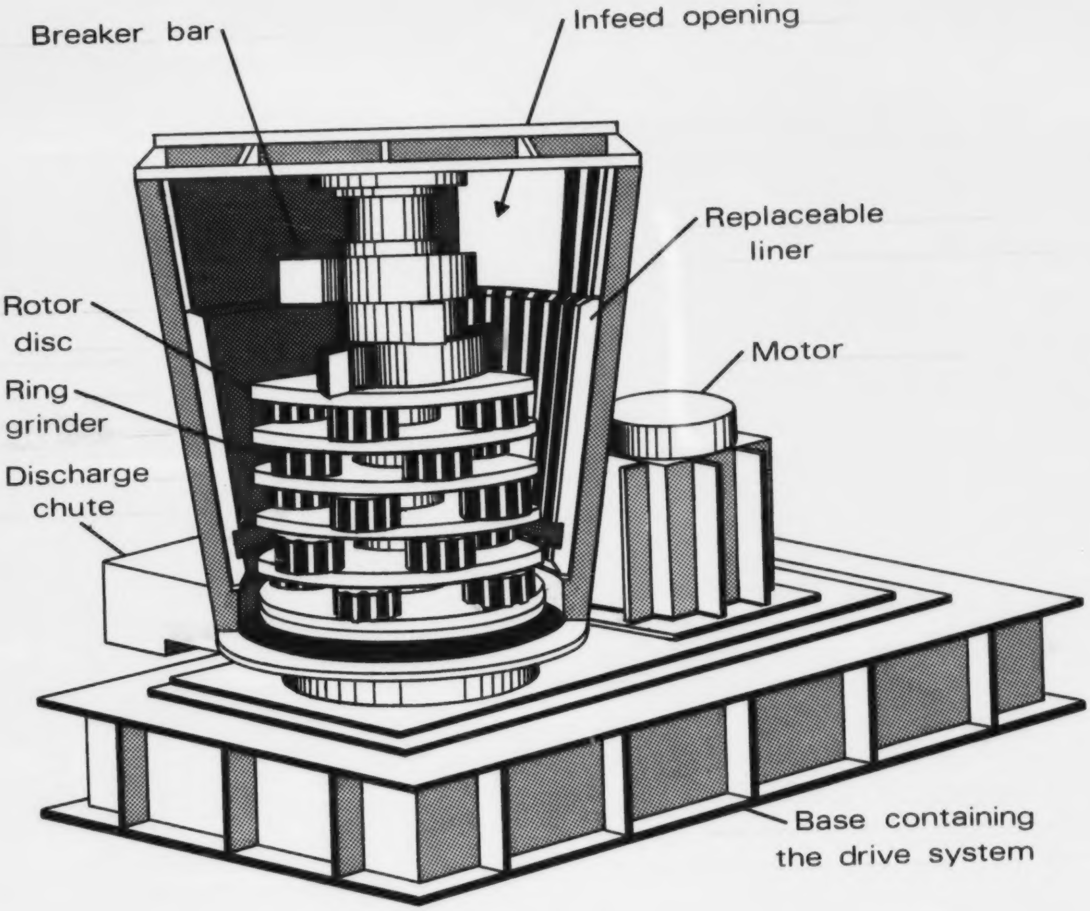

Figure 8. Vertical ring shredder.

of causes, many of the facilities are not operational. The shredders listed in reference 7 have rated capacities ranging from 2 to 90 Mg/h, and the facilities are designed to process from 10 to 1800 Mg per day. Some facilities have parallel shredding lines. A listing of refuse shredders is given in Appendix B.

SHREDDER MANUFACTURERS

Municipal requirements for refuse size reduction generally fall within the range of 10 to 80 Mg/h. In the United States, approximately ten reputable and proven manufacturers produce shredders that have capacities within that range. A partial listing of manufacturers is given in Appendix C.

SECTION 4

DESIGN OF REFUSE SIZE REDUCTION SYSTEMS

PRINCIPLES OF REFUSE SIZE REDUCTION

Introduction

Despite the fact that the size reduction (synonymously, milling, comminution, grinding, or shredding) of solid waste and waste-derived fractions is a key unit process in resource recovery, the development of machine designs and the modeling of the size reduction process continues to rely primarily upon empiricism, rather than upon fundamental principles. As a result of this reliance, presently available literature on size reduction and its principles is almost completely based on the size reduction of homogeneous brittle materials (e.g., coal). Therein lies a problem in that the contents of such literature are applicable only in part to the size reduction of MSW, because as one would expect from the data in Figure 1, MSW is a mixture of ductile and low-tear strength materials (e.g., metal containers, paper) and of brittle materials. The delay in the development of literature on the size reduction of refuse, especially with respect to principles, arises in great part from the heterogeneity of the material and an accompanying lack of documentation regarding the mechanical properties of the diverse objects in the waste stream. Another reason is the absence of a previously developed theory that relates machine-specific parameters for the types of shredding equipment used in the solid waste industry (e.g., hammermills) to the mechanisms and physics of refuse size reduction. While empiricism is of use in design and modeling, it is not enough for the optimal designing of advanced processing systems, because refuse processing involves the control and manipulation of product size distributions to ensure efficient particle and material segregation.

To formulate a valid comminution theory, a variety of factors must be taken into consideration. Two such factors are machine design and particle characteristics of the feedstock. The two factors are among those that determine the dominant mechanisms of the size reduction that takes place within the machine. The mechanisms have a direct bearing upon the size distribution of the final product in that the resultant particle size distribution is the collective result of many single-event distributions brought about by the the particular mechanisms of size reduction peculiar to the piece of equipment.

All too often, theories and so-called laws discussed in the literature do not give information on the machine parameters that govern the particle size-throughput relations of a size reduction device or of an optimum operating condition. Hence, the utility of the theories and laws in machine design is limited. By realizing that the breakage (fracture) process brings about changes throughout all size classes of a complete size distribution and depends upon both the characteristics of the material and the design of the machine, a rational groundwork may be fashioned for the development of a design theory. The theory would include all of the principal factors that govern refuse size reduction. Among the latter are the properties and size distribution of the components of the feedstock, the design and operating specifications of the size reduction equipment, and the rate of throughput. Of itself, a single parameter (e.g., surface area) is incapable of describing changes of such complexity [8,9]. Attempts have been made to fill the gaps in the existing knowledge; the attention remains focused on homogeneous collections of brittle materials. Progress made along those lines is described in a review by Snow [10]. More recently, studies dealing with mixtures, and especially heterogeneous materials, have been reported [11-13].

Elementary Forces

Generally, three types of basic forces are involved in the size reduction of municipal solid wastes, namely, shear, tensile, and compressive. Because of the heterogeneity of MSW with respect to composition and physical and mechanical properties, each of the three forces plays an important part in the size reduction process. The three basic forces are a result of a variety of shredding mechanisms that include impact, crushing, and tearing. The mechanisms generally produce a combination of the three basic forces. For example, tearing results in a combination of tensile and shear stresses within a particle of material.

Pertinent details of concepts described in the literature are presented in this paragraph to demonstrate possible extensions of the principles and knowledge of the size reduction of brittle materials to the comminution of nonbrittle heterogeneous materials. The application of a tensile load to a body is accompanied by the development of normal and shear stresses within the body and the internal transfer of energy. When the resultant stresses exceed mechanical strength of the material, failure (i.e., breakage or fracture) occurs. Failure within the material occurs at points where the stresses are concentrated such as around voids in the material and the tips of cracks. Similar to the case of failure of a material under tension, the fracture of a body under a compressive load also results when the developed normal and shear stresses exceed the mechanical strength of the material. Shear stresses within a material may also develop from the offset application of tensile and compressive loads.

In general, shearing, tearing, and compression in refuse size reduction predominate in those pieces of equipment that operate at relatively low rotational speeds (and therefore low velocities). Examples of relatively low velocity machines are low-rpm and vertical ring shredders. On the other hand, the failure (breakage) of material is predominately due to compression and tearing in those size reduction devices that operate at relatively high rotational speeds, such as vertical and horizontal hammermills.

Early Energy Theories

The emphasis in early theories regarding the energy aspects of size reduction was on the development of a characteristic index for a given brittle material that could be related to a standard degree of size reduction, and therefore could be used to determine the amount of energy required to accomplish other degrees of size reduction. This index, c, depends physically on material properties and operating variables of the system and is described mathematically by the equation,

$$\frac{dE}{dx} = -\frac{c}{x^n} \tag{1}$$

where E is the net energy required per unit weight in a given process of comminution, x is the mean particle size, and n is an exponent. In terms of theoretical development, a problem originates in the difficulty of expressing particle size in terms of one variable, x. The difficulty arises from the fact that the material being comminuted is characterized by a broad range of sizes (cumulatively termed a size distribution) upon entering and leaving the process. The difficulty of representing particle size by a single index is compounded by variations in the shapes of the particles among different materials and over the complete size range of a particular material.

The general form of Equation 1 has been modified by Rittinger [14], Kick [15], and Bond [16] with respect to its solution for specific values of n. The values are obtained as follows: The integration of Equation 1 becomes an expression of Rittinger's law when n = 2. Thus,

$$\Delta E = c_R \left(\frac{1}{x_2} - \frac{1}{x_1}\right) \tag{2}$$

The integration of Equation 1 becomes Kick's law when n = 1,

$$\Delta E = c_K \log \left(\frac{x_1}{x_2}\right) \tag{3}$$

To obtain Bond's third theory of comminution, n = 1.5 is substituted in Equation 1, and the equation is integrated, and rearranged to arrive at

$$\Delta E = C_B \quad \frac{1}{X_2^{1/2}} - \frac{1}{X_1^{1/2}} \tag{4}$$

where C_B is defined as the "bond work index" and commonly denoted in the literature as "w_i". Obviously, the energy requirement in Bond's theory must be between the two predicted by Kick's and Rittinger's laws.

The definitions of x_1 and x_2 distinguish the three theories from each other. As far as Rittinger's theory is concerned, the energy used in comminution is proportional to the resulting increase in surface area (surface theory). Consequently, x_1 and x_2 are defined as the particle sizes that correspond to those particles whose specific surface area (surface per unit weight) is equal to the specific surface of the mixture of particles comprising the feed and product, respectively. Kick's theory states that analogous changes of configuration of geometrically similar bodies vary with the volumes of the bodies (volume theory). According to this theory, x_1 and x_2 are the sizes of those particles whose specific volume (volume per unit weight) is the same as the specific volume of the mixture of particles comprising the feed and product, respectively. In Bond's theory, particle sizes are defined as the apertures through which pass 80 percent by weight of the feed or product.

In contrast to Kick's theory, which is better suited to large particles, Rittinger's theory best fits the size reduction of relatively small particles. When considering the two theories, it should be kept in mind that there is evidence that the numerical value of n in Equation 1 is a function not only of the material being comminuted, but also of the design of the size reduction equipment. Bond accommodates the latter variation through the work index, w_i. To determine the work index for a given material, Bond established an arithmetic mean value of energy per ton through the use of data collected in several types of crushers and grinding equipment, each of which had a characteristic efficiency. Bond's theory would be useful principally in the codification of a mass of industrial experience for the purpose of making interpolations and limited extrapolations for known materials and equipment.

Although the Bond equation was derived for the purpose of describing the breakage of friable materials, several investigators have explored its use to describe the relationship among energy requirements, feed size, and product size in refuse size reduction. The basis for the theory's use in the case of refuse stems primarily from its simplicity in that only the energy requirements and the feed and product sizes must be considered. Stratton and Alter [17], utilizing product sizes from ten different shredders and an energy relationship developed by Trezek and Savage [18], found the Bond work index to be in the range of 426 to 529 kWh/Mg for the size reduction of MSW. The above range is in contrast to that measured by them for individual components, namely glass (8 to 9 kWh/Mg), mixed office waste paper (215 to 218 kWh/Mg), flattened steel cans (275 to 309 kWh/Mg), and aluminum beverage cans (497 to 839 kWh/Mg). In a separate study, Vesiland, Rimer, and Worrell [19] found the work index for MSW to be approximately 253 kWh/Mg.

The wide range in the work index as evidenced above for MSW may be attributable to a number of factors, probably the chief of which are the lack of consideration of machine characteristics and operating conditions in the derivation of the Bond equation and the fact that MSW only contains on the order of 25 percent brittle materials. Regardless of whether or not the above range of the work index as determined from references [17] and [19] (i.e., 253 to 529 kWh/Mg) is typical of refuse size reduction, the reason for the wide spread remains an unanswered question and requires further investigation.

Results of studies reported by other investigators [20-22] indicate indirectly that energy-size relations can have as a common base the simple relationship

$$\Delta E = ck^{-m} \quad (5)$$

where c is a machine constant, k is a measure of particle size, and m is a constant.

The conclusion to be drawn from the preceding paragraphs is that the energy-size relationships described in the pre-1960 literature do not make possible a complete theoretical analysis of the comminution process, and certainly are inadequate for a meaningful process simulation. This is true even though in some instances the approach proposed by the workers of that period may provide a basis for a partial correlation of experimental data.

Representation of Particle Size Distribution

Inherent in the description of the process of size reduction is the concept of particle size, or more appropriately of particle size distribution. The appropriateness of the latter follows from the fact that uniform particle size is seldom encountered in mineral and refuse processing. Associated with the size reduction of a mixture of particles from one size, or more correctly one size distribution, to a finer one is an expenditure of energy, the magnitude of which is a function of a number of factors that have been cited previously.

In an effort to relate theoretically the degree of size reduction to the energy expenditure for achieving it, a description of both feed and product sizes is generally required, the reason being that the energy expenditure is related to the shifts in the distribution. Consequently, the feed and product size distributions and their relationship to one another must be represented in such a manner so as to allow their incorporation into a governing relationship with the energy required for size reduction.

The size distribution of a mixture of particles is characteristically represented in terms of weight percent of material passing specific screen sizes, the spacing of the latter being chosen at regular intervals spanning the entire distribution of particle sizes. From the size distribution data, characteristic sizes can be computed in terms of one size (e.g., the screen size through which 50 percent by weight of the material passes) and in terms of the mass fraction of material retained between two screen sizes (e.g., 25 percent by weight of the material is retained in the size class -5 cm +2 cm). Each of the above manners of representing size distributions have been used in the theoretical development of relationships among: 1) shifts in particle size distributions of a mixture; 2) the energy required to achieve the shifts; and 3) the breakage mechanisms that occur within the size reduction equipment.

Equations formulated by Gaudin-Schuhmann [23,24] and Rosin-Rammler [25] are examples of the the empirical equations for size distributions that have been formulated to describe the physical nature of the comminuted product. The fraction of undersize Y(x) to relative size x/k is related by the Gaudin-Schumann equation

$$Y(x) = (\frac{x}{k})^{\alpha} \tag{6}$$

In Equation 6, $Y(x)$ is the cumulative weight fraction finer than size x, and k is a quantity termed the "size modulus," which together with the slope parameter, α, characterize the size distribution.

In the Rosin-Rammler equation, the mass fraction of undersize is related to the size modulus (X_o) by an equation having an exponential form

$$Y(x) = 1 - \exp[-(\frac{x}{X_o})^{n}] \tag{7}$$

where n is a numerical constant, and X_o is the size (termed the characteristic particle size) corresponding to the case where $Y(x)$ equals 63.2 percent cumulative passing, i.e., the value of $Y(x)$ where x equals X_o.

Several studies (Stratton and Alter [17]; Vesiland, Rimer, and Worrell [19]; and Trezek and Savage [18]) have shown the usefulness and goodness-of-fit of the Rosin-Rammler equation for representing the size distributions of shredded refuse. In the studies, product size distribution data from several different types of refuse shredders were subjected to analysis using the Rosin-Rammler equation. Among the conclusions to be drawn from the three studies is the range of the exponent n for shredded MSW, $0.6 \leq n \leq 1.0$.

Gaudin and Meloy [26] propose the following theoretical size-distribution equation for single fracture:

$$Y(x) = 1 - (1 - \frac{x}{x_o^*})^{r} \tag{8}$$

In Equation 8, x_o^* is a characteristic dimension of the feed particle before fracture, and r is the size ratio, which is a measure of the number of breaks in the particle. The Gaudin-Meloy equation was modified empirically by Bergstrom [27] through the addition of another parameter, q. The following equation is the result:

$$Y(x) = [1 - (1 - \frac{x}{x_o^*})^{r}]^{q} \tag{9}$$

Thus, a combination of the fine and coarse size curve-fitting capacities of the Gaudin-Schuhmann and Gaudin-Meloy equations is embodied in Equation 9.

For greater curve-fitting flexibility, other size distribution equations with additional parameters have been proposed as further generalizations of the preceding relations. However, at the time of this writing, such other equations have not seen use in the area of refuse comminution.

Degree of Size Reduction

When the need arises to compare the operation and performance of size reduction equipment under differing conditions (e.g., comparison of shredders at two different sites and shredding MSW to dissimilar particle sizes), the question of normalization of the performance data must be considered and resolved. Some researchers rely upon the concept of degree of size reduction, Z_o, when making comparisons between the performances of size reduction equipment that produce different product size distributions from refuse feedstocks differing in size distribution [28,29]. The term Z_o is defined as unity minus the ratio of the product characteristic size (X_o) to the feedstock characteristic size (F_o).

Values for degree of size reduction range from zero (no size reduction) to a maximum of 1.0, which corresponds to a product size of zero and therefore to an infinite amount of size reduction. Of course, the latter limit is unachievable in practice.

An example of the utility of employing the degree of size reduction is indicated by its use in the evaluation of the specific energy required to size reduce the different types of waste encountered in a resource recovery facility. The relative energy requirements for a given degree of size reduction for selected waste fractions are indicated by the curves in Figure 9, in which are plotted data taken from reference 28. The shredder used in the study was a 187 kW horizontal swing hammermill.

Matrix Modeling of Breakage

The possibility is remote that all of the types of breaking that occur in refuse comminution can be described by a single breakage "law", inasmuch as refuse is a mixture of materials each of which has different mechanical properties. The impossibility is confirmed by the fact that experimental results indicate that the feed cannot be characterized by any of the preceding theoretical relations for size distributions. Possibly, the process of comminution could be described through the use of the matrix method to simulate the breakage process so as to arrive at predictions of feed and product size distributions.

In the matrix method, vector notation represents the size distribution as described by sieve analysis. This is done by considering the range of size of the collection of particles to be subdivided into n intervals, with the coarsest size being x, and the finest as x_{n+1}. The ith size fraction is bounded by x_i above and x_{i+1} below and $x_i = rx_{i+1}$ ($i=1,2,3,---, n-1$), with $r(>1)$ being the geometric sieve ratio. Where it is necessary to specify the size of particles in a particular size fraction by a single number, the geometric mean is used. When the particle size distribution is expressed logarithmically, the geometric progression of sizes appears as equally spaced points on the abscissa.

In the matrix representation, P_i refers to the cumulative mass fraction of product material less than size x_i, and F_i is the cumulative mass fraction of feed material less than size x_i where $i = 1,2,3, ---, n$. Consequently, the size distributions of the feedstock and comminuted product can be described by n x 1 column vectors $\underline{f}$ and $\underline{p}$ with elements f_i and p_i, where f_i and p_i are, respectively, mass fractions of feed and product materials that fall between sizes x_i and x_{i+1}, thus:

BEGIN FIRST LINE OF TEXT HERE
CENTER OF PAGE
TOP OF IMAGE AREA
DROPPED HEAD; BEGIN SECTION HERE

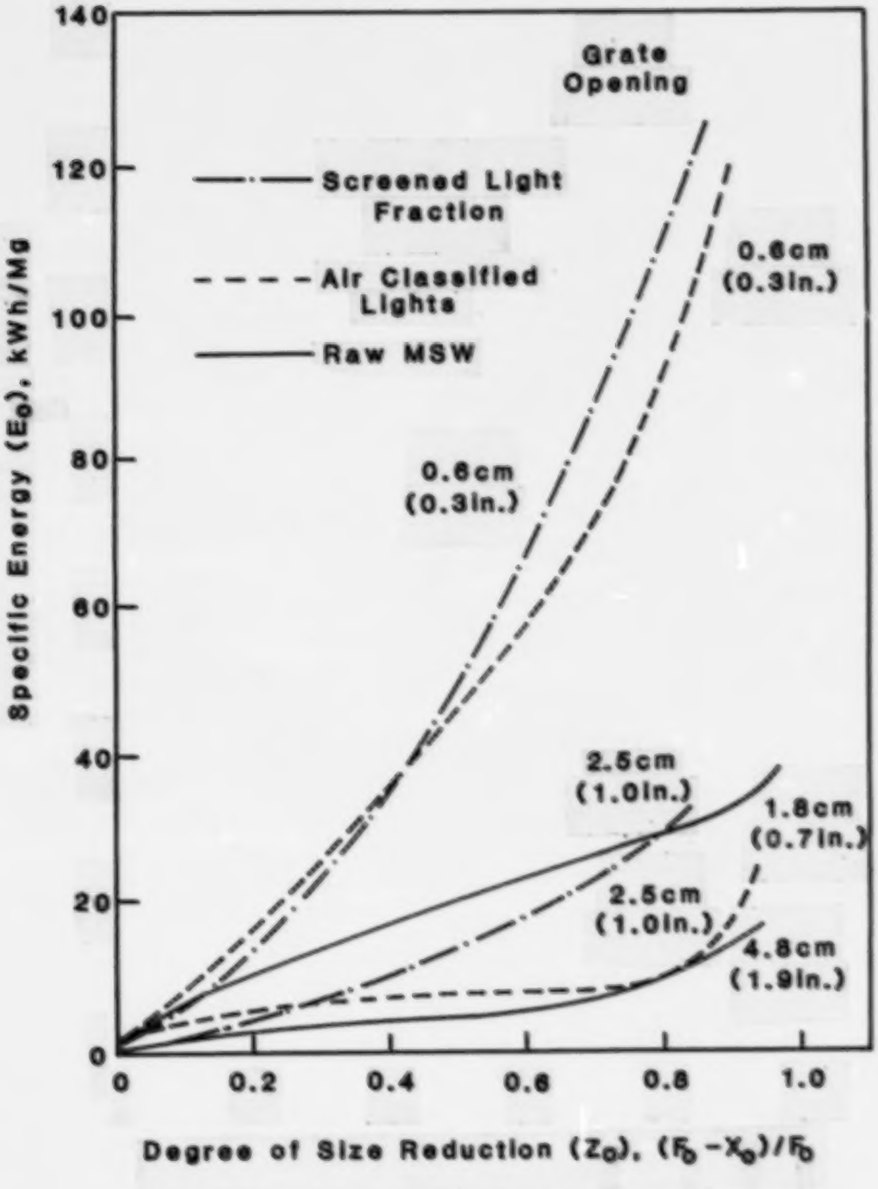

Figure 9. Energy requirements for selected solid waste fractions using a 187-kW horizontal swing hammermill.

BEGIN LAST LINE OF TEXT
3/8"
BOTTOM OF IMAGE AREA; OUTSIDE DIMENSION FOR TABLES AND ILLUSTRATIONS

PAGE NUMBER
EPA Form 2350-4 (4-80)
(PREVIOUSLY CIN. EPA FORM 247)
TYPING GUIDE SHEET

$$\underline{f} = \left|\begin{matrix} f_1 \\ f_2 \\ \cdot \\ \cdot \\ \cdot \\ f_n \end{matrix}\right| \quad ; \quad \underline{p} = \left|\begin{matrix} p_1 \\ p_2 \\ \cdot \\ \cdot \\ \cdot \\ p_n \end{matrix}\right| \tag{10}$$

where

$$f_i = F_i - F_{i+1} \tag{11}$$

$$p_i = P_i - P_{i+1} \tag{12}$$

The percentage or mass fraction of material less than the smallest size is described by

$$f_{n+1} = F_{n+1} = 1 - \underline{e}'\underline{f} \tag{13}$$

$$p_{n+1} = P_{n+1} = 1 - \underline{e}'\underline{p} \tag{14}$$

where $\underline{e}'$ is the transposition of the n x 1 column vector $\underline{e}$ with unity elements. The transformation of the feed to the product is thus expressed mathematically by matrix algebra:

$$\underline{p} = X^*\underline{f} \tag{15}$$

where X^* expresses the breakage process.

The sequence of rows and columns in the matrix, X^*, which describes a transformation of a size distribution, bears a definite relationship to particle size. If i and j refer to the ith row and jth column of X^*, with elements X_{ij}, then X_{ij} will denote the proportion of particles that initially were in size range j and afterwards were in product size range i. For size reduction, X^* is a lower triangular matrix, and a knowledge of the n elements of $\underline{p}$ and the n elements of $\underline{f}$ is not sufficient to arrive at a unique solution from the n equations of the $n/2(n+1)$ unknowns $X_{ij}(i \geq j)$.

An empirical evaluation of the matrix for an open-circuit grinding process can be made by representing the process by the equation

$$\underline{p}_j = X^*\underline{e}_j \qquad (j = 1,2,3, \ldots, n) \tag{16}$$

where X^* is unknown and $\underline{e}_j$ is the unity vector with all elements zero except the jth element (=1). The experimental determination of $\underline{p}_j$ gives the jth column of X^*. If particle interaction does not occur and it is possible to use graded feeds ($\underline{e}_j$) down to the smallest size x_n, the experimental evaluation of X^* should satisfactorily predict the output size distribution ($\underline{p}$) obtained on feeding ungraded material ($\underline{f}$).

The analysis of the size reduction of refuse may be made through an adaptation of a matrix method similar to that developed by Callcott [30] for size reducing coal in a swing hammermill. Considering first the case of low throughput (i.e., a dilute concentration of particles within the mill cavity), it may be assumed as a first order approximation that a hammermill is essentially a "once-through machine", that is, the material passing through the mill is exposed to one cycle of breakage. (It should be noted, however, that operation conditions different from that considered above (e.g., higher throughput) would lead to a more extensive recirculation, and hence to repeated exposure to breakage.) If the process is considered as "once-through", the residence time of the material in the machine would be brief. The above assumption of a "once-through grinder" was used by Calcott in the development of a comminution theory for coal. Two of four models based on such a matrix method [31] seem to offer the most utility. The two are the π-breakage model and the repeated breakage cycles model. Both utilize the concepts of a selection function and a breakage function. The former represents the fractional amount of a given size material that is selected for breakage while the latter represents the proportion of particles initially in a given size class that is redistributed to each of the other size classes after breakage. A description of the two models follows:

In the π-breakage model, the selection function S(Y) equals a constant, π, for all sizes Y, whereby a proportion, π, of the particles independent of particle size is selected for breakage according to the breakage function B(x,y). In matrix notation where I* represents the identity matrix and the selection function is represented by, $S^* = \pi I^*$, the equation describing the breakage process is

$$\underline{p} = [\pi B^* + (1-\pi I^*)]\underline{f} \tag{17}$$

The process is completely described by the parameter π if B* is assumed to be known. It is a useful measure of the breakage accomplished in the process. Broadbent and Callcott [32] describe techniques for determining the value of π from known feed and product distributions through the use of iterative methods. They warn that because of the errors that might attend measurements, the simple simultaneous solution of the elements of Equation 17 usually should not be attempted. In place of the equation, they recommend the use of the least-square technique outlined by them.

The breakage process can be assessed in terms of a series of cycles of mild breakage, or repeated breakage cycles when the feed size distribution differs considerably from that of the product. Such would be the case if high throughputs were being processed through the size reduction device, i.e., a large concentration of particles existed within the mill cavity. The repeated breakage cycle may be expressed as

$$p = \prod_{n=1}^{N} (B^* S^*_n + I^* - S^*_n)\ \underline{f} \tag{18}$$

where n equals 1,2,..., N refers to the nth cycle in which the probability of breakage is S^*_n. It should be noted that it is impossible to evaluate each S^*_n and for each cycle n if only $\underline{p}$, $\underline{f}$, and B* are given. However, if it is assumed that the probability of breakage S^*_j is the same for all the cycles, Equation 18 becomes

$$\underline{p} = (B^*S^* + I^*-S^*)\ N\underline{f} \tag{19}$$

where S^* is the selection matrix common to all N cycles. If

$$D = (B^*S^* + I^*-S^*) \tag{20}$$

then $\underline{p}$ can be represented simply as,

$$\underline{p} = D^*N\underline{f} \tag{21}$$

The entire size reduction process that occurs in the mill is treated as a sequence of operations in which the product from the jth cycle becomes the feed for the (j+1)th cycle. To ensure that the undersize from any cycle of the process is correctly described, $\underline{p}$ and $\underline{f}$ are (n+1)- column vectors, and the last elements, p_{n+1} and f_{n+1}, describe the undersize for the product and feed, respectively. D^* is written as a (n+1) square matrix, with the (n+1)th row describing the proportions of the various size ranges that end up as undersize.

In his analyses, Calcott [30] assumed that a hammermill has N obstructions or grinding zones. Material from the jth zone in passing through the (j+1)th zone is said to have undergone a single cycle of breakage. In Trezek's and Savage's modification of the model [18], the number of cycles, N, is not identified with the grinding zones. Instead, N is introduced arbitrarily as a way of repeatedly applying the single matrix D^* to the feed vector $\underline{f}$ to obtain $\underline{p}$ when there is considerable difference between the the top sizes of the feed and product distributions. If x_1 is the largest size of the initial feed and x_m the largest size of the final product (where $x_i = rx_{i+1}$, $i = 1,2,\ldots, m,\ldots,n-1$), then N is as in the relation

$$N = (m - 1) \tag{22}$$

In his reaseach, Obeng [31] found that of the two models, the π-breakage model more adequately describes the process of refuse comminution.

An example of the method of matrix modeling of size reduction is given in Appendix D.

Internal Shredder Configuration

Thus far, no published attempt has been made to correlate the performance characteristics of refuse shredders with the internal design of the machine. Consequently, even though the designer might know the particle size that must be produced by the shredder and the power requirements for doing so, he lacks the analytical relationships that would enable him to calculate the internal configuration of a machine needed to attain the performance required for a given throughput. With respect to internal design, it is necessary to depend upon previous results from an identical (or similar) shredder, or to construct a machine such that machine operation and performance could be varied. It is readily apparent, therefore, that there is an urgent need to develop an analytical method for designing the internal configuration of a shredder. The availability of such a method would circumvent the reliance upon trial-and-error solutions and would potentially contribute to an improvement in shredder design.

Research conducted by Cal Recovery Systems, Inc. with the use of horizontal hammermills as a part of its attempt to meet the need for an analytical design method [33], has led to the development of empirical relations among the shredding variables power (P), holdup (H), specific energy (E), and characteristic particle size (X_o) and the internal configuration of the equipment, i.e., grate spacing, number and volume of hammers, etc. Data used in the development of the relationships were derived from previous field tests [18,29].

Although the findings of the research continue to be preliminary in nature, they are presented herein as a means of indicating the state-of-the-art as applied to relationships between shredder performance and internal configuration of the machine.

Much of the notation in the CRS analysis is the same as that used in this manual. However, additionally in the manual are defined some fundamental quantities that have been found to be of use in the description of the interaction between hammermill performance and the configuration of the shredding cavity. Volume was selected as a key parameter, since from the standpoint of designing a shredder cavity, it describes in a general manner the geometry of the cavity. After considering various volume parameters, open volume, closed volume, and total hammer volume appear to be the ones of greatest significance and of the greatest utility for design purposes. The three volume parameters are defined and described in the paragraphs that follow.

The swept volume (V_s) was taken as being the cylindrical volume defined by the tip-to-tip diameter of the rotating hammers and the length of the shredder shaft within the shredding zone. The swept volume is composed of two quantities: 1) the closed volume within the swept cylinder, i.e., volume of the internal shredder hardware (V_c) (e.g., rotor, rotor pins and disks, hammers, etc.); and 2) the open volume (V_o). The open volume is defined as the difference between the swept volume and the closed volume. The hammer volume (V_h) is the total volume of all hammers in the mill and is equal to the volume of one hammer multiplied by the number of hammers. Relations that have been developed for mill holdup and throughput, for power requirements and mill holdup, and for specific energy requirement and product size in terms of the shredder's internal parameters are given in Table 2.

The complexity of the relations are readily apparent from the form of the equations in Table 2. Despite their complexity, however, the relations reflect results that are intuitively consistent. For example, the expressions relating mill holdup and throughput (Equations 1, 2, and 3 in Table 2) reflect the fact that at a constant throughput, an increase in the open volume will result in an increase in the mill holdup. The latter increase is due to a drop in number of hammer-particle collisions. In effect, the mean distance

TABLE 2. EMPIRICAL RELATIONS AMONG THROUGHPUT, HOLDUP, POWER, SPECIFIC ENERGY, AND PRODUCT SIZE IN TERMS OF MACHINE PARAMETERS FOR HORIZONTAL HAMMERMILLS

Throughput/Holdup

$$\dot{m} = aH^b \qquad (1)$$

$$b = 0.58 \exp\left[2.13V_h^{\,2}S/V_o\right] \qquad (2)$$

$$a = 20.62 \left(\frac{d^{0.75}}{V_o}\right)^{2.15b} \qquad (3)$$

where: V_h = total hammer volume (m^3)
V_o = mill open volume (m^3)
S = hammer tip speed (m/s)
d = grate opening (m)
$\dot{m}$ = throughput (Mg/h)
H = mill holdup (kg)

Power/Holdup

$$P = aH^b \qquad (4)$$

$$b = 0.7 \exp\left(0.071SV_h\right) \qquad (5)$$

$$a = 9.4\left(\frac{V^*}{SV_h}\right)^{1.36b} \qquad (6)$$

where: P = power (kW)
H = mill holdup (kg)
S = hammer tip speed (m/s)
V_h = total hammer volume (m^3)
V^* = percent open volume, [open volume/swept volume]

Energy/Product Size

$$E = a\left(\frac{25.4}{X_o}\right)^b \qquad (7)$$

(continued)

BEGIN FIRST LINE OF TEXT HERE
CENTER OF PAGE
TOP OF IMAGE AREA
DROPPED HEAD: BEGIN SECTIONS HERE
BEGIN LAST LINE OF TEXT
3/8"
PAGE NUMBER
BOTTOM OF IMAGE AREA; OUTSIDE DIMENSION FOR TABLES AND ILLUSTRATIONS
EPA Form 2350-4 (4-80)
(PREVIOUSLY CIN. EPA FORM 287)
TYPING GUIDE SHEET

TABLE 2. (continued)

For the coefficient a:

if,

$$\frac{V_o d}{SV_c} \leq 0.0127 \tag{8}$$

then,

$$a = 751 \left(\frac{V_o d}{SV_c}\right)^{1.12} \tag{9}$$

if,

$$\frac{V_o d}{SV_c} > 0.0127 \tag{10}$$

then,

$$a = 0.011 \left(\frac{V_o d}{SV_c}\right)^{-1.44} \tag{11}$$

For the coefficient b:

if,

$$(V^*)^a\, d \leq 0.065 \tag{12}$$

then,

$$b = -6.32 - 2.34 \ln\left[(V^*)^a d\right] \tag{13}$$

if,

$$(V^*)^a\, d > 0.065 \tag{14}$$

then,

$$b = 4.23 + 1.49 \ln\left[(V^*)^a\, d\right] \tag{15}$$

where: X_o = characteristic particle size (mm)
E = specific energy in (kWh/Mg)
d = grate spacing (m)
S = tip speed (m/s)
V_c = closed volume (m^3)
V_o = open volume (m^3)

EPA Form 2350-4 (4-80)
(PREVIOUSLY CIN. EPA FORM 287)
TYPING GUIDE SHEET

between particles and hammers is increased, and therefore, the probability of breakage is reduced.

Due to this empirical development, the relations given in Table 2 are appropriate for use only in connection with the design of horizontal hammermills and only within the range of parameters specified in Table 3.

TABLE 3. APPLICABLE RANGE OF PHYSICAL PARAMETERS OF HORIZONTAL HAMMERMILLS FOR THE EMPIRICAL RELATIONS GIVEN IN TABLE 2

Grate spacing (d)	0.013m	to	0.343m
Total hammer volume (V_h)	0.0272m^3	to	0.2026m^3
Total swept volume (V_s)	0.765m^3	to	8.15m^3
Percent open volume ($V_o/(V_o + V_c)$)	63.5	to	86.9
Hammer tip speed (S)	54.5m/s	to	75.6m/s
Product size (X_o)	7.4mm	to	140 mm

SHREDDER OPERATION AND PERFORMANCE

Three characteristics are of especial importance in the evaluation of the performance of a size reduction device, namely, size distribution of the product, specific energy requirement (kWh/Mg), and machine wear. The quantification of the three characteristics is a function of the physics of the comminution mechanisms that occur in the individual machine. Hence, they constitute three dependent variables. The three dependent variables are influenced by a a set of five independent variables in the form of operational factors. The five factors are: 1) size distribution of the feed; 2) the flow rate of material through the device; 3) moisture content of the feedstock; 4) grate opening size or size of the discharge opening; and 5) the relative velocities of the size reduction elements in the device (e.g., rpm or tip velocity of the rotating hammers).

Particle Size Distribution

As stated in the Introduction, solid waste as discharged from a collection vehicle is a highly variegated collection of objects of all shapes and sizes. The size distribution of the objects spans approximately an order of magnitude. A range of 90 percent cumulative passing between 30 and 65 cm is typical of unprocessed refuse. In evaluating shredder performance, it is convenient to assign one number as representative or characteristic of the size distribution of a material, hence, the term "characteristic particle size." In practice, the term is expressed as the size of the screen openings through which 63.2 percent of the particles pass. Thus, if 63 percent of the particles of a given waste have a characteristic particle size of 40 mm or less, it is referred to as having a characteristic particle size of 40 mm. Another commonly used term is "nominal particle size." "Nominal particle size" is the size the corresponds to 90 percent cumulative passing. Size distribution and its characterization are affected by a number of factors, chief among which are: 1) feed rate; 2) number of passes through the mill; 3) rotational velocity of the hammer tips; 4) moisture content of the input material; 5) grate spacings; and 6) condition of the hammers (degree of wear).

The description of a product size analytically makes it possible to develop a semi-empirical theory in terms of breakage and selection functions. This development in turn can serve as the basis upon which to devise a predictive method for calculating the product size distribution to be obtained in the size reduction of a given feed. It is possible to extend the theory thus developed to include an investigation of the interrelation and effects of the comminution variables as they occur in a machine. However, practically speaking, it is better to confine the application of the theory to the examination of the size distribution itself. By so doing a useful insight into the behavior of the other variables can be gained.

Judging from observations reported in the literature [17-19,34,36], product distributions can be represented by a Rosin-Rammler relation of the type:

$$y(x) = 1 - \exp\left[-(x/X_0)^n\right] \tag{23}$$

where $y(x)$ is the cumulative percent passing screen size x. In effect, the exponent n ("n index") is the slope of the line $\ln[1/(1-y)]$ versus x when plotted using log-log coordinates. The numerical value of X_0 is the size that corresponds to 63.2 percent cumulative passing, or alternatively, the value of x where $\ln[1/(1-y)] = 1.0$. In observations made thus far, individual values of n for shredded refuse were within the range of values reported as being characteristic in the grinding of brittle materials in hammermills ($0.5 \leq n \leq 1.3$). Lower n values are associated with a rather scattered distribution over a wide spectrum of particle sizes, whereas high n values indicate a rather uniform particle size, i.e., particle sizes limited to a narrow size range.

Effect of Multiple Size Reduction

Successive cycles of grinding characteristically lead to a shift in product size distribution towards the finer sizes. The shift becomes more extensive with successive cycles of grinding as is evidenced by downward shifts of X_0 and n, respectively. For example, in an investigation conducted with the use of a hammermill in which the rotor revolved at 1,200 rpm, Savage and his colleagues [18] found that the characteristic particle size (X_0) dropped from 1.5 to 2.5 cm in the primary grinding (i.e., first pass), to 0.825 cm in the second grinding (second pass), and to 0.575 cm in the third grinding (third pass). The corresponding n values were 0.99, 0.87, and 0.75, respectively.

Rotational Velocity

Some data [18,34,35] are available on the effect of rotational velocity of the hammer tip (tip speed), and are interpreted herein in terms of rpm of the rotor. Such an interpretation is a valid one inasmuch as one and the same machine was used to obtain the results upon which the interpretation is based. An important consequence was the fact that hammer circle diameter (i.e., tip to tip diameter) was constant throughout the tests. During the tests, the shredder was operated successively at 1200, 790, and 555 rpm. The measured n indexes of the Rosin-Rammler distributions at 1200 rpm was 0.81; at 790 rpm, 097; and at 555 rpm, 0.91. The corresponding X_0 values were 1.95, 2.7, and 2.2 cm respectively. The larger values of n and X_0 obtained at 790 rpm and 555 rpm velocities indicate that a coarser product may be an accompaniment of lower operating speeds.

The smaller X_0 and n values characteristic of higher rotational velocities may be functions of the resulting increased number of impacts per unit of time. Not to be overlooked is the increase in force of the impacts that is another result of increase in velocity. Because velocity apparently ceases to exert a prevailing influence on the overall description of the size reduction process, values for X_0 and n more or less plateau at the lower velocities.

Moisture Content

Because of a lack of agreement among observations reported in the literature, the effect of moisture content on particle size distribution cannot be ascertained with certainty at this time. Despite that fact, it can be stated unequivocally that moisture does have a definite effect.

The lack of agreement is with respect to the extent and nature of the effect. Thus, according to results obtained in one reported study [18], a definite increase in coarseness of particle size characterized increase in moisture content (wet weight basis) within the observed range (viz. 25 to 57 percent). Observations reported by a second group of researchers in another locale [36] were quite the contrary in that the group noted a smaller average particle size and a more uniform size distribution to take place as the moisture was increased (i.e., 32 to 48 percent). Reasons for the discrepancies may include difference in the procedures followed during the preparation of samples for size distribution analyses, in the methods and equipment used for sample sieving, and in the composition of the feedstock.

Regardless of the resolution of the effect of moisture content on product size, it can be stated with certainty that during sample preparation and the sieving of moist samples, a certain amount of clumping and matting of particles occurs -- at times to such an extent as to render impossible the task of obtaining a meaningful measurement of particle size distribution. This latter is especially true when the moisture content exceeds 60 percent.

There is a limited amount of available test data [18,35] to indicate the existence of a drop in the specific energy requirement for refuse size reduction with increase in the moisture content of the feedstock. However, the same reports indicate the possibility of a renewed gain in energy consumption when the moisture exceeds 50 percent [18,35]. The curves in Figure 10 illustrate the relation between moisture content and power requirement. (Incidentally, the figure also shows the effect of a decrease in rotor speed on energy requirements.)

Condition of Hammers

Undoubtedly, the condition of the hammers constitutes an important factor in the determination of particle size distribution. The effect exerted by hammer wear on size distribution has been described in terms of exponential decay with time by Gawalpanchi, et al [36]. In their description, the relation for cumulative percent of material passing a specified size (y) is expressed as:

$$y = b_0 + b_1 \exp(-b_2 t) \tag{24}$$

where t is the cumulative tons of refuse shredded after the installation of new hammers. According to Gawalpanchi, the size distribution of particles becomes increasingly coarse as the hammers lose their cutting edges, i.e., become worn. The change is greatest immediately after new or resurfaced hammers are installed. A reason for the increased coarseness with advance in wear is the progressive widening of the space between the hammer tips and the housing that is the accompaniment of the gradual wearing down of the hammers. Another reason is the obvious one that worn hammers do not shred as effectively as do new hammers.

It should be noted that the results obtained by Gawalpanchi, et al differ drastically from the experience had by many plant managers. The latter report a progressive increase in fineness of particle size of the shredded product with increase in extent of wear of the hammers. A reason proffered for the plant managers' observation is that less efficient cutting occurs with dull hammers and thereby brings about a prolongation of the residence time, and therefore an increase in number of hammer impacts as material moves through the shredder.

Specific Energy Requirement

The energy requirement for size reduction constitutes a decisive factor in the practical and economic feasibility of a shredding process. A useful way of characterizing the energy requirement is by the "specific energy requirement" (kWh/Mg). The "specific energy requirement" is defined as the quantity of gross minus the freewheeling energy divided by throughput rate. The implication therefore is that in the consideration of power requirements, a distinction should be made between "gross power," "net power," and "freewheeling power." "Gross power" refers to the total energy required; "net power," to the gross energy minus the freewheeling energy; and "freewheeling power," to the energy requirement of the shredder under idling conditions. Inasmuch as approximately 5 to 15 percent of the full load rating usually is taken for freewheeling power, from 85 to 95 percent remains available for size reduction. Factors of importance in terms of energy

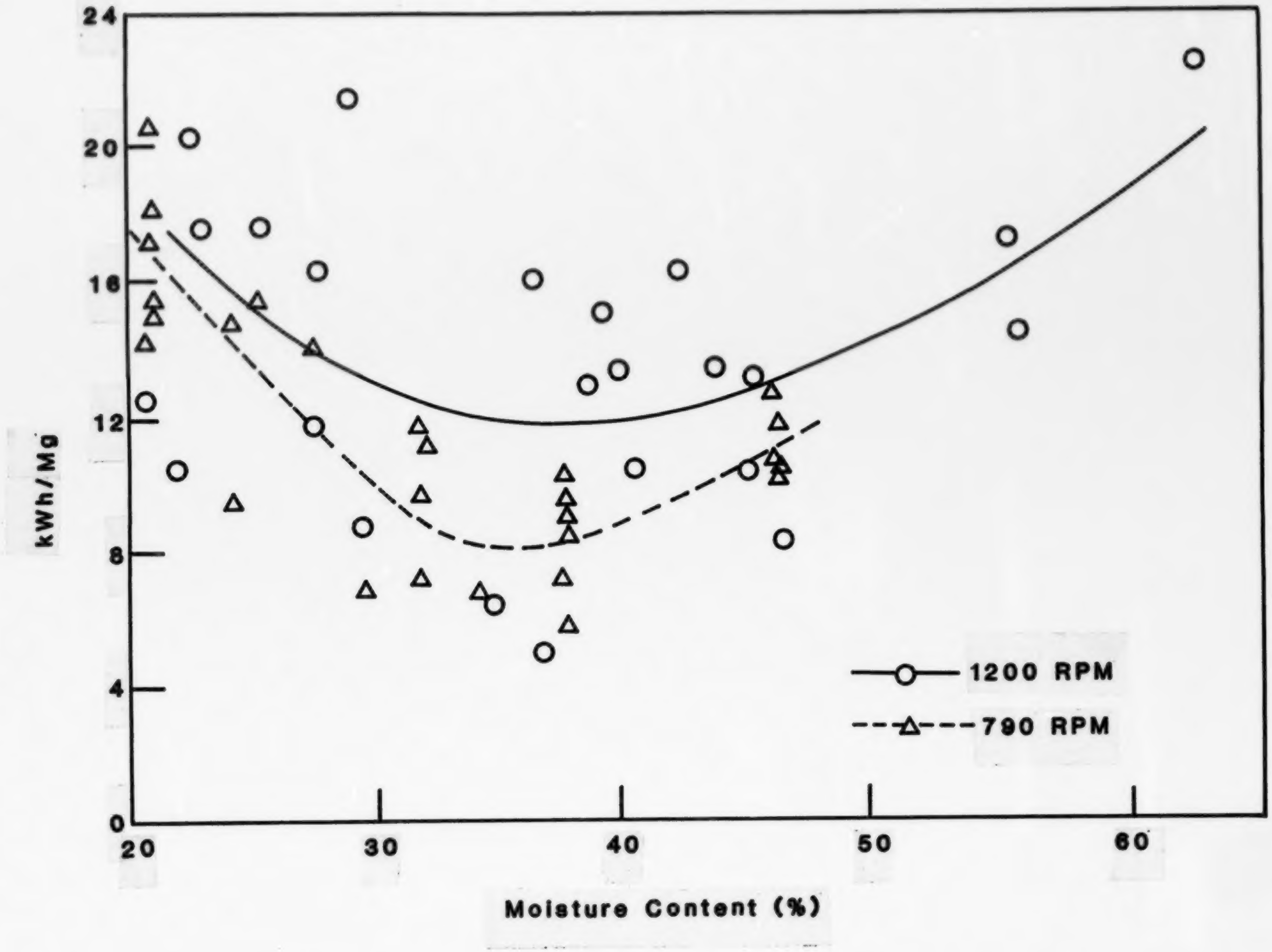

Figure 10. Effect of moisture on specific energy consumption.

consumption by a shredder system are characteristic particle size, feed rate, moisture content, machine design (including hammer placement and state-of-repair of the machine), and efficiencies of the motor and drive system.

The specific energy consumption for a hammermill was found empirically by Trezek and Savage [18] to be a function of characteristic size when the range of n values is from 0.7 to 1.3. It is at its maximum when the particle size (X_o) is small, and at its least when the particle size is large. Accordingly, the amount of energy to produce a given percent change in X_o is less with coarser particles that it is with finer particles. For example, Trezek and Savage found that on the one hand a 50 percent reduction in characteristic particle size could be obtained at an expenditure of about 2.4 kWh/Mg if the reduction in size is from a feed size of 15 cm down to a product size of 7.5 cm. On the other hand, if the particle size of the feed is 1.5 cm, to reduce it to 0.75 cm would require a power input of 7.2 kWh/Mg.

The results of field studies of shredders conducted during 1978-80 served as a groundwork for the development of relationships with which predictions can be made on an as-received basis (as received weight, E_o) regarding specific energy as a function of characteristic size (X_o) and of the nominal (X_{90}) product size [29]. The following two equations were formulated in the development of a functional relationship between E_o and the size parameters:

$$E_o = 17.91\ X_o^{-0.90} \tag{25}$$

$$E_o = 35.5\ X_{90}^{-0.81} \tag{26}$$

in which E_o is expressed in kWh/Mg (as received), and X_o and X_{90} in cm. The corresponding coefficient of correlation for Equation 25 is 0.87, and for Equation 26, 0.89. The equations have a practical value in estimating net power requirements in general, because they are based on data covering throughputs of 15 to 82 Mg refuse/h. (Such estimates must serve as generalities inasmuch as other variables also influence power requirements such as those addressed previously in the section "Internal Shredder Configuration.")

The net power required to produce a specific particle size can be estimated by multiplying the specific energy (E_o) by the anticipated flow rate.

Power and Throughput Relationship

Power requirement as a function of throughput rate may be determined by way of the following equation taken from reference 29:

$$P_n = a\ \dot{m}^b\ (1 - MC)^c \tag{27}$$

where P_n = net power (kWh); $\dot{m}$, the flow rate of refuse through the shredder (Mg/h); and MC, the fractional moisture content of the refuse. If the exponents b and c have a positive value, the implication is that power requirement increases with flow rate, and decreases with increase in moisture content. The numerical value of the coefficient a indicates the magnitude of the power requirements. It is postulated as being influenced by machine design characteristics such as size of grate openings, internal geometry, and the geometry and number of hammers. The units of the coefficient are $(Mg/h)^{-1}$. In Table 4 are listed coefficient values characteristic of several full-scale operations [29]. According to the nine equations listed in the table, the calculated value of the exponent b for the nine shredders would be positive, and with two exceptions would approach unity. This fact justifies the conclusion that in the operations referred to in the table, the net power requirements were in direct proportion to flow rate. One of the exceptions from the trend towards unity was the rise in the value of coefficient b regarding the Ames secondary shredder. An explanation for the rise may be the extremely worn condition of the hammers noted at the time of the observations. The second exception (Great Falls) differed from the first in that the value of coefficient b dropped sharply. No reason is conjectured for the decline, although it was noticed that the power drawn by the machine was almost independent of feed rate.

The relations indicated by the sign of the exponent c in the equations in Table 4 are somewhat incongruous with the data reported in the literature. If the sign of exponent c is positive in the equations, the indication is that energy requirements drop as the moisture content is increased. Conversely, a negative sign is indicative of an increase in power requirement with decrease in moisture content. The incongruity is in the fact that the exponent is negative in four of the equations. More research will have to be conducted before the incongruity can be explained.

Hammer Wear

An important feature of municipal solid waste seldom addressed in tables on the composition of refuse is its extreme abrasiveness. The abrasiveness stems from the cellulosic constituents in the refuse. The severity of the abrasiveness is attested by the fact that after a throughput of only 1000 to 3000 Mg, hammers are typically worn to an unusable condition even when tipped with the hardest of feasibly applied alloys. (A throughput of 1000 to 3000 Mg represents little more than two or three days throughput in the average processing installation.) According to the data in Table 5, the erosion rates may be as little as 0.013 or as much as 0.106 kg/Mg of refuse processed. It should be noted that the attrition because of abrasion should not be lumped with mechanical and structural failures that may result from an overload in the form of a bulky item or an over-sized piece of tramp metal. Such overloads can be avoided by good management practice. Unfortunately, attrition by erosion is unavoidable because abrasiveness is a wellnigh universal characteristic of refuse. Consequently, the economics of shredding is greatly affected by the attrition factor.

Normally, the hammers and the grate bars in a horizontal hammermill and the hammers and the lining in the neck of a vertical hammermill receive more wear-and-tear than do the other machine parts. The reason for the disproportionate share of wear and tear is obvious: The area between the hammers

TABLE 4. RANGE OF COEFFICIENT VALUES SHOWING EFFECT OF FLOW RATE AND MOISTURE CONTENT IN FULL-SCALE OPERATIONS [29]

Shredder	Correlation coefficient	Number of data points	Equation
Appleton east	0.85	11	$P_n = 6.33\ \dot{m}^{0.94}\ (1-MC)^{1.54}$
Ames primary	0.74	10	$P_n = 0.62\ \dot{m}^{1.20}\ (1-MC)^{-7.04}$
Ames secondary	0.93	10	$P_n = 0.28\ \dot{m}^{1.92}\ (1-MC)^{-2.84}$
Cockeysville No. 1, forward rotation	0.92	6	$P_n = 47.04\ \dot{m}^{0.82}\ (1-MC)^{4.79}$
Cockeysville No. 1, reverse rotation	0.96	6	$P_n = 6.04\ \dot{m}^{1.18}\ (1-MC)^{2.01}$
Cockeysville No. 1, combined rotation	0.91	12	$P_n = 21.85\ \dot{m}^{0.90}\ (1-MC)^{2.25}$
Great Falls	0.28	12	$P_n = 39.97\ \dot{m}^{0.27}\ (1-MC)^{-0.63}$
Tinton Falls	0.85	12	$P_n = 4.05\ \dot{m}^{0.94}\ (1-MC)^{1.66}$
Odessa, forward rotation	0.91	12	$P_n = 0.14\ \dot{m}^{0.84}\ (1-MC)^{-12.64}$

EPA Form 2350-4 (4-80)
(PREVIOUSLY CIN EPA FORM 287)
TYPING GUIDE SHEET

TABLE 5. OBSERVED RATES OF HAMMER WEAR IN REFUSE SHREDDING

Shredder location and hammer alloy	Hardness (R_c)	Average weight loss (ω_i) (kg/hammer Mg)	Wear of full hammer complement (W_o) (kg/Mg)	Reference
Appleton, WI				
East Mill				A
Stoody 2134	48	9.44×10^{-4}	0.023	
West Mill				A
McKay 48	38	4.84×10^{-4}	0.023	
McKay TiC	45	3.30×10^{-4}	0.016	
Stoody 2134	48	3.60×10^{-4}	0.017	
Amsco Super 20	56	2.73×10^{-4}	0.013	
Ames, Iowa				A
Manganese steel	14	5.50×10^{-4}	0.026	
Cockeysville, MD				A
Shredder 1				
Mangjet	21	2.88×10^{-3}	0.069	
Abrasoweld	36	1.87×10^{-3}	0.045	
McKay 55	49	0.89×10^{-3}	0.021	
Faceweld 12	57	1.57×10^{-3}	0.038	
Shredder 2				
Manganese steel	14	4.40×10^{-3}	0.106	
Great Falls, MT				A
1060 Steel	11	3.33×10^{-3}	0.086	
Stoody 2134	41	1.52×10^{-3}	0.040	
Amsco Super 20	51	1.48×10^{-3}	0.039	
Odessa, TX				A
Modifid Hatfielde manganese steel	33	2.15×10^{-3}	0.030	
Tinton Falls, NJ				A
Nickel-manganese steel	43	4.5×10^{-4}	0.027	

Table 5. (Continued)

Shredder location and hammer alloy	Hardness (R_c)	Average weight loss (ω_i) (kg/hammer Mg)	Wear of full hammer complement (W_o) (kg/Mg)	Reference
Madison, WI (Tollemache) Amsco Super 20	56	1.6×10^{-3}	0.054	B,C
Pompano Beach, FL Amsco Super 20	50	1.8×10^{-3}	0.047	C
Kent, England (Gondard Mill)	NA*	5.2×10^{-4}	0.025	D
Johnson City, TN	NA	7.4×10^{-4}	0.032	E

*NA = Not Available

A. Savage and Shiflett, "Processing Equipment for Resource Recovery Systems: III - Field Test Evaluation of Shredders," EPA Report No. 600/2-80-007c, July 1980.

B. Reinhardt and Ham, "Final Report on a Demonstration Project at Madison, Wisconsin to Investigate Milling of Solid Wastes Between 1966 and 1972," Volume 1, EPA Grant No. 3-G06-EC-00000-0051, March 1973.

C. Reinhardt and Ham, "First Interim Report on a Continuation of a Project on Milling Refuse for Landfill Without Daily Cover at Madison, Wisconsin," U.S. EPA.

D. Holmes, "A Shredding Station in Great Britain," Waste Age, 8(10), 1977.

E. U.S. EPA, "Composting at Johnson City," Final Report on Joint U.S. EPA-TVA Composting Project, 1967 to 1971, Volumes I and II, SW-31r.2, 1975.

EPA Form 2350-4 (4-80)
(PREVIOUSLY CIN. EPA FORM 257)
TYPING GUIDE SHEET

and the grate bars (or liners) constitute the working face of the shredder, and is the area where most of the refuse size reduction occurs.

Although several factors have a bearing on attrition, only few have been adequately defined in terms of design, operation, and maintenance parameters. Type of material being processed is one of the few. On the basis of hammer weight loss per unit weight of refuse shredded, wear on hammers apparently is intensified if the refuse has a large percentage of paper. Wear becomes less intensive if the moisture content is in the upper range. If the degree of size reduction (defined as one minus the ratio of product to feed size) is small, wear is less intensive. Another factor is rotor speed. Wear is less intensive at lower speeds. Thus, Trezek and Savage observed a 31 percent decline in material lost from hard-tipped hammers and 43 percent drop with bare hammers when the rpm of the rotor was reduced from 1200 rpm to 790 rpm [18,36,38].

Experience indicates that the hardness of the metals of which the hammers are fabricated, or if they are tipped, of the alloy used for tipping them, surpasses the other factors in the determination of rate of hammer wear [18,29,35]. In Table 6 are listed and identified groups of alloys available for hardfacing. Factors to take into account when deciding which of the five groups is best suited for hardfacing are cost, ease of application, compatibility with the base hammer material, and abrasion and impact resistance. Unfortunately, costs rise in proportion to the hardness of alloy. The useful "life-span" of a hammer tipped with a subgroup 2c alloy (hardness, 33 to 40 R_C) is on the order of 30 percent to 57 percent longer than that of an untipped hammer (at 790 rpm) [18,35]. Hammer wear can be reduced significantly through the use of alloys having a hardness that exceeds 40 R_C [29]. A limiting factor with respect to hardness is the tendency of the welds to chip under high impact loadings. The influence of

TABLE 6. PRINCIPAL GROUPS OF HARDFACING ALLOYS

Group	Description*
1	2 to 12 percent alloy content (soft and ductile)
2	12 to 25 percent alloy content (Cr and Mo are major alloying elements)
3	25 to 50 percent alloy content (Cr is the major alloying element)
4	Co and Ni-based alloys
5	Carbide-based alloys (extremely hard and brittle deposits)

* The facings increase in hardness in the order listed. Thus, group 1 is ductile, whereas group 5 is extremely hard and brittle.

alloy hardness and that of degree of size reduction (feed size-product size)/(feed size) on hammer wear are shown by the curves in Figure 11. For example, the figure indicates that if the degree of size reduction is 0.8, the hammer wear rates will be approximately 0.05 and 0.02 kg/Mg respectively at alloy hardnesses of 28 and 56 R_c.

Apparently wear is most severe if the hammers are fabricated of manganese or of carbon steel (hardness 14 R_c or less) and are not hardfaced [29,34]. For example, in one operation Savage and his colleagues observed that with the hardness at 11 R_c, the hammer wear in the form of weight loss was 3.33×10^{-3} kg/hammer-Mg of refuse processed. With the hardness at 51 R_c, the loss was 1.48×10^{-3} kg/hammer-Mg [29]. Judging from experience and the curves in Figure 12, the optimum range for hardness is between 48 and 56 R_c. The selection of the facing most suitable to a specific shredding operation would have to be based upon experimentation. This could be done by testing a group of hardfacing alloys, the collective hardness of which would span the optimum range. Ideally, all alloys to be tried should be tested simultaneously.

Operational Problems

A survey of sixteen facilities wherein size reduction of refuse is practiced indicated that in general, refuse shredder operators were satisfied with the operation and performance of their machines. When requested to report specific problems encountered in the operation of their shredders, 44 percent of those queried reported no problems. The two most prevalent problem areas mentioned by the respondents were the shredding of "special" waste components (30 percent of the respondents) and problems related to wear of the shredding elements in the machine (13 percent). Examples of the "special" waste components are tires, "white goods," wire, and rug rolls.

MILL HOLDUP

The determination of the effect of machine characteristics upon net power requirements (P_n) and throughput ($\dot{m}$) can be facilitated through the application of the measurement for machine "holdup" [38,39]. "Holdup" (H) refers to the amount of material within the shredder at a given instant in time. Power requirement increases and product size becomes smaller with increase in amount of holdup. A typical relation between net power requirement and size of holdup is plotted in Figure 13. Experimental and field-scale data available at the time of this writing can be made to fit the following two curves:

$$P_n = aH^b \tag{28}$$

$$\dot{m} = cH^d \tag{29}$$

where a, b, c, and d are numerical constants.

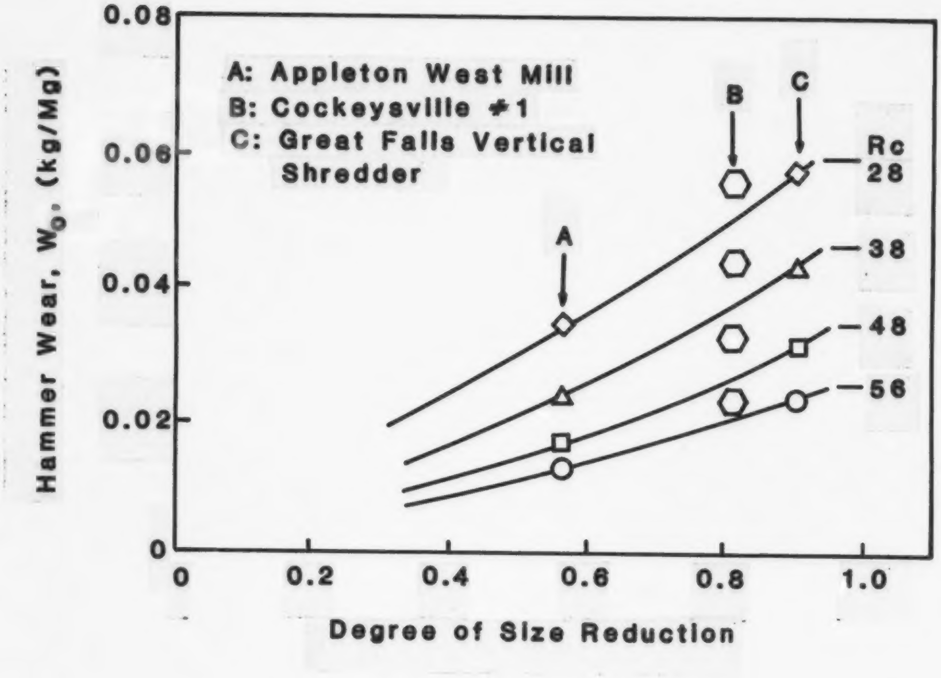

Figure 11. Hammer wear associated with MSW size reduction as a function of alloy hardness and degree of size reduction.

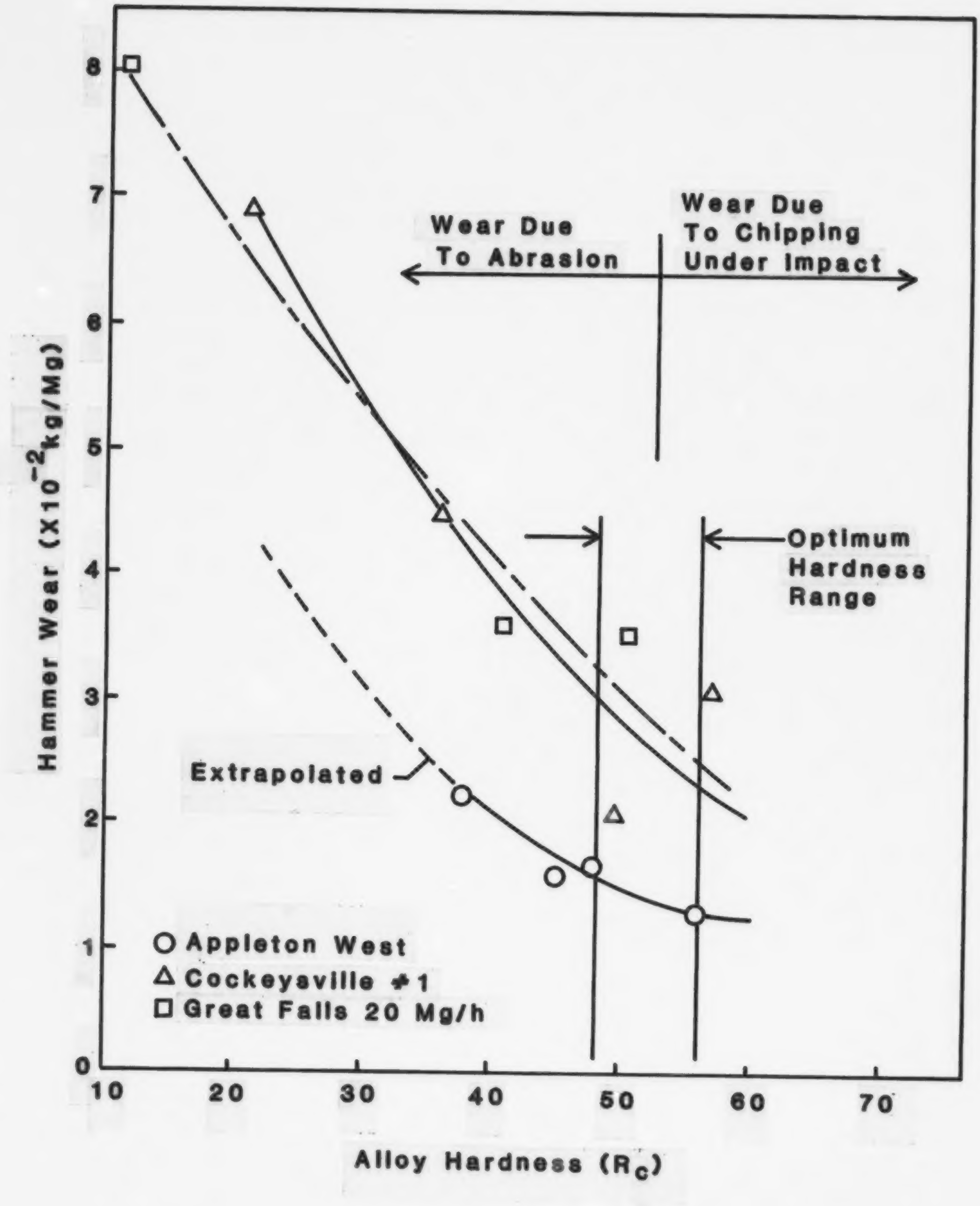

Figure 12. Hammer wear associated with MSW size reduction as a function of alloy hardness.

BEGIN FIRST LINE OF TEXT HERE
CENTER OF PAGE
TOP OF IMAGE AREA
DROPPED HEAD; BEGIN SECTIONS HERE

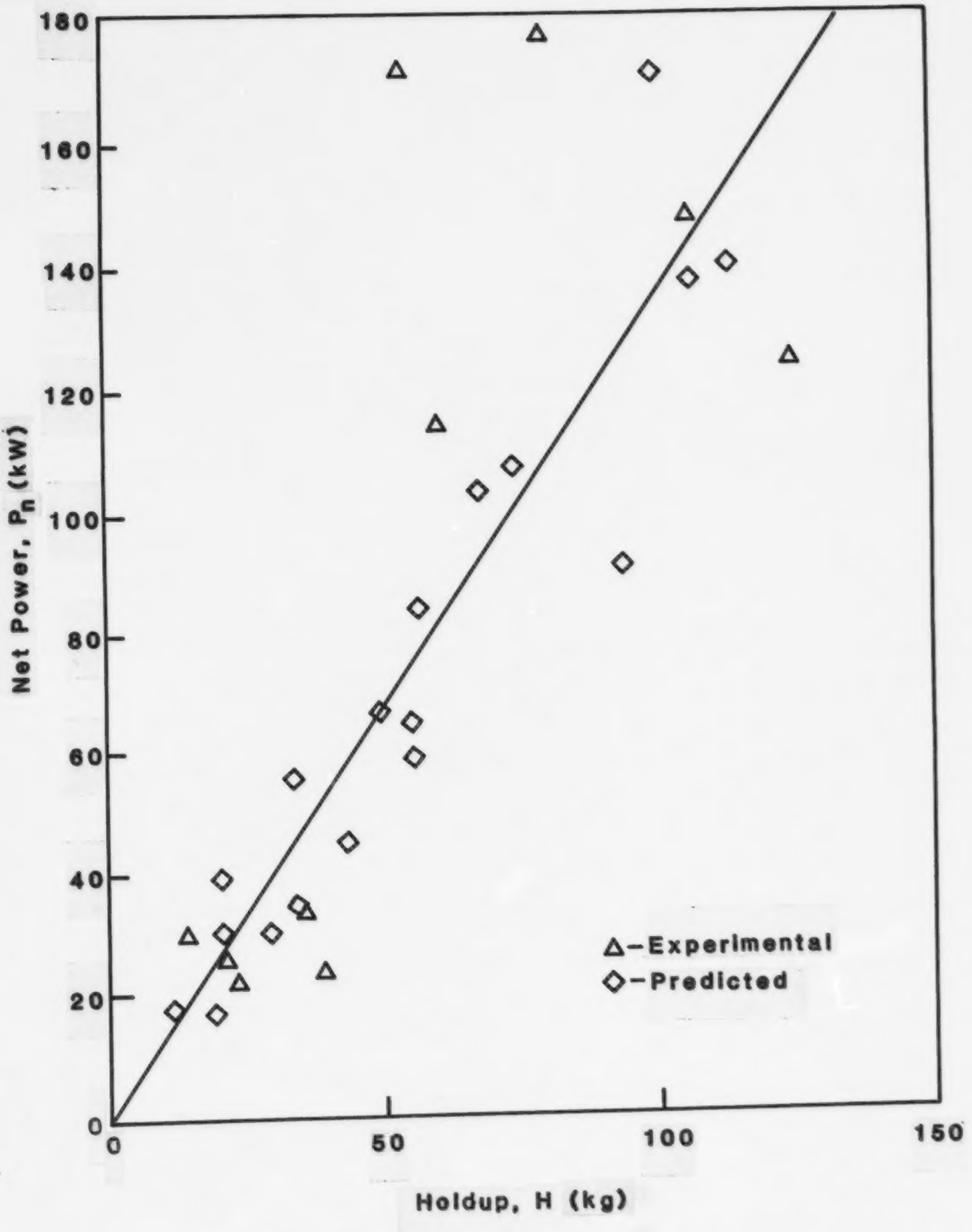

Figure 13. Relation of holdup to power requirement.

BEGIN LAST LINE OF TEXT
3/8"
PAGE NUMBER

EPA Form 2350-4 (4-80)
(PREVIOUSLY CIN. EPA FORM 287)
TYPING GUIDE SHEET

THE MOTOR AND SHREDDER AS A SYSTEM

Shredder Motors

Because the motor used to drive the shredder is a key element of a refuse size reduction system, the selection of a motor and the integration of the motor and shredder are major considerations in the design of an efficient and reliable size reduction process. Longevity of a motor depends in large part upon proper loading. Therefore, in the selection of a motor, care should be taken to decide upon one capable of effectively accommodating the anticipated load cycle (i.e., the time-dependent torque), and thereby avoid the possibility of placing excessive strain on the motor. An adequate estimate of the anticipated loads is a key consideration, since the purchase of an over-designed motor would be an unnecessary additional capital expense. The estimate must take into account the type of solid waste to be processed, variations in throughput, and the required particle size distribution of the shredded product.

Motors used on solid waste size reduction equipment usually are of the squirrel cage or wound rotor type. The wound rotor motor differs from the squirrel cage motor in that the rotor resistance of the wound rotor motor can be changed during operation by automatic control of an external variable resistance, whereas the rotor resistance of a squirrel cage motor is fixed. In general, for motors rated in excess of 400 kW, direct coupling is employed between the motor shaft and shredder rotor. Shaft speeds for shredder motors rated higher than 400 kW are in the range of 600 to 900 rpm. For motors having ratings lower than 400 kW, the rpm range normally is 1200 to 1800 rpm. Within specific ranges, the higher rpm units tend to be less expensive than the lower rpm models.

With respect to the selection of a motor for refuse size reduction, the primary consideration is to remain within the thermal limits of the motor components. The thermal loads generated within the motor are a consequence of the load torque, and result from the dissipation of power through the resistive elements of the motor. Large, transient torques in particular are conducive to the generation of heat. In a wound rotor motor, the heat is effectively dissipated through an external resistance, whereas in a squirrel cage motor, the heat must be dissipated through the motor itself. The primary modes of heat transfer in a squirrel cage motor are conduction and convection. Their rates of heat transfer govern the capability of the motor to cope with the magnitude and rapidity of transient torques that require a capacity in excess of the motor rating.

With regard to squirrel cage motors, manufacturers recommend that the external torque should never exceed 150 percent of the rated torque of the motor, where rated torque is defined as the full load power rating divided by the motor rpm at full load. The 150 percent torque level is the limit of the capability of the motor to adequately dissipate the heat buildup that takes place during operation.

Due to the rapidly fluctuating loads characteristic of refuse size reduction, it might be appropriate to substitute some other motor sizing criterion or criteria for the specification of a 150 percent of rated motor torque as being the upper limit for torque delivered by the motor. The reason is that the root mean square (RMS) value of the motor torque could be considerably greater than the continuous torque rating of the motor, despite the fact that no motor torque peak exceeds 150 percent of the rated torque. If the RMS exceeds the continuous torque rating of the motor (rated motor torque multiplied by the nameplate service factor), thermal failure of the motor is likely to follow. From the preceding rationale it becomes apparent that an appropriate design criterion for a refuse shredder motor would be the following: The RMS value of the motor torque does not exceed the continuous torque rating of the motor. The thermal fatigue caused by fluctuating loads in excess of the design rating of the motor can cause the failure of the rotor in a squirrel cage motor.

It often is preferable to have a motor capable of a high starting torque when equipment having a high inertial load must be started. This is true with some size reduction equipment. A high starting torque capability (approximately 200 percent of rated torque) is characteristic of wound rotor motors. For any desired starting torque, a squirrel cage motor can be found that would meet that specification. To impart a high starting torque capability to a squirrel cage motor, a large rotor resistance is required. Squirrel cage motors that have a high starting torque characteristic also normally have a high "slip." "Slip" is defined as the percentage difference between the synchronous speed and the actual running speed of the motor at 100 percent load. A slip in excess of five percent is referred to as a "high slip."

High slip motors must be capable of dissipating the large amount of heat that is built up in the rotor. Consequently, such motors are designed to have a relatively large heat sink (i.e., a large motor frame) -- an added cost to that of the motor.

The breakdown torque of wound rotor and of squirrel cage motors are typically in the range of 200 to 250 percent of rated torque, where rated torque (T_r) is defined by the relation,

$$T_r = (\text{Constant})(\text{Full Load Power Rating})/(\text{Full Load RPM})$$

For purposes of design, maximum torque levels normally are near 150 percent of rated torque.

The relation between the location of the breakdown torque value and motor rpm and rotor resistance is illustrated in Figure 14. The breakdown torque in a wound motor can occur at a very low rotational speed, because the motor circuitry can automatically increase the rotor resistance. Consequently, a wound rotor motor can withstand a start-up under high load (torque) conditions (e.g., a shredder in a jammed condition) because the maximum torque will be available. Start-up under a jammed condition is not possible with a Class A or B squirrel cage motor, because NEMA Class A and B squirrel cage motors normally approach breakdown torque when the rotational speed reaches approximately 85 percent of the synchronous value, i.e., 15 percent slip. To provide a capability for start-up under a jammed condition

BEGIN FIRST LINE OF TEXT HERE
CENTER OF PAGE
TOP OF IMAGE AREA
DROPPED HEAD, BEGIN SECTIONS HERE

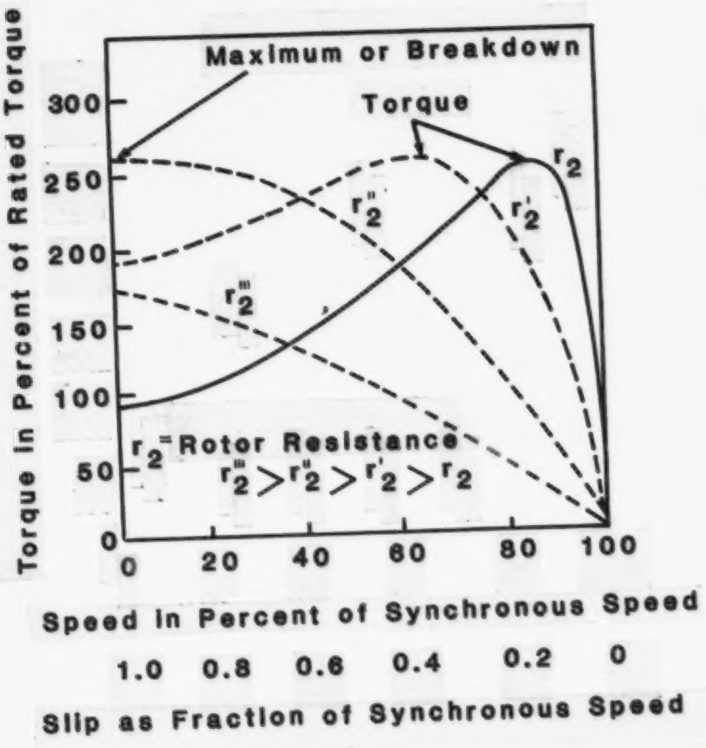

Figure 14. Torque-slip diagram for polyphase induction motor.

BEGIN LAST LINE OF TEXT
3/8"
BOTTOM OF IMAGE AREA; OUTSIDE DIMENSION FOR TABLES AND ILLUSTRATIONS

PAGE NUMBER
EPA Form 2350-4 (4-80)
(PREVIOUSLY CIN EPA FORM 257)
TYPING GUIDE SHEET

with a squirrel cage motor, a high start-up torque characteristic must be specified, e.g. a NEMA Class D or E design.

The derivation of a time-dependent load (torque) cycle for rotating equipment in most instances is not an easy task; and with respect to size reduction, it becomes even more difficult. The reason for the difficulty rests in the fact that the measurement of shaft torque is virtually impossible in a production situation because of the sophisticated procedures that must be used to make the measurement. Consequently, the load torque must be determined through the use of an indirect method. For example, one can be made through the use of measured power levels and of motor design specifications.

The integration of a motor and shredder to achieve a given degree of size reduction under an anticipated range of operating conditions involves a great number of considerations. Among them are: 1) a decision as to whether or not start-ups under jammed conditions would be made; 2) the establishment of an adequate safety factor, such that the motor will not be loaded beyond its capacity; 3) an assessment of local utility restrictions for the installation and operation of a large prime mover; 4) determination as to the degree of sophistication of motor control circuitry required or desired; 5) determination of the anticipated load cycle for the motor; and 6) establishment of the relative contributions of motor torque and inertial torque in meeting the applied loading.

Generally the selection of a type and size of motor involves a communication with the local utility representative and with the shredder manufacturer. Shredder manufacturers specify the motors for their size reduction equipment according to the requirements of the customer. For special cases, as for example where the optimum design for the shredder electro-mechanical system is being sought, the system designer would do well to consult the local utility, the shredder manufacturers, and the electric motor vendors concerning their opinions regarding types of equipment.

To determine a load cycle for a shredder, the delivered torque must be derived as a function of time. The delivered torque is comprised of the motor torque and the torque delivered by the system inertia. The motor and inertial torques are the system response to changes in rotational speed brought about by the application of an external load. In size reduction, the loads are transmitted through the shredding elements to the rotating shaft. The relation for the load torque can be represented as follows,

$$T_L = T_m + T_I \tag{30}$$

where T_L = load torque; T_m = torque delivered by the motor; and T_I = torque delivered by the system inertia. The load cycle placed on a shredder during the size reduction of refuse can be estimated through the use of: 1) a curve representing the power drawn by the shredder motor (P_{in}) as a function of time; 2) curves representing motor performance (e.g., torque and efficiency versus rotational speed); and 3) the application of a knowledge of the system inertia (i.e., shredder and motor rotor inertias). The power drawn (P_{in}) by the shredder can be determined through the instrumentation of the shredder motor such that an active (real) power measurement can be made, and the power levels can be recorded on a strip chart recorder over an appropriate time interval.

The torque delivered by the motor during size reduction (T_m) must in most circumstances be calculated from input power measurements on the motor and from motor performance data. The reason for a calculation instead of a direct measurement is that the latter would be so difficult as to be impractical. The principle upon which the indirect method (i.e., calculation) is based is as follows: When the angular velocity of the motor and shredder rotors are decelerated because of an applied load, energy stored in the flywheel and other rotating mass is delivered to the system. This inertial torque is applied to meet a part of the load torque requirements. The torque delivered by the system inertia (T_I) is given by the relation,

$$T_I = -IC_2 \frac{d\omega}{dt} \qquad (31)$$

where T_I = the torque delivered by the system inertia; I = system mass moment of inertia; $d\omega/dt$ = the rate of change of angular velocity; and C_2 = a constant of proportionality depending upon the units of I, ω, and t. The presence of a negative sign in Equation 31 is an indication that deceleration of the mass is accompanied by delivery of torque to the system, i.e., the system undergoes a negative acceleration. Since the mass moment of inertia of a shredder rotor typically is much larger than that of the motor rotor, T_I can be calculated with sufficient accuracy by considering only the change in speed of the shredder rotor and the flywheel, i.e., if the system includes a flywheel.

Mass Moment of Inertia

The occurrence of transient loads within the shredder and motor system, due (for instance) to poor feedrate regulation or difficult-to-shred materials, are inevitable in refuse processing. Consequently, the design of refuse shredders employs the use of rotor inertia to store rotational energy for the purpose of responding to such loads. Since the energy stored in a rotating mass is proportional to the product of its mass moment of inertia and the square of its angular frequency, energy would be added to the system if its angular frequency were suddenly decreased. Such a case exists if a difficult-to-shred item, such as a water heater, enters a shredder and causes a momentary reduction in rotor speed while the system responds to the sudden change in the load. Equilibrium is restored to the system as it regains speed after the difficult-to-shred item has been size reduced, i.e., the transient load has been removed.

While published data are lacking for the selection of the required mass moments of inertia for refuse size reduction, a review of manufacturer's equipment specifications shows a range of 30 to 100 kg-m^2 per Mg/h for primary shredders handling typical MSW and 150 to 200 kg-m^2 per Mg/h for shredders that are designed to handle oversize, bulky waste. The breadth of each of the above ranges is most likely a consequence of a number of job specific considerations, including the manufacturer's estimate of the amount of energy storage required for the application, the standard driven speed of the manufacturer's shredder, and the type of motor selected for use.

For a detailed discussion of the shredder mass moment of inertia, please see Appendix E.

Motor Torque, Inertial Torque, and Load Torque

It is possible to determine the torque delivered by the motor, T, through the use of: 1) data on power levels measured during shredder operation, P_{in}; 2) data supplied by motor manufacturers regarding motor operation and performance; and 3) the following equations: (The equations are subsequently used for the purpose of system evaluation and design.)

$$T_m = C_1 P_m / \omega \tag{32}$$

where C_1 is a constant of proportionality depending upon the units in which P_m and ω are expressed. Inasmuch as the electro-mechanical power of a system, P_{em}, may be represented in terms of P_m and the freewheeling power, P_{fw}, the governing equation may be expressed as

$$P_{em} = P_m + P_{fw} \tag{33}$$

and solved for P_m,

$$P_m = P_{em} - P_{fw} \tag{34}$$

In order to complete the evaluation of P_m, it is necessary to calculate P_{em} and P_{fw}. The electro-mechanical power may be derived from fundamental motor theory. The governing relation for a 3-phase system is:

$$P_{em} = (P_{in} - I_m (P_f)_{nl} V \sqrt{3})(1 - s) \tag{35}$$

where P_{in} = real power input into the motor; I_m = exciting current; $(P_f)_{nl}$ = power factor under no-load conditions; V = line-to-line voltage; and s = slip expressed as a fraction. (The complete derivation of Equation 35 is presented in Appendix D.) The variables P_{in}, I_m, and P_f are known variables in that P_{in} and V are measured directly, and I_{im} and P_f are data obtained from the manufacturer.

By definition,

$$\begin{aligned} s &= \frac{\omega^* - \omega}{\omega} \\ &= 1 - \frac{\omega}{\omega^*} \end{aligned} \tag{36}$$

where ω = angular velocity under a given load; and ω^* = synchronous angular velocity, i.e., angular velocity under zero external torque. Through the substitution of the expression for s given in Equation 36 into Equation 35, the expression for P_{em} becomes

$$P_{em} = (P_{in} - I_m(P_f)_{nl}V\sqrt{3})(\omega/\omega^*) \qquad (37)$$

Substitution of the expression for P_{em} given in Equation 37 yields,

$$P_m = (P_{in} - I_m(P_f)_{nl}V\sqrt{3})(\omega/\omega^*) - P_{fw} \qquad (38)$$

Equation 38 specifies motor power in terms of the unknown variables ω and P_{fw}.

The determination of P_m follows from the use of Equation 38 and the fact that P_m equals zero and $\omega = \omega^*$ when the system is not burdened with an external load, i.e., the system is in a no-load condition. Hence,

$$P_m = 0 = [(P_{in})_{nl} - I_m\,(P_f)_{nl}V\sqrt{3}]\,(1) - P_{fw}$$

where $(P_{in})_{nl}$ = input power measured when the system is operating under a no-load (nl) condition.

Consequently,

$$P_{fw} = (P_{in})_{nl} - I_m(P_f)_{nl}V\sqrt{3} \qquad (39)$$

Having derived an expression for P_{fw} in terms of the measured variables (P_{in} and V) and of the characteristics of the motor I_m and $(P_f)_{nl}$, the expression for P_{fw} may be substituted into Equation 38 to obtain the following expression for P_m in terms of one unknown variable (ω):

$$P_m = (P_{in} - I_m(P_f)_{nl}V\sqrt{3})(\frac{\omega}{\omega^*}) - (P_{in})_{nl} + I_m(P_f)_{nl}V\sqrt{3} \qquad (40)$$

It is necessary to develop a relation for ω in terms of measured or known quantities, in order to complete the expression for P_m (Equation 40) in terms of measured or known variables. This step yields two equations in two unknowns, i.e., P_m and ω. Such a relation for ω may be developed to an accuracy within ten percent if the following two assumptions are made: 1) The motor torque is linear with ω and within the range of zero to 150 percent of rated torque of the motor, thus limiting ω to greater than or equal to approximately 0.95 ω^* for Class A, B, and C motors. 2) The freewheeling power of the motor averages less than 5 percent of P_{em}. This is true if the load on the motor is greater than 20 percent of the rated torque of the motor.

With the use of the preceding two assumptions, it becomes possible to represent the angular velocity by the linear relation,

$$\omega = \omega^* - K\,\frac{P_{em}}{P_r} \qquad (41)$$

where P_r = rated power of the motor, and K = constant of proportionality. Equation 41 may be solved for P_{em},

$$P_{em} = (\omega^* - \omega)\ P_r/K \tag{42}$$

and through the use of Equation 33, it is possible to derive the second relation for P_m, namely,

$$P_m = (\omega^* - \omega)\ P_r/K - P_{fw} \tag{43}$$

Using Equation 39, P_{fw} may be eliminated from Equation 43, and thus

$$P_m = (\omega^* - \omega)\ P_r/K - (P_{in})_{nl} + I_m(P_f)_{nl} V \sqrt{3} \tag{44}$$

A simultaneous solution of the two equations for P_m in terms of the unknown ω (Equations 40 and 44) yields:

$$\frac{\omega}{\omega^*} = \frac{\omega^* P_r}{K\ (P_{in} - I_m(P_f)_{nl} V \sqrt{3}) + \omega^* P_r} \tag{45}$$

and

$$P_m = [P_{in} - I_m(P_f)_{nl} V \sqrt{3}]\ \ K\ (P_{in} - I_m(P_f)_{nl} V \sqrt{3}) + \omega^* P_r$$

$$- (P_{in})_{nl} + I_m(P_f)_{nl} V\ \sqrt{3} \tag{46}$$

Through the substitution of the expression for ω (Equation 45) and of the expression for P_m (Equation 46), it now becomes possible to calculate the motor torque, T_m, by way of Equation 32.

On the basis of the preceding analysis, the inertial torque (T_I) may now be calculated from measured data and known information through the use of Equation 45 and the definition of inertial torque (Equation 31). The derivation is as follows,

$$T_I = -Ic_2 \frac{d\omega}{dt} \tag*{(Equation 31)}$$

$$= -Ic_2 \frac{\Delta\omega}{\Delta t} \tag{47}$$

The change in ω, $\Delta\omega$, during a time interval, Δt, may be calculated by way of Equation 45 and index notation, i.e.,

$$\Delta\omega = \omega_j - \omega_{j-1} \tag{48}$$

and

$$\Delta t = t_j - t_{j-1} \tag{49}$$

Consequently,

$$\frac{\Delta\omega}{\Delta t} = \frac{\omega_j - \omega_{j-1}}{t_j - t_{j-1}} \tag{50}$$

and therefore,

$$(T_I)_j = -Ic_2 \left(\frac{\omega_j - \omega_{j-1}}{t_j - t_{j-1}}\right) \tag{51}$$

Having derived expressions for T_m and T_I, the load torque (T_L) may be expressed in terms of measured data and known information. For a given power level (e.g., a particular power level recorded at time j during recording of input power to the shredder motor), the load torque at time j may be represented by Equation 30 if it is re-written in index notation, i.e.,

$$(T_L)_j = (T_m)_j - (T_I)_j \tag{52}$$

where $(T_m)_j = C_i(P_m)_j/\omega j$.

Equation 52 is amenable equally to algebraic and to computerized solution. Data needed for solutions are measured input power levels to the system, specified motor data, and the system mass moment of inertia.

System Analysis and Design

The utility of the analytical methods discussed and described in the preceding sections is well illustrated by three examples based in large part upon field test data reported in references 18 and 29. The first example is the development of a diagram of load (torque) as a function of time. Evaluation of a particular design and the design of shredding equipment are illustrated by the second and third examples.

Example 1--

A diagram of load (torque) as a function of time is shown in Figure 15. In the development of the diagram use was made of data obtained by measuring the actual power input of the 187 kW motor of a hammermill located at the University of California waste processing facility and of motor data supplied by the manufacturer of the unit. The power measurements are shown in Figure 16 and were made while refuse was being processed at 4.5 Mg/h. The characteristic size of the shredded product was approximately 1 cm. A second curve in Figure 15 shows the torque delivered by the motor together with that contributed by the inertia of the system (i.e., the difference between the load torque and the torque delivered by the motor). The relation of the two curves to each other in Figure 15 illustrates the effectiveness of system inertia (energy stored in the rotating mass of the system) in reducing the peak loads on the motor.

The establishment of a load torque curve based upon the size reduction of refuse under a given set of operating conditions makes it possible to

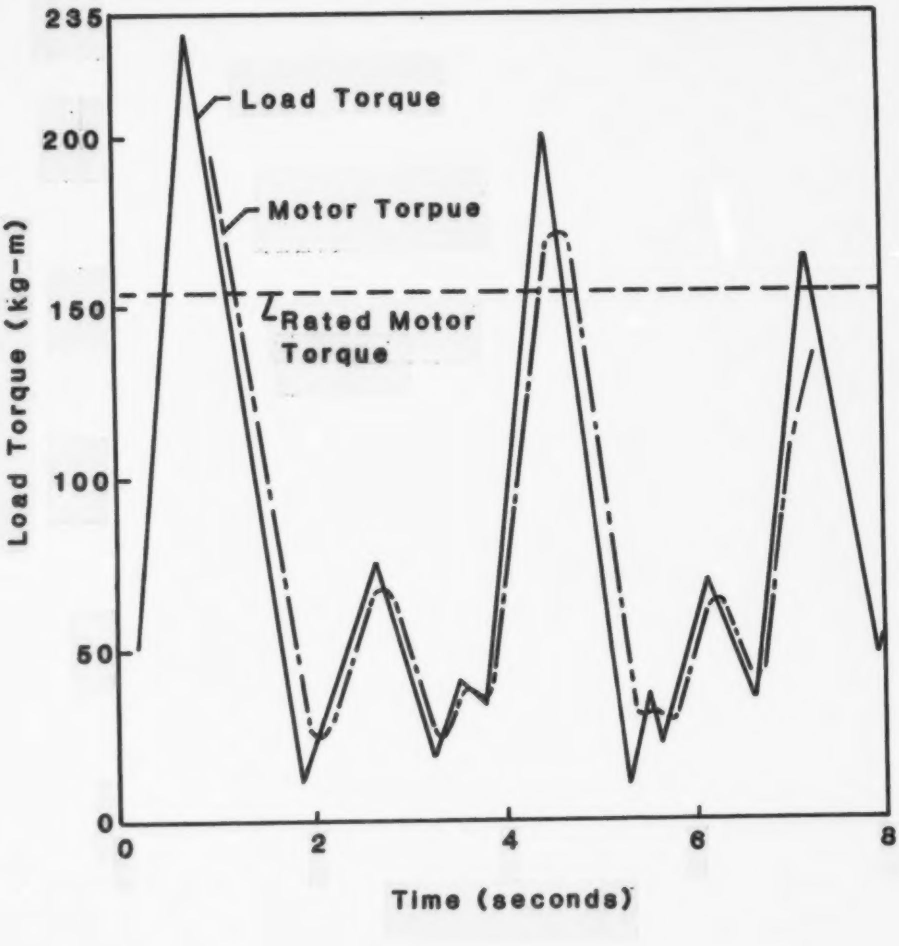

Figure 15. Load diagram developed from shredder power measurements and motor performance data.

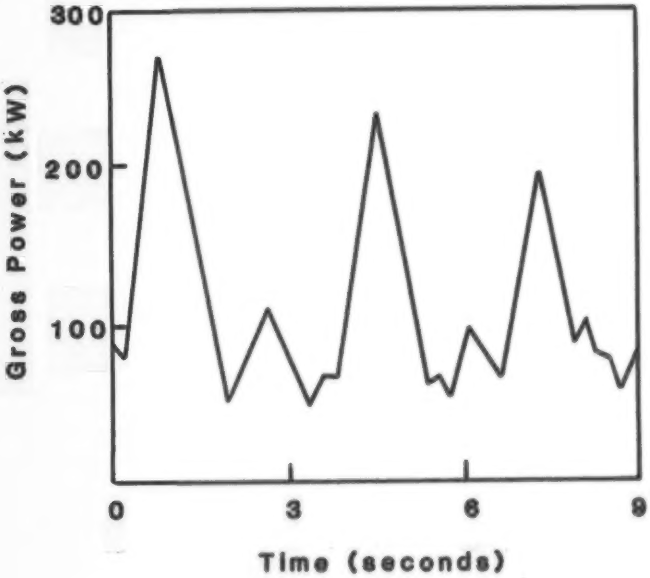

Figure 16. Power recording for a refuse shredder located at the University of California.

evaluate a particular system design or to utilize the load torque information in the design of refuse shredding equipment. The evaluation and design are illustrated by the second and third examples.

Example 2--

The second example deals with the determination of the optimum value of shredder mass moment of inertia as based upon the load cycle shown in Figure 16. In making the determination, it is stipulated that the torque delivered by the motor is not to exceed 150 percent of rated motor torque, and the motor is to have a full load power rating of 150 kW, and a slip of 1.7 percent at full load. In the determination, various levels of mass moment of inertias are selected for trial calculations. The mass moment of inertia would consist of a fixed contribution from the rotating elements in the shredder and incremental contributions supplied by an external flywheel.

The load torque and the motor torque for each mass moment of inertia are calculated according to procedure described in the preceding paragraphs. The performance of the system with respect to the applied load at four different levels of system inertia is shown in Figures 17a through 17d. Given the design criterion of maintaining the motor torque below 150 percent of rated torque, it is apparent from the figures that the mass moment of inertia should be on the order of 190 kg-m^2.

Example 3--

Again, using the procedure described, curves for load torque and motor torque were derived for a vertical ring shredder operated at the Manmouth County Reclamation Center in Tinton Falls, New Jersey. The curves are shown in Figure 18, and represent the load cycle placed upon the motor and shredder system when the shredder is processing approximately 70 Mg/h. Data used in the calculations of load and motor torques were field measurements [29] of input power to the motor, motor specifications, and the value of the system mass moment of inertia (6340 kg-m^2).

The large inertia of the Tinton Falls shredder (6340 kg-m^2) resulted in a minimal fluctuation in the motor torque despite wide fluctuations in the load torque shown in Figure 18. According to the figure, the motor torque varied between approximately 15 and 35 percent of rated motor torque; whereas the load torque fluctuated between 5 and 60 percent. The expense of the relative smoothness of the motor torque cycle is in the system start up. In order to bring the shredder up to speed, a 75 kW starter motor is used at the Tinton Falls facility.

Tradeoffs encountered in the integration of an electric motor and a shredder are illustrated by the following: During operation of the vertical ring shredder, the machine's large moment of inertia is conducive to a relatively uniform motor torque. Consequently, the thermal loads generated within the motor are relatively constant -- a situation that is conducive to reliable motor operation. However, the smoothness of the motor torque curve is accomplished at the expense of the utilization of a 75 kW starter motor to initially accelerate the large inertia without imposing an excessive current draw during startup.

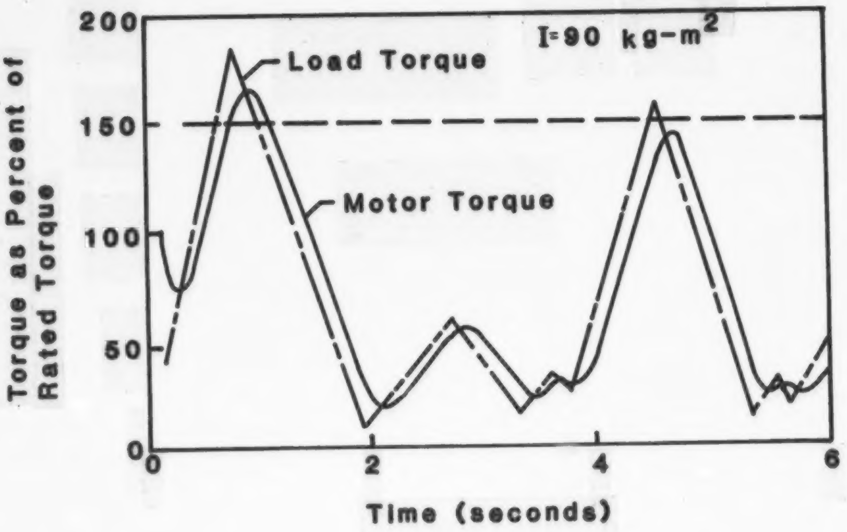

Figure 17a. Load torque and motor torque for a 150 kW shredder motor with slip = 1.7% and I = 90 kg-m^2.

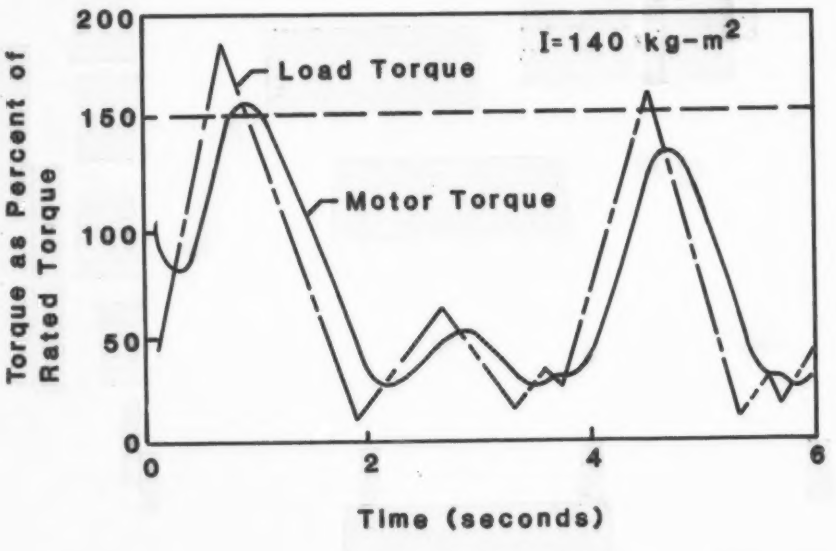

Figure 17b. Load torque and motor torque for a 150 kW shredder motor with slip = 1.7% and I = 140 kg-m^2.

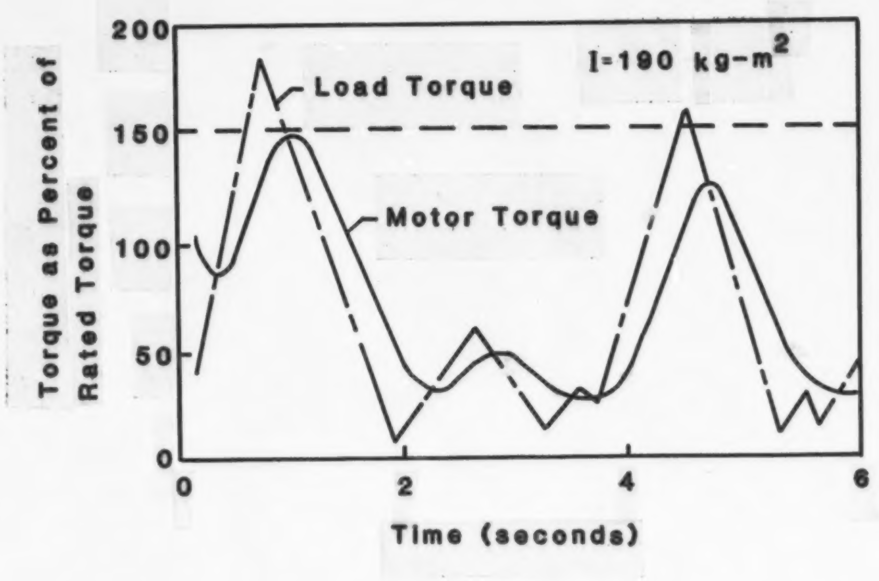

Figure 17c. Load torque and motor torque for a 150 kW shredder with slip = 1.7% and I = 190 kg-m^2.

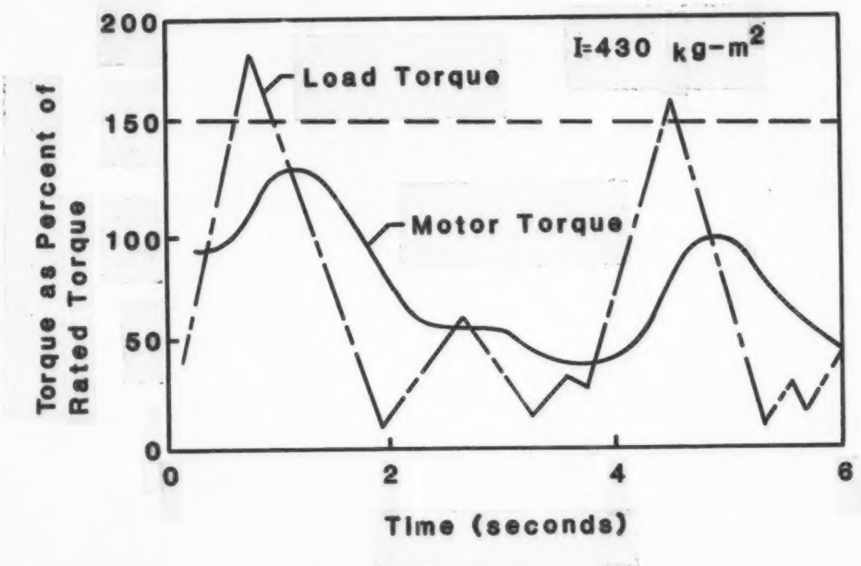

Figure 17d. Load torque and motor torque for a 150 kW shredder motor with slip = 1.7% and I = 430 kg-m^2.

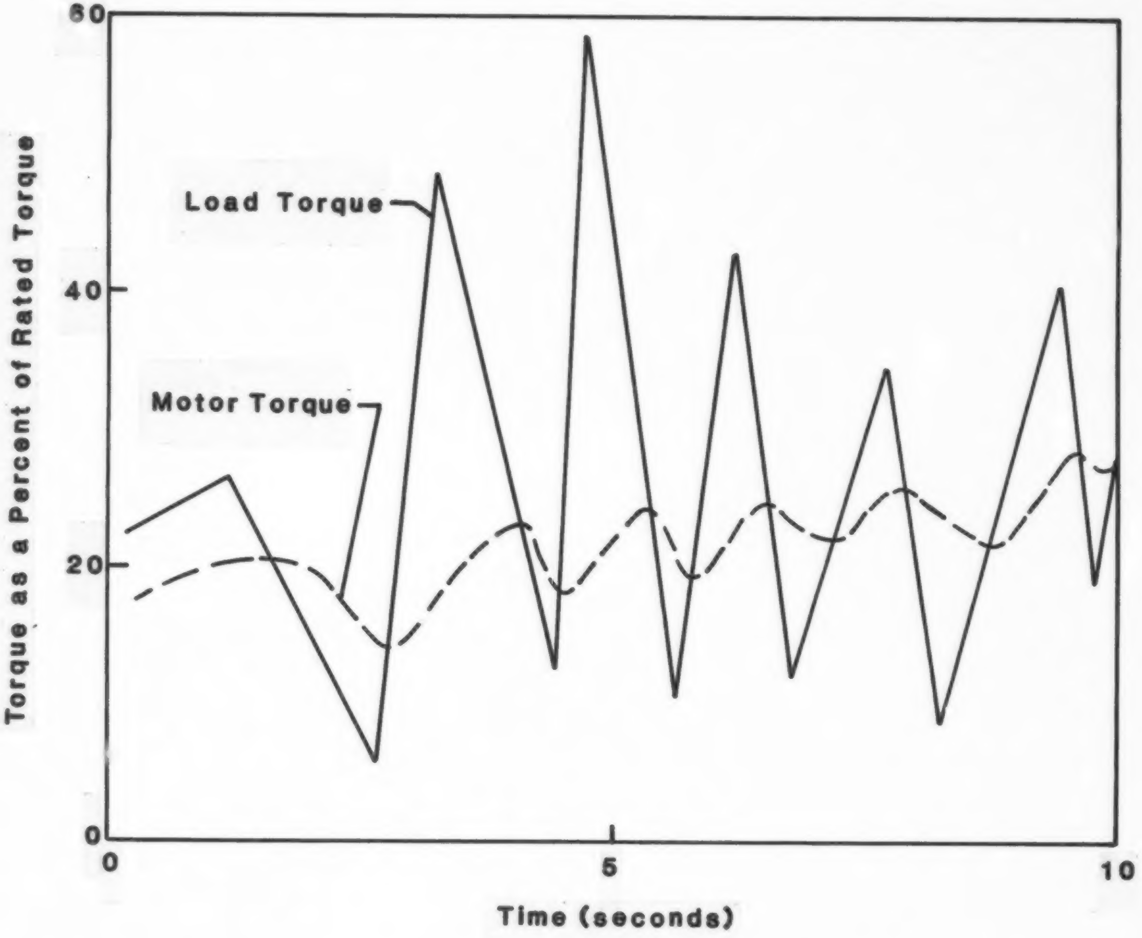

Figure 18. Motor torque and load torque for the Tinton Falls vertical ring shredder.

SECTION 5

MAINTENANCE CONSIDERATIONS

Maintenance is one of the major elements of cost in size reduction systems, and maintenance cost is largely a function of the amount of labor involved. Labor is required for changing and replacing worn hammers and other internal elements (e.g., breaker bars, grate bars), retipping worn machine elements, cleaning out the shredder when it is jammed with refuse, carrying out routine preventative maintenance (e.g., greasing bearings, checking oil levels), and performing cleanup of fugitive dust and particulate matter disposed and deposited around the shredder.

The type of labor category utilized for shredder maintenance and degree of maintenance labor performed are highly site-specific. For example, in certain plants, certified contract welders are hired to retip hammers; and in other plants, in-house labor may be employed. A third approach is not to retip the hammers, and instead to use them until they are worn-out, and then simply to scrap them. In the third approach, relatively unskilled labor suffices since it is only a matter of changing hammers.

Certain items of shredder maintenance are generic to heavy duty electromechanical equipment. Such items should be made a part of a regular and documented schedule. They include cleaning the motor control equipment, cleaning and greasing the drive and the motor, lubricating the bearings, and servicing the hydraulic and pneumatic equipment.

An important feature of shredder maintenance should be the provision of an adequate inventory of replacement parts; and where retipping is practiced, a stock of welding wire or electrode. The parts inventory can be very small (e.g., a set of spare hammers) or very extensive (e.g., spare hammer pins, wear liners, stocking of a spare shaft bearing).

The relation between the actual capacity of a primary shredder and manhours required to change hammers or grates is shown by the two curves plotted in Figure 19. According to the curves, the time required for hammer and grate changes is approximately proportional to shredder capacity. The longer time required for grate and hammer changes in the larger shredders is due mainly to the greater mass of steel that must be moved. The figure also indicates the existence of significant fluctuations in time requirements for hammer and for grate changes, probably due to differences among maintenance procedures followed at each plant.

Information given by the curves in Figure 19 is valuable in the establishment of a reasonable goal for plant maintenance personnel with respect

BEGIN FIRST LINE OF TEXT HERE
CENTER OF PAGE
TOP OF IMAGE AREA
DROPPED

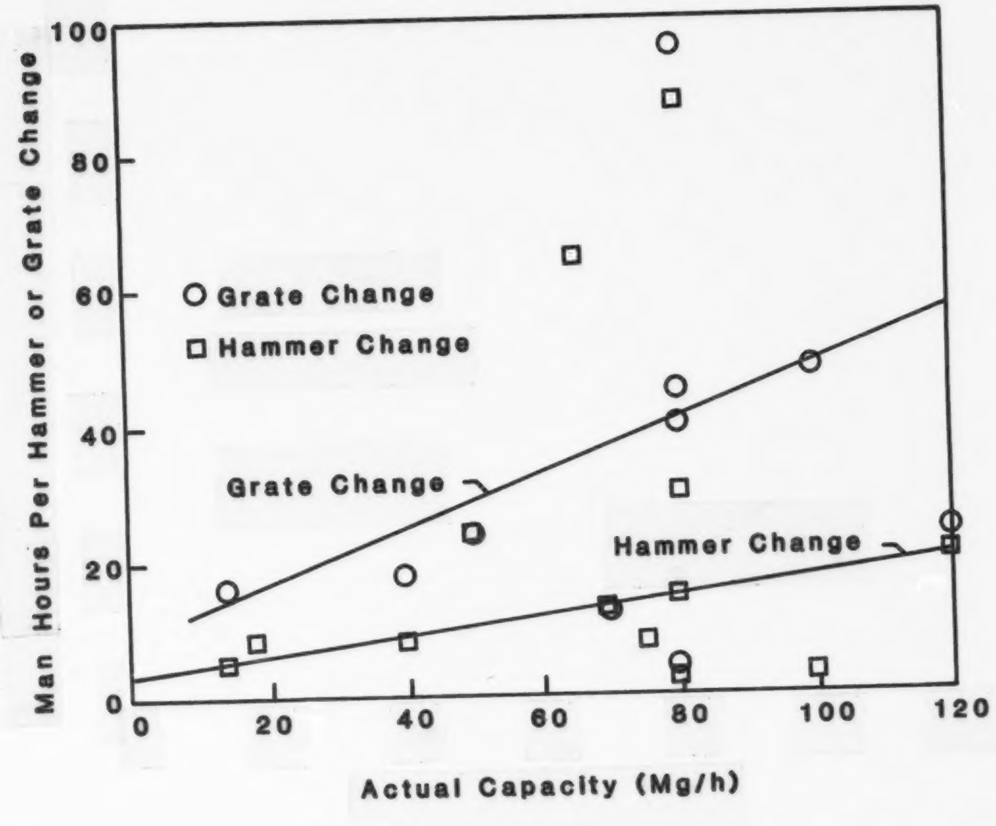

Figure 19. Time requirements for hammer and grate change in primary shredders as a function of throughput capacities.

BEGIN LAST LINE OF TEXT
3/8"
BOTTOM OF IMAGE AREA OUTSIDE DIMENSION FOR TABLES AND ILLUSTRATIONS

PAGE NUMBER
EPA Form 2350-4 (4-80)
(PREVIOUSLY CIN. EPA FORM 257)
TYPING GUIDE SHEET

to the time to be spent in changing hammers and grates. Although the general maintenance categories apply to most refuse shredding facilities, the amount of time spent on maintenance varies significantly from plant to plant. A key factor in determining time requirements for maintenance is the existence or non-existence of an adequate dust collection system in the vicinity of the shredder, and of well designed interfaces between the shredder and the feed and discharge conveyors. The absence of an adequate dust collection system or of well-designed shredder and conveyor interfaces typically results in emissions of fugitive particulate matter and spillage of material from the size reduction system. Because of these two undesirable developments, a significant amount of time must be spent housekeeping around the equipment. More than one plant manager has commented that for each hour of refuse processing, an hour of housekeeping is required.

The type of laborer involved in the maintenance of a shredder ranges from the unskilled worker required for housekeeping chores to the skilled technicians employed in the overhauling of bearings and the retipping of hammers. In some instances, the labor force may extend from correctional facility labor to certified journeyman welders.

Access to a manual in which are described in detail types of maintenance needed, maintenance intervals, types of personnel and equipment required, and step-by-step procedures and methods would facilitate the performance of the necessary shredder maintenance. The manual preferably should be supplied by the purveyor of the shredder. In some plants, considerable time was spent accomplishing the first hammer or grate bar change. The additional time was due to the fact that a maintenance manual was not supplied by the manufacturer. On the other hand, a well-trained crew provided with the proper equipment can make a hammer change ten times faster than can an untrained and poorly supervised crew burdened with an inadequate supply of tools and equipment.

SECTION 6

HEALTH AND SAFETY

A number of related health and safety issues must be given due consideration in the design and operation of a refuse size reduction system. Most, if not all, of the safety issues are a consequence of the brute force approach to size reduction and of the magnitude of the forces that are generated. One of the more noticeable characteristics of shredders and of other types of similar heavy-duty rotating equipment is the generation of extreme levels of noise and vibration. Another characteristic is the inherent risk of worker injury if work safety features are not incorporated into the equipment design. As with any system in which rotating equipment is a part, shredder designs incorporate the standard industrial safeguards required for the minimization of the risk of injury to operating and maintenance personnel. Among such safeguards are enclosures (or guards) around rotating components (e.g., belt drives, coupling connections, flywheels, shafts) and electrical lock-out systems. Attention is also called to three other hazards to health and safety that may be encountered in the size reduction of refuse. They are: 1) dust particle generation, 2) shredder explosions, and 3) discharge of projectiles.

NOISE

The nature of size reduction makes noise generation almost inevitable. Usually, in a resource recovery system the size reduction equipment is the major offender in terms of noise generation. Noise levels that have been measured around shredding equipment are summarized in Table 7. As the table indicates, the levels are in the range of 86 to 105 dBA. Not surprisingly, noise levels rise as the metal content of the waste is increased, i.e., providing all other conditions remain the same. It is not uncommon for the noise level around refuse shredding equipment to be above the level permitted at specific periods of exposure. (The OSHA standard is 90 dBA for an eight-hour exposure.) However, in response to the high noise levels and the danger of explosions, workers seldomly are stationed around operating shredders over long periods of time.

NUISANCE DUST

As is apparent from the data listed in Table 8, shredders can, in some cases, produce a significant amount of nuisance dust. The degree of dust generation is highly site-specific. For example, the shredder at the University of California Richmond Field Station is characterized by a dust generation 40 to 100 times greater than that from the commercial shredders listed in Table 8. It should be pointed out that the University shredder is

TABLE 7. NOISE LEVELS AROUND SIZE REDUCTION EQUIPMENT

Site	dBA	Reference
U.C. Richmond Field Station	94 - 105	A
Plant A	88 - 98	B
Plant B	86 - 95	C
Plant C	96 - 98	D
Plant E	86 - 90	E
Plant F	90 - 95	F

References

A. Diaz, L.F., *et al*, Health Aspect Considerations Associated with Resource Recovery. Compost Science, Summer 1976.

B. Midwest Research Institute. Industrial Hygiene Characterization of Resource Recovery Systems. Draft Survey Report - Plant A. NIOSH Contract No. 210-0013, June 1980.

C. Midwest Research Institute. Industrial Hygiene Characterization of Resource Recovery Systems. Draft Survey Report - Plant B. NIOSH Contract No. 210-0013, June 1981.

D. Midwest Research Institute. Industrial Hygiene Characterization of Resource Recovery Systems. Draft Survey Report - Plant C. NIOSH Contract No. 210-0013, February 1981.

E. Midwest Research Institute. Industrial Hygiene Characterization of Resource Recovery Systems. Draft Survey Report - Plant E. NIOSH Contract No. 210-79-0013, April 1981.

F. Midwest Research Institute. Industrial Hygiene Characterization of Resource Recovery Systems. Draft Survey Report - Plant F. NIOSH Contract No. 210-79-0013, June 1981.

TABLE 8. TOTAL AND RESPIRABLE DUST LEVELS REPORTED AROUND REFUSE SIZE REDUCTION EQUIPMENT*

Shredder location	Total dust (mg/m^3)	Respirable dust (mg/m^3)	Reference
U.C. Richmond Field Station, CA	118 - 202	ND	A
Outagamie County, WI	2.2 - 5.5	ND	B
Baltimore County, MD	0.5 - 5.5	ND	B
Plant A			
Primary Shredder	2.7 - 3.4	0.35	C
Secondary Shredder	16.4 - 27.1	0.41	
Plant C	0.7 - 1.9	0.2	D
Plant F	1.8	ND	E

* Recommended (ACGIH/NIOSH) 8-hour exposure level for total nuisance dust = 10 mg/m^3, for respirable dust = 5 mg/m^3.

ND = no data reported.

References

A. Diaz, L.F., et al. Health Aspect Consideration Associated with Resource Recovery. Compost Science, Summer 1976.

B. Simister, B.W., and Bendersky, D. Processing Equipment for Resource Recovery Systems. Volume II, EPA-600/2-80-007b, July 1980.

C. Midwest Research Institute. Industrial Hygiene Characterization of Resource Recovery Systems. Draft Survey Report - Plant A. NIOSH Contract No. 210-79-0013, June 1980.

D. Midwest Research Institute. Industrial Hygiene Characterization of Resource Recovery Systems. Draft Survey Report - Plant C. NIOSH Contract No. 210-79-0013, February 1981.

E. Midwest Research Institute. Industrial Hygiene Characterization of Resource Recovery Systems. Draft Survey Report - Plant F. NIOSH Contract No. 210-79-0013, June 1981.

operated solely for research, produces a product that is much finer (particle size) than that by commercial shredders, and lacks the dust control features generally found in commercial shredders.

Factors that influence the extent of dust generation are composition and moisture content of the feedstock, size distribution of the shredded product, and obviously, methods employed for dust control. The influence of fineness of the shredded product is indicated by the difference between the primary shredder and the secondary shredder in Plant A in terms of dust generation (see Table 8). The measured dust levels at the secondary shredder (fine product) were approximately 4 to 10 times those at the primary shredder (coarse product). In general, if the feedstock contains significant amounts of paper and materials made of powdery substances (e.g., gypsum board) and has a low moisture content, the generation of dust will be increased. Finally, the few data in Table 8 provide some basis to the generalization that the dust levels generated in the size reduction of refuse seem to be within the limits recommended by ACGIH and NIOSH.

Dust emission from size reduction equipment can be controlled through the application of one or more of several methods. Among the methods are moistening the wastes before or during size reduction, and the use of a pneumatic dust collection system. The wastes can be moistened by sprinkling or by injecting water into the mass.

Dust can constitute a hazard not only to health, but also to the efficient operation and maintenance of the equipment and the equipment control apparatus. For example, if the dust should settle in the control apparatus and in the shredder motor, overheating could result from dirty contacts and circuitry. Furthermore, additional manpower would be required to remove the dust -- thus significantly increasing the operational costs of the facility.

EXPLOSIONS

The coming of resource recovery operations having processing capacities on the order of 1000 Mg/day has been accompanied by a surge in the incidence of shredder explosions sufficiently large as to constitute a significant health and safety issue. Thus, during the period 1971 through 1975, approximately 100 shredder explosions were reported, of which 69 resulted in significant damage [41,42]. During the same period, an incidence of two to five explosions per 100,000 Mg of refuse shredded apparently was a typical operating experience. Such an incidence resolves into one explosion per one to two months in a plant that processes 1000 Mg/day.

Because of the magnitude of the explosive energy released, of the vulnerability of adjacent equipment, and of the inevitable blast wave propagation, injury to personnel and damage to structures cannot be warded off simply by designing the shredder to have a heavier construction. To avoid damage to the shredder and its ancillary equipment, with most shredder explosions, it is necessary to vent the resulting gases immediately upon the initiation of the explosion and if no provision has been made for extinguishing the flame front.

The most common cause of explosions in refuse size reduction is the ignition of a flammable vapor by one or another means. Sparks generated by metal-to-metal contact within the zone of size reduction seems to be the most common means of ignition. The term "lower flammable limit" (LFL) has been given to the minimum concentration of flammable vapor at which an explosion can be initiated, given a source of ignition.

Data on the sources of ignition and on the materials that can develop into an explosive charge are few in number. The scarcity of data stems mostly from the practical impossibility of visually identifying an explosive material as it enters the shredder and the destruction of the evidence in the subsequent explosion. The problem of identification is complicated by the time increment between an explosive material entering the shredder and its eventual ignition. The increment may be on the order of tens of seconds. The consequence is an extreme paucity of detail in most reports of shredder explosions.

Measures to control deflagrations constitute the usual approach to the minimization of the incidence of explosions and of the accompanying losses. "Deflagrations" are explosions in which the flame propagates subsonically through the combustible fuel-oxidant mixture. Among the several methods for controlling deflagrations, explosion venting is traditionally the most popular. Venting results in the dissipation of pressure buildup and of explosive energy into the ambient atmosphere. Another method of control in explosion suppression, i.e., the rapid injection of extinguishing agents (such as water, dry chemicals, or halogenated hydrocarbons) to extinguish the expanding flame front. Micro-mist fogging systems [41], which utilize water as the working fluid, and commercially available suppression systems utilizing halogenated hydrocarbon extinguishing agents [42] have been employed in refuse size reduction systems.

Unlike deflagrations, the detonation type of explosion is not subject to the aforementioned methods of control. In a detonation explosion, the flame or reaction front is propagated at supersonic velocities. The extremely rapid release of energy during a detonation makes the use of explosion venting and suppression ineffective as control measures.

Blast-resistant construction for the shredder and building, the use of blast mats to protect areas near the shredder occupied by plant personnel, and isolation of the shredder are useful measures of explosion protection for detonations, as well as for deflagrations. Fortunately, in the case of refuse size reduction, detonations are much less likely occurrences than deflagrations. As one would expect, waste materials subject to detonation include discarded hand grenades, ammunition, blasting caps and dynamite. The single most effective means of preventing the occurrence of detonations most probably is institution of a public awareness campaign to eliminate the discard of detonable materials. Of course, another method is the visual inspection of the waste as it is fed to the shredder.

Among the recent reports on studies on shredder explosions, two by Zalosh and Coll [42,43] especially merit attention. To identify the key factors that affect the severity of shredder explosions and thereby make it possible to identify measures for their control, the two researchers embarked upon an experimental program that involved the use of a mock-up shredder. The design of their experimental shredder simulated a typical horizontal hammermill with respect to rotor configuration and size. Important features of the mock-up were an infeed enclosure at top of the shredder, simulated grate bars, and a discharge enclosure typical of industry practice. In the mock-up, the rotor of the mock-up was operational. However, no refuse was processed during the course of experiments involving explosions. Explosions were set off at several locations in the mock-up shredder and under a range of operating conditions with respect to rpm and number of hammers.

Even though refuse shredding was not a part of their test program, the findings and conclusions made by the two researchers have a definite significance with respect to loss prevention. Thus, they made definitive findings regarding the degree of dilution and mixing of the combustible vapor and the oxidant (i.e., oxygen in the air) within a shredder enclosure at which an explosion becomes imminent. This factor has a fundamental influence on the probability of and the energy release from an ensuing explosion. In tests in which the flammable vapor release in the mock-up shredder was 0.9 kg or less [43], concentrations of the vapor did not exceed the LFL, excepting in the quiescent areas of the shredder, e.g., near the inboard side of the shredder bearings. In these areas the concentration of flammable vapor could exceed the LFL for periods of 6 to 31 seconds.

From the findings made by Zalosh and Coll, one may make the following two conclusions:

1. A sufficiently large air flow within a shredder may reduce the risk of explosion by keeping the concentration of flammable vapors lower than the LFL. Therefore, air-sweeping of the shredder enclosure or the maintenance of a sufficient air flow through the shredder may serve to minimize the risk of explosions. However, the considerations for establishing the design of such an air flow system have not been developed.

2. In horizontal hammermills of present design, concentrations of flammable vapors exceeding the LFL may occur for significant periods of time (i.e., several seconds to half a minute) near the end of the rotor shaft, even when the vapor release is as small as 0.9 kg. From this finding, one may conclude that ignition may occur at some time between the shredding of the flammable container and its discharge. This time interval may render impossible the identification of the source of the explosion. The fact that flammable vapor concentrations may occur within flammable limits in quiescent volumes and over time periods on the order of tens of seconds dictates that all sources of ignition should be kept away from operating shredders, and any ancillary equipment in or around which flammable vapors may accumulate. As for the design of shredders, the shredder designers should consider hardware improvements aimed at eliminating stagnant zones within the shredder and reducing the prevalent ignition sources (hammer heating and impact sparks), or

else include in their designs a provision for gas detection in the stagnant zones.

An important conclusion reached by Zalosh and Coll concerns the design of venting systems and contemporary design criteria. On the basis of the results of the mock-up tests, they suggest that if existing venting design guidelines are used for predicting overpressure from shredder explosions, little of the inlet and discharge areas should be used in the calculations. The reason for the latter is the fact that apparently only the vent area directly above the shredder acts effectively as a source of venting. The reason for its effectiveness presumably is the fact that the force of the explosion follows the path of least resistance; which in the case of the test mock-up and of most shredders in the field, is in the vertically upward direction.

Zalosh and Coll found that the severity of a shredder explosion is a strong function of the level of turbulence existing within the shredder as a consequence of the rotating rotor assembly and hammers. Their report shows that the design guidelines in NFPA [44] provide reasonable estimates of peak explosion pressures when the turbulence levels within the mock-up shredder are characterized as being moderate (16 hammers and 260 to 690 rpm). However, the NFPA guidelines drastically underestimate the peak pressures at high turbulence levels (48 hammer, 700 rpm). High turbulence levels may be more indicative of commercial shredding operations than would be moderate turbulence levels, because commercial hammermill shredders generally have hammer complements of 24 to 48 hammers and operate in the range of 900 to 1200 rpm.

With respect to detailed design guidelines for explosion protection, at the time of this writing two sets of guidelines were in preparation: 1) Guidelines for Explosion Protection prepared by the E-38 Committee (Solid Waste) of the American Society for Testing and Materials and available through the society at its headquarters in Philadelphia, PA; and 2) The Guidelines for Shredder Explosion Venting contained in reference [45].

PROJECTILES

The size reduction of solid waste in most cases is accompanied by the generation of projectiles that fly out of the shredder unless precautionary measures are taken to curtail their discharge. Generally, the projectiles are difficult-to-shred metallic objects, such as reinforcement bars, hardened steel items, and nuts and bolts. Fragments produced during size reduction can be discharged from the shredder by way of the feed or discharge opening as a result of a direct contact with a rotating shredding element (e.g., a hammer) or indirectly after a rebound. Ejections of projectiles from shredders that process waste fractions from which the metal components have been removed (e.g., air classified light fraction) tend to be fewer in number and to have less momentum than do those produced in primary size reduction.

The extent of the generation of projectiles during primary size reduction can be reduced by means of source separation and through the use of restraining systems. In source separation, objects that would disintegrate into high velocity fragments are removed. Examples of restraining systems are chain-link curtains or rubber mats suspended over the shredder infeed opening. In the latter method, propelled fragments are intercepted and their kinetic energy is absorbed as they leave the feed opening.

While from the standpoint of personnel safety, the primary mode of projectile discharge from a shredder is through the feed opening, injury to personnel also may result from fragments propelled through the discharge opening and then rebounding from ancillary equipment (e.g., hopper sides, conveyor belting). In addition to discharge through the feed and discharge openings, fragments can also be discharged from the shredder through holes that may be in the shredder structure (e.g., space between the feed conveyor and the shredder).

Projectiles do not necessarily leave the shredder in a direction perpendicular to the axis of the shredder rotor. Because of the high incidence of multi-rebound possible for the high-energy fragments, it is possible for particles to leave the shredder in a direction parallel to the axis of the shredder rotor -- oftentimes to the surprise of the operating personnel.

SECTION 7

ECONOMICS OF SIZE REDUCTION

COSTS OF SIZE REDUCTION

The costs associated with size reduction can be broken down into the following elements:

1. Capital and installation costs
    a) shredder
    b) motor
2. Operating and maintenance costs
    a) energy
    b) labor
    c) replacement parts (e.g., grate bars, hammers, hardfacing electrode, etc).

Normally, costs other than the two sets of primary capital and installation cost elements named in the outline may or may not be charged to the size reduction system. For example, the costs of laying the foundation for the shredder, of providing motor control and explosion control systems, and in some instances of capital and installation costs for the infeed and discharge conveyors, are allocated to the size reduction system.

A sampling of typical unit costs associated with size reduction is given in Table 9 (capital costs) and in Table 10 (maintenance costs). Although Table 9 shows a wide range, unit capital costs (1981 dollars) for primary and secondary shredders having nominal capacities of 30 to 70 Mg/h average approximately $6,000 to $7,000 per Mg/h. For estimating the unit cost of primary shredding, the average cost range ($6,000 to $7,000 per Mg/h) is suitable in those cases where oversize, bulky waste (OBW) is to be removed from the shredder infeed. For the shredding of OBW, the figure of $8,000 to $9,000 per Mg/h should be used. Unit capital cost (1981 dollars) for motors and cutting elements used in primary and secondary size reduction average respectiveley, $1,500 to 1,600 per Mg/h and approximately $200 per Mg/h, as shown in Table 9. The unit capital costs for ferrous and glass size reduction are also shown in Table 9. The wide range of costs associated with each cost category and type of shredder is primarily a function of the structural strength of each device, which ultimately reflects the ability of the shredder to do an effective job of size reduction and withstand abuse over its design life.

TABLE 9. ESTIMATED CAPITAL COSTS IN 1981 DOLLARS FOR MSW SHREDDERS

Item	Primary	Secondary	Ferrous	Glass
Capacity range (Mg/h)	30 to 70	30 to 60	6 to 20	10
Estimated life (yrs)	10 to 20	10 to 20	10 to 20	5 to 20
Capital cost ($1000)/(Mg/h)				
Shredder				
Range	5.0 to 9.4	3.7 to 13.8	6.1 to 16.5	1.5 to 4.8
Average	6.3	7.0	10.7	3.0
Motor				
Range	0.9 to 2.4	0.7 to 3.6	0.7 to 5.2	0.3 to 0.6
Average	1.5	1.6	3.0	0.4
Cutting Elements (e.g., hammers)				
Range	0.02 to 0.4	0.03 to 0.7	0.03 to 1.5	0.1 to 0.2
Average	0.2	0.2	0.8	0.1

EPA Form 2350-4 (4-80)
(PREVIOUSLY CIN. EPA FORM 287)
TYPING GUIDE SHEET

TABLE 10. BREAKDOWN OF MAINTENANCE COSTS (1981 DOLLARS) FOR MSW SHREDDERS

	Primary shredding		Secondary shredding	
	Range	Average	Range	Average
Maintenance (man-hours/Mg)^{a,b}	0.1 to 37	9	3 to 43	16
Maintenance labor ($/Mg)^{a,b,c}	0.002 to 0.75	0.175	0.075 to 0.858	0.322
Hammer costs ($/(Mg/h))^{a}	0.02 to 0.9	0.3	0.03 to 0.07	0.2
Hardfacing alloy ($/Mg)^{a}	0.1 to 0.3	0.15	I^{d}	I

a) Mg refers to Mg of MSW shredded.
b) Includes hammer changes and retipping.
c) Labor costs = $20/man-hour.
d) I = insufficient data.

EPA Form 2350-4 (4-80)
(PREVIOUSLY CIN. EPA FORM 247)
TYPING GUIDE SHEET

From this sampling it is possible to estimate the cost of a size reduction system. For example, if a primary shredder nominally rated at 60 Mg/h is required, an average capital cost for the motor, shredder, and hammers can be estimated as being $8,000 per Mg/h (1981-cost of a 60 Mg/h primary shredder) x 60 (Mg/h) = $480,000.

In Table 10 are given unit costs for maintenance labor. The dollar values were developed from data collected from operating resource recovery facilities and data reported in reference 29. The primary breakdown is by man-hours. Labor costs are estimated on the basis of an average pay scale of $20 per hour. Direct operating costs are not included. For primary and secondary shredders, the average reported cost (1981) of maintenance labor is within the range of $0.18 to $0.32 per Mg. The reported cost is relatively low when compared to the range of $0.25 to $0.75 per Mg typically quoted by shredder manufacturers for primary and secondary shredders.

Inasmuch as the costs for operating labor (i.e., non-maintenance labor) are seldom broken down separately for the size reduction station in a processing facility, an adequate data base does not exist for estimating operating labor costs. The estimation of operating labor costs would entail proportionally allocating the labor associated with the labor for the overall operation of the processing plant, e.g., loading of refuse into the shredder, plant supervision, and control room operation.

HAMMER MAINTENANCE

Costs associated exclusively with hammer maintenance are significantly affected by operational procedures. This relation is illustrated by the following examples: (Numbers in the examples were derived from actual test data and by observation of practices in the field.) The first example is a procedure in which the hammers are built up (re-surfaced, re-tipped) once during each five days of operation. The procedure in the second example is to re-tip the hammers each day (during the second shift). The third example involves the application of a wear-and-scrap program. In a wear-and-scrap program, the hammers are allowed to wear down to a point at which the incoming refuse can no longer be effectively shredded. A summary of the costs for the three procedures is presented in Table 11. (The table is reproduced from reference 29.)

Certain important factors are neglected when the analysis is restricted to costs alone. The factors are: 1) variations between plants with respect to operational procedures for hammer maintenance; 2) availability of suitable equipment for changing and welding hammers; 3) availability of trained maintenance personnel; and 4) the fact that badly worn hammers, an inevitable occurrence in the wear-and-scrap method, affect particle size, energy requirements, and throughput. It is highly likely that the two means most effective in minimizing costs of hammer maintenance are the proper training of maintenance personnel and the ready availability of suitable maintenance equipment. Regarding the latter area (i.e., availability of equipment), the location of the necessary utilities and welding equipment adjacent to the shredder station is an effective method of minimizing the costs attributed to maintenance downtime.

TABLE 11. TYPICAL COSTS FOR HAMMER MAINTENANCE

Cost Items	Man-hours	$ Per Man-hour	Total $	Tonnage Mg	Unit cost $ per Mg	Annual cost[g] $	Percent of cost
Case I: Buildup once per week							
Labor							
Remove and install	12	7	84	1,800[d]	0.047	4,900	11.0
Welder[a]	40	11	440	1,800[d]	0.244	25,400	61.8
Materials							
Hardfacing[f]			126	1,800[d]	0.070	7,300	17.8
Hammers (2 sets)[b,c]			3,538	104,000[e]	0.034	3,500	8.5
Totals					0.395	41,100	100.0
Case II: Daily buildup							
Labor							
Welder[h]	9	13	117	400	0.292	30,400	73.6
Materials							
Hardfacing[i]			35	400	0.088	9,100	22.0
Hammers (1 set)[c,j]			1,769	104,000	0.017	1,800	4.4
Totals					0.397	41,300	100.0
Case III: Wear and scrap							
Labor							
Remove and install	12	7	84	7,200	0.012	1,200	2.6
Materials							
Hammers (1 set)[k]			3,154	7,200	0.438	45,600	97.4
Salvage credit[l,m]			(235)	7,200	(0.033)	(3,400)	--
Totals					0.417	43,400	100.0

(continued)

EPA Form 2350-4 (4-80)
TYPING GUIDE SHEET

TABLE 11. (continued)

[a] Welder for re-tipping, regular time charge, 40 hours per set of 24 hammers.

[b] 1 set = 24 hammers x 73 kg x $1.80/kg = $3,154; 2 sets needed, one for installation, one for retipping.

[c] Amortized 2 years at 8 percent per annum, capital recovery factor = 0.5608.

[d] Tonnage per hammer change.

[e] Annual tonnage: 50 Mg/d x 8 hr/d x 260 d/yr.

[f] 1800 Mg x 0.020 kg/Mg x $3.50/kg = $126.

[g] Rounded dollars.

[h] Welder for re-tipping, overtime charge, 9 hours to re-tip 24 hammers in place.

[i] 50 Mg/h x 8 h/d x 0.020 kg/Mg x $4.40/kg = $35/d.

[j] 1 set = 24 hammers x 73 kg x $1.80/kg = $3,154; 1 set only, hammers welded in place.

[k] 1 set = 24 hammers x 73 kg x $1.80/kg = $3,154; worn and scrapped.

[l] Scrap value: $150/Mg = $0.15/kg.

[m] Credit = 1,752 kg/set - (7200 Mg x 0.026 kg/Mg)($0.15/kg) = $235 per set.

EPA Form 2350-4 (4-80)
(PREVIOUSLY CIN. EPA FORM 287)
TYPING GUIDE SHEET

COST ESTIMATION

The capital and maintenance costs of size reduction can be estimated with the use of the data presented in Tables 9, 10, and 11 and the application of basic design criteria for the shredding application (i.e., the nominal throughput and the desired particle size). For example, the elements of cost for 60 Mg/h primary shredder designed to produce a nominal particle size of 10 cm would consist of $480,000 for equipment, and an energy and maintenance cost totaling $0.86/Mg, as shown in Table 12.

The cost estimate given in Table 12 allows the sensitivity of the cost elements to be examined. For example, if depreciation and amortization of the capital expenditures are neglected, the unit cost for the shredder, assuming an operation of 8 hours per day and 260 days per year, and a 20-year life, is approximately $0.19 per ton. This cost would be two to fourfold greater if depreciation and amortization of the shredder were included; and potentially 15 to 30 times greater, if the building and ancillary equipment were charged to the size reduction system.

However, on the simple premise of examining the key elements that compose costs directly attributable to the size reduction system, the data in Table 12 indicate that cumulatively the energy and maintenance costs overshadow the capital cost by a factor of four to five when all are expressed on a unit weight basis.

TABLE 12. ESTIMATED COST ELEMENTS FOR A 60 Mg/h PRIMARY SHREDDER DESIGNED TO PRODUCE A NOMINAL PRODUCT SIZE OF 10 cm*

I. Capital

a) Shredder	(\$6,300/(Mg/h)) x (60 Mg/h) =	\$378,000
b) Motor	(\$1,500/(Mg/h)) x (60 Mg/h) =	90,000
c) Hammers	(\$200/(Mg/h) x (60 Mg/h) =	12,000
	Total	\$480,000

II. Energy and Maintenance

a) Energy Costs:

(Assume average gross power requirement (P_G) as calculated in Table 14, P_G = 330 kW)

$$\begin{aligned}\text{1980 Energy Cost} &= (P_G/(\text{throughput}))(\text{energy cost})\\ &= (330\ \text{kW}/(60\ \text{Mg/h}))(\$0.06/\text{kWh})\\ &= \$0.33/\text{Mg}\end{aligned}$$

b) Maintenance Costs:

(Assuming hammer buildup once per week and costs from Table 11 escalated at 10 percent per annum)

1980 Maintenance Cost = \$0.53/Mg

c) Total Estimated Operating and Maintenance

	\$/Mg
Energy	0.33
Maintenance	0.53
Total	0.86

---

* Nominal size is defined as the screen size corresponding to 90 percent cumulative passing.

SECTION 8

SELECTING A SHREDDER

The selection of a shredder for refuse size reduction involves an assessment of a number of criteria of a type applicable in the selection of any piece of electro-mechanical processing equipment. An obvious criterion is the relation of the performance of the equipment to the performance claimed for it by the manufacturer in terms of throughput capacity, energy requirement, maintenance, and product characteristics. A second criterion pertains to the shredded product. This criterion pertains to the extent to which the product produced by the shredder is within the set of specifications determined by the requirements of downstream processing or by use of the product. For example, the product size distribution must be within a specified range. The shredder must not only meet the criterion for product characteristics, it must also be capable of doing so with a reasonable degree of uniformity and continuity over a specified period of time. Meeting this latter criterion implies a high degree of reliability on the part of the machine. Because maintenance is a function of reliability, the shredder should not require maintenance over and above that which is normally expected for a machine of its type, and the maintenance should be of a type that is easily applied. Yet another important criterion is the efficient use of energy. A final criterion relates to economics, namely, the overall cost per unit of mass processed.

TYPE OF MACHINE

The rational selection of a machine is made difficult by the absence of reported definitions of the relations between physical characteristics of a shredder and its performance parameters (e.g., specific energy, hammer wear) with respect to machine design. The lack of definition becomes especially noticeable when one wishes to compare the advantages and disadvantages of horizontal hammermills with those of vertical hammermills. Regardless of other uncertainties, sturdiness of construction should be an important factor in the selection, because municipal refuse is difficult to grind and it exacerbates normal wear-and-tear on the machine.

No specific statements can be made regarding specific design features and power requirements, although some tentative associations are indicated. One such association is that between the lowering of the rpm of the rotor and the drop in power consumption and hammer wear. Unfortunately, the lower rpm would be characterized by a product of coarser size.

In selecting a machine, it should be kept in mind that proper maintenance is materially facilitated through the inclusion of mechanical or hydraulic pin pullers for pin removal and installation in the machine, as well as a hydraulically activated system for opening the shredder and an overhead crane for hammer removal and installation. All working parts should be easily accessible and should be readily replaceable.

VERTICLE-SHAFT VERSUS HORIZONTAL-SHAFT HAMMERMILLS

With respect to design, there is a relative abundance of published data on the performance of horizontal as contrasted to the few on vertical hammermills. A second difference is in the relative ease of modeling and controlling of the operation of the two types of machines. The existence of a regular array of grate openings in the horizontal shredder provides a means of developing analytical relationships between grate opening size, percent open area, throughput, and product size. Grate bars (or a screen) in the bottom of the horizontal shredder provide a convenient means of controlling the size of the shredded product by varying the size and shape of the spacing between the grate bars. (If the bars are replaced by a screen, size of product is determined by the size and shape of the openings in the screen.) With a vertical hammermill, the particle size of the product is controlled either by varying the number, shape, and clearance of the hammers, or by changing the size of the discharge opening, or by relying upon a combination of all four variables. Modeling is made difficult by the non-specific and poorly defined nature of such control measures.

MACHINE COMPONENTS

Motor

The size of the motor needed to power a particular shredder at a specified throughput rate must be based on gross power requirement. The gross power requirement is the sum of the net power required to size-reduce the waste and of the freewheeling or "idling" power. The freewheeling power is the power consumed by the machine when no refuse is being milled. Within the power ranges commonly used in refuse size reduction, freewheeling power accounts for 5 to 10 percent of the total energy consumed.

A determination of the net power required to produce a product of a particular particle size can be made by multiplying the specific energy (E_0) by the anticipated flow rate ($\dot{m}$). The product divided by 0.9 approximates the necessary gross motor power. However, such an estimate would not include the factor of safety in the form of the power needed for transient surges in the throughput to the machine or for the presence of materials that are difficult to size reduce. According to observations made in the course of field testing of refuse shredders in the United States [29], shredder motors typically are operated at 13 to 73 percent of their full-load rating. The average was about 36 percent.

Hammers

Number of hammers per machine; metallic composition of the parent material of the hammer and of its hardfacing (cutting edge); geometry of the individual hammers; placement; and ease of access, removal, and replacement are key points in the selection of hammers.

Due to its toughness and resistance to abrasion, an austenitic manganese steel is a good base hammer material. The steel is particularly suited to resist the combined effects of abrasion resulting from glass, dirt, and paper, and impacts upon concrete and metallic objects in the refuse. If hammers are to be hardfaced, the alloy used for the facing must be compatible with the steel body of the hammer. In Table 6 are listed groups of alloys that can meet this requirement.

OPERATIONAL ALTERNATIVES

Multiple-Stage Size Reduction

A feature characteristic of coarse or primary shredding in most resource recovery facilities is the production of particles having a nominal particle size of about 10 cm. If a particle size smaller than 10 cm is desired, the product is shredded again ("secondary" shredding), and if need be, even a third time (hence, "tertiary" shredding). ("Secondary" and "tertiary" shredding often are collectively termed "fine" grinding.) An example of a need for fine grinding is the production of "fluff" RDF. In such a product, the particle sizes usually are within the range of 90 percent passing 2.5 to 7.5 cm. Another example is the requirement of a small particle size for pelletization of RDF. For efficient and reliable densification, the particle size of feedstock for RDF pelletization usually must be in the range of 1 to 2.5 cm. Other applications in which fine shredding may be involved are the recovery and processing of ferrous, aluminum, and glass scrap to meet user specifications.

Shredding of Homogeneous Feedstocks

As used in this manual, the shredding of homogeneous feedstocks refers to size reduction of the low density, pliable components (e.g., paper, plastics) of MSW in one operation, and of the brittle components (e.g., glass, metal) in another, separate operation. Judging from the general experience, the efficiency of the size reduction process apparently is increased by separating the components and subsequently grinding them. Several factors are responsible for the increase, and they all seem to be based on the fact that the specific energy and the wear-and-tear exerted on the shredder generally are greater in the size reduction of low density, pliable components, than in the size reduction of high density, brittle components.

The separation of the low density, pliable components of refuse from the highly dense, brittle components has an important bearing in fine size reduction. Because separate grinding constitutes a means of reducing the high energy consumption generally characteristic of fine grinding, it would seem that separation of refuse into its two constituent types should precede fine grinding.

Fine Grinding

Conflicting data are reported regarding the relative benefits of the separate and of multiple stage approaches to fine grinding in terms of energy consumption. Thus, Savage and Shiflett [29] report results of research that give reason for concluding that the use of the multi-stage approach to fine size reduction might be the more efficient of the two in terms of energy consumption. In contrast, Shiflett and Trezek report data from other research [39] that would make single stage size reduction the more efficient approach, if the shredder is operated near its maximum capacity. The difference between the two sets of data and the resulting conflicting conclusions most likely are explained by the many unknowns presently characteristic of the principal machine parameters, especially those related to grate spacing, number and shape of hammers, and the internal volume of the shredders. Until these machine parameters and their influence on the mechanisms of size reduction are more fully understood, a definitive answer cannot be given regarding the validity of either of the two conclusions. Certainly, each has some justification. Until the conflict is resolved, the better course to follow probably would be the coarse size reduction of the incoming raw MSW in a single-stage operation. The coarse size reduction would be followed by processing sequences in which high density, brittle materials are separated from low density, pliable materials. A final step would be the secondary shredding of either or both of the segregated streams.

ESTABLISHMENT OF EQUIPMENT SPECIFICATIONS

Despite the fact that shredding has been a basic unit process almost from the inception of large scale resource recovery, it is only recently that attention has been directed to the relation of composition and particle size of the shredded product to energy consumption and machine wear. A result has been the equipping of many recovery facilities with shredders that are either too large or too small. Another common occurrence is the equipping of a shredder with a motor that is incompatible with it. An example of such an incompatibility is the provision of a shredder that has an internal capacity too small to permit the desired degree of size reduction at a given throughput with an oversized motor.

The rational design or selection of a shredder depends upon the specification of three basic criteria, namely: 1) the characteristics of the input material (type and physical properties such as moisture content, bulk density, composition, and particle size distribution); 2) the desired product size distribution; and 3) the mass throughput. Through the application of the three criteria it is possible to assess the magnitude of the operating and performance parameters of the shredder to be designed or selected. Among the operating parameters are rotor rotational velocity, motor power rating, grate spacing or exit clearance, shredder moment of inertia and number of hammers. Energy required per unit weight of material size reduced, hammer wear per weight of material shredded, and magnitude of size reduction are among the performance parameters.

HAMMER TIP VELOCITY

Among the more important performance factors is the angular velocity of the shredder rotor, or expressed more fundamentally, its hammer tip velocity. Examples of hammer tip velocities are those of seven MSW shredders observed by Savage and Shiflett in field tests conducted by the two [29]. They found that the seven machines collectively covered a range of 55 to 70 m/s. However, this range does not include the hammer tip velocities of all machines on the market. Thus, some manufacturers sell machines for shredding MSW that have lower hammer tip velocities. For example, shear type shredders operate at tip speeds in the range of only a few meters per second, and vertical ring shredders operate at a tip velocity of 29 m/s. Finally, investigations have been reported by Savage and Trezek in which MSW was successfully shredded at tip velocities of 26 and 38 m/s with the use of a horizontal swing hammermill [18,37].

There is some evidence for concluding that hammer wear declines with the slowing of hammer tip velocity, especially if the velocities are slower than 40 m/s [18,35]. It should be remembered, however, that the beneficial effect of a slower velocity may be accompanied by an important disadvantage, namely, a lessening of the "flywheel effect," i.e., of the energy storage capacity of the shredder rotor assembly and flywheel. Because of the reduction in energy storage capacity, less energy is available for shredding transient peak loads. Aside from the increase in startup torque, the disadvantage (i.e., loss of flywheel effect) can be lessened to some extent by designing additional inertia into the equipment to compensate for the loss of energy storage that results from a reduction in rotational velocity.

The possibility of reducing hammer wear is not the only advantage of resorting to a lower hammer tip velocity; there is also the important factor of a potential lessening of the danger of an explosion in the shredder. Although no documentation exists to substantiate their belief, several manufacturers hold that the use of a slower tip velocity does reduce the likelihood of an explosion. The rationale underlying the belief that a lower tip speed and fewer explosions go together is the reduction in the generation of sparks because of fewer contacts between the hammers and the metals in the refuse, or because the contact between the two may not be sufficiently forceful to generate a spark. However, the complete explanation involves more than that rationale, because the processes involved in shredding refuse are truly complex.

DESIRED PARTICLE SIZE

Because of the effect exerted by throughput on the size of the shredded product, grate bar spacing serves only as an approximate guide in the determination of the particle size range of the product. A governing relationship between product size, size of grate opening, and throughput that would be universally applicable remains to be developed, although specific governing relationships have been defined for particular shredders [29,38].

Test data [29] regarding the effect of throughput and the relationship between product size and the dimension of grate openings are listed in

Table 13. It is of interest that according to the data, approximately doubling the size of the grate opening (i.e., from 12.7 cm to 24.1 cm) and simultaneously increasing the throughput by 230 percent (i.e., from 22.5 Mg/h to 74.4 Mg/h) did not materially alter the characteristic size of the product (i.e., 3.2 cm vs 3.7 cm).

TABLE 13. AVERAGE PRODUCT SIZE AT VARIOUS GRATE OPENINGS AND REFUSE THROUGHPUTS [29]

Minimum Grate Opening (cm)	Throughput (Mg/h)	Average Product Size Characteristic (cm)	Nominal (cm)
12.7	22.5	3.7	9.8
22.9	16.9	5.0	12.7
20.3	35.6	2.2	6.4
24.1	74.4	3.2	9.2

POWER AND ENERGY REQUIREMENTS

The average net specific energy required to shred raw MSW to a specified particle size can be determined through the application of empirical relationships developed from field test data [29]. The data are observations made in test runs with nine shredders located at seven U.S. resource recovery facilities. Collectively, the capabilities of the nine shredders ranged from 9 to 90 Mg/h. The relationships are:

$$E_o = 17.91\ X_o^{-0.90} \qquad (53)$$

or

$$E_o = 35.55\ X_{90}^{-0.81} \qquad (54)$$

where E_o is the average net specific energy (kWh/Mg) on an as-processed weight basis; X_o is the characteristic product size in cm; and X_{90} is the nominal product size in cm.

The average gross power requirements for size reducing MSW can in turn be estimated with the use of Equations 53 and 54, certain basic identities, and elementary algebra. Gross power (P_g), net power (P_n), and freewheeling power (P_{fw}) can be related through the following equation:

$$P_g = P_n + P_{fw} \qquad (55)$$

where $P_n = E_o\dot{m}$; (56)

E_o is the average net specific energy (kWh/Mg); and $\dot{m}$ is the mass throughput (Mg/h) on an as-processed weight basis.

The freewheeling power, P_{fw}, can be expressed as

$$P_{fw} = \alpha P_g \tag{57}$$

where α is the ratio of P_{fw} to P_g, and generally is within the range of 0.05 to 0.15.

Substitution of Equations 56 and 57 into Equation 55 yields,

$$P_g = E_o\dot{m} + \alpha P_g \tag{58}$$

The gross power required for size reduction can be expressed in terms of net specific energy and mass throughput by rearranging terms as follows:

$$P_g = \frac{E_o\dot{m}}{(1 - \alpha)} \tag{59}$$

Because of an existing empirical relationship between average net specific energy requirement and nominal product size, which is,

$$E_o = 35.55\, X_{90}^{-0.81} \quad \text{(from Equation 54)} \tag{60}$$

Equation 59 can be rewritten as,

$$P_g = \frac{35.55\, X_{90}^{-0.81}\, \dot{m}}{(1 - \alpha)} \tag{61}$$

or P_g can be expressed in terms of the characteristic product size, X_o, with the use of Equation 53,

$$P_g = \frac{17.91\, X_o^{-0.90}\, \dot{m}}{(1 - \alpha)} \tag{62}$$

Estimated gross power requirements for the size reduction of MSW, based upon Equation 61 and a value of 0.10 for α, are shown in Figure 20 as a function of product size and throughput.

Through the application of Equation 53 or 54 it is possible to predict the average net specific energy required to size reduce a given raw MSW to a specified particle size. It is possible to determine the average net power requirement of the shredder's prime mover (e.g., electric motor or diesel

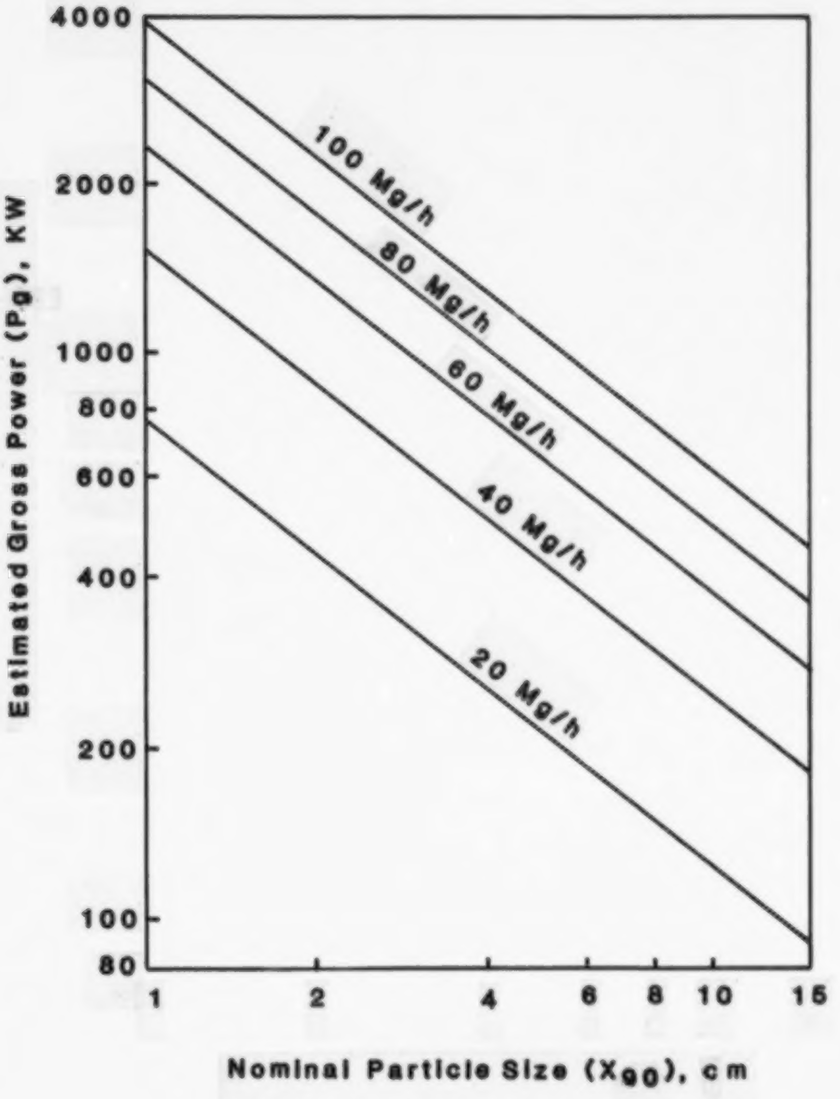

Figure 20. Estimated gross power requirements for size reduction of MSW as a function of throughput and nominal size of product given P_{fw}/P_g = 0.10.

BEGIN FIRST LINE OF TEXT HERE
CENTER OF PAGE
TOP OF IMAGE AREA
DROPPED HEAD: BEGIN SECTIONS HERE
BEGIN LAST LINE OF TEXT
3/8"
PAGE NUMBER
BOTTOM OF IMAGE AREA OUTSIDE DIMENSION FOR TABLES AND ILLUSTRATIONS
EPA Form 2350-4 (4-80)
(PREVIOUSLY CIN. EPA FORM 387)
TYPING GUIDE SHEET

engine) by multiplying the average net specific energy by the throughput. In the latter determination, consideration must be given to the freewheeling power contribution. This is done by adding it to the average net power required as is shown in Equations 55 and 58. According to a report by Savage and Shiflett [29] the freewheeling power requirements of shredders observed by them typically was from 5 to 15 percent of the power rating of the motor. Equation 61 is used to determine the average gross power required to produce a given characteristic particle size and Equation 62 for required gross power and nominal product size.

Lacking a complete engineering analysis of the shredder and motor system for a specific application, for example as described in the section "The Motor and Shredder as a System," a suitable safety factor should be applied to P_g, inasmuch as Equations 61 and 62 are estimations of average rather than of site-specific gross power requirements in size reduction. Composition of the waste and amount of the rotary inertia (Wk^2) are the main points to be considered in arriving at a safety factor. In the absence of evidence to the contrary, a safety factor of 1.2 to 1.7 can be assumed to be a reasonable range. Within this range, the throughput variations almost inevitable in the loading and conveyance of MSW would not excessively tax the capacity of the prime mover, even though this range is only a little more than 50 percent of the 2.8 that Savage and Shiflett report as being average for the shredders observed in their field studies [29]. At this time, it can only be conjectured as to whether the high safety factors reported by them were consequences of deliberate over-design or of an inadequate throughput. Not to be overlooked in the conjecturing is the fact that the 1.2 to 1.7 range pertains to the primary shredding of typical MSW. It does not allow for the shredding of heavier or bulkier wastes, as for example, automobiles, refrigerators, and water heaters.

By defining the safety factor as η, Equations 61 and 62 can be rewritten to express the average design power requirement, P_d,

$$P_d = \eta P_g \qquad (63)$$

or

$$P_d = \frac{\eta 17.9\, X_o^{-0.90}\, \dot{m}}{(1 - \alpha)} \qquad (64)$$

and

$$P_d = \frac{\eta 35.55\, X_{90}^{-0.81}\, \dot{m}}{(1 - \alpha)} \qquad (65)$$

If the range is 1.2 to 1.7, Equation 64 for P_d can be recast as

$$21.49\, \frac{X_o^{-0.90}\, \dot{m}}{(1 - \alpha)} \leq P_d \leq 30.45\, \frac{X_o^{-0.90}\, \dot{m}}{(1 - \alpha)} \qquad (66)$$

and Equation 65 as

$$42.66 \frac{X_{90}^{-0.81} \dot{m}}{(1 - \alpha)} \leq P_d \leq 60.44 \frac{X_{90}^{-0.81} \dot{m}}{(1 - \alpha)} \qquad (67)$$

If an average value of α is chosen as 0.10, Equation 66 can be further simplified to

$$23.88\ X_o^{-0.90}\ \dot{m} \leq P_d \leq 33.83\ X_o^{-0.90}\ \dot{m} \qquad (68)$$

and Equation 67 to

$$47.40\ X_{90}^{-0.81}\ \dot{m} \leq P_d \leq 67.15\ X_{90}^{-0.81}\ \dot{m} \qquad (69)$$

The range of design power for the prime mover of the shredder as a function of the product particle size in the primary size-reduction of raw MSW can be expressed either by Equation 68 or by Equation 69. The choice of which of the two equations is to be used depends upon whether characteristic size or nominal product size is the criterion governing design. If power is to be estimated, the choice probably would be characteristic size, inasmuch as it would permit a better correlation with power requirement than would be possible if nominal product size were the criterion [29]. A procedure for calculating the shredder power requirements for a specific case is illustrated in Table 14.

Experience gained through the shredding of several types of MSW is perhaps, the best guide in the selection of the specific level of design power within the estimated range. If actual test data are not available, it is well to decide upon a design power level that is on the higher side of the power range.

MAINTENANCE

The nature, extent, and frequency of maintenance are three extremely important considerations in the selection of a shredder. It follows, therefore, that to rationally evaluate the many presently available shredder designs, it is essential to be cognizant of the many and varied maintenance problems that are encountered in a shredder operation.

The cost of maintaining a shredder is aggravated by the fact that maintenance is a labor intensive operation. Because of this fact it is important that a machine be selected that has features designed to expedite maintenance. Therefore, to be complete, the specifications for a shredding system should call for the following five features:

1. Appropriate equipment (overhead cranes, hydraulic or pneumatic devices for opening the shredder for access to the internal parts and for closing it, mechanical pin-pullers, hammer removal jigs, and reversible hammers);

TABLE 14. CALCULATION OF SHREDDER POWER REQUIREMENTS

A. DESIGN SPECIFICATIONS

1. Feedstock: Municipal Solid Waste
2. Throughput ($\dot{m}$): 60 Mg/h
3. Desired particle size: 90 percent cumulative weight percent passing 10 cm (X_{90})
4. Freewheeling power to gross power ratio (α): 0.10
5. Safety factor (η): 1.5

B. POWER CALCULATIONS FOR SHREDDER DESIGN

Gross Power, P_g, required:

$$P_g = \frac{35.55\, X_{90}^{-0.81}\, \dot{m}}{1 - \alpha}$$

$$= \frac{35.55(10)^{-0.81}(60)}{1 - 0.1}$$

$$= 330 \text{ kW}$$

Design power, P_d, required:

$$P_d = \eta\, P_g$$

$$= 1.5\, P_g$$

$$= 496 \text{ kW}$$

$$= 665 \text{ hp}$$

---

2. Necessary and well-kept welding equipment and facilities that include a carefully-designed ventilation system;

3. The lighting required for the safe performance of maintenance operations;

4. Movable scaffolding or permanent walkways about the shredder to permit easy access to all pieces of equipment that may require maintenance, including sufficient crawlways and walkways below and adjacent to the shredder and its auxiliary equipment, especially the conveyors; and

5. Adequate space around the shredder to accommodate the removal and re-installation of grate bars, hammers, wear plates, breaker bars, and other parts.

A request for a price quotation should stipulate that the responding manufacturer specify all equipment and material inventory required to maintain his shredder. Examples of such equipment are the equipment used in bearing and rotor replacement and overhaul, and of the equipment employed in the removal and re-installation of hammers, liners, wear plates, breaker bars, and of grate bars or cages. Furthermore, an operating and maintenance manual should be provided in which are given detailed descriptions of operating data and procedures for performing the various functions required in shredder maintenance.

MANUFACTURERS' REPUTATION

As one would expect, a weighty consideration in the selection of a particular piece of equipment is the quality of the past performance by the manufacturer. Things to be considered in an evaluation of performance are the longevity of the business (e.g., several refuse shredder manufacturers failed during the 1970's) and its record of service. An effective means of determining quality and reliability of a company's performance is through communication with users of similar equipment supplied by the manufacturer. A list of users may be requested in the formal request for bids or it may be sought informally through a communication with the manufacturer. Users contacted for information regarding their experience with the proposed piece of equipment should be queried as to:

1. The condition of the machine upon delivery by the manufacturer.

2. Type and cost of guidance and consultation provided by the manufacturer during equipment installation and shakedown.

3. The manufacturer's record for expeditiously supplying replacement parts and the reasonableness of the costs of such parts.

4. Type and cost of consultation supplied by the manufacturer after the acceptance period was completed and the general receptiveness of the manufacturer to plant inquiries.

SECTION 9

PERFORMANCE EVALUATION IN THE FIELD

The selection of a piece of equipment, shakedown of in-house equipment, and research on the principles of equipment design, all may involve at one point or another, an evaluation of the performance of the equipment. With respect to the evaluation of a shredder, major considerations are throughput capacity, energy consumption, product characteristics, and hammer wear. These considerations or elements are explained in summary fashion in the paragraphs immediately following this one, and in some detail in a later part of this section under the heading "Test Methods for Shredder Performance Evaluation."

Throughput capacity can be considered to be either the design mass flow rate, or a mass flow rate that has been determined under operating conditions established as being optimum through previous experience. One method of determining the mass flow rate involves the removal of material from a given length of belt that is moving at a known speed. The weight of the sample times the speed of the belt constitutes the mass flow rate.

In an evaluation, rate and amount of energy consumption are monitored. The information thus obtained is used in the calculation of the specific energy consumed in the production of a given product size at a specified throughput. An essential element in the monitoring and determination of specific energy consumption is a precise synchronization between energy consumed and the collection of the "mass flow rate" sample.

An element of major importance in the determination of product characteristics is that the collected sample be truly representative of the material being processed. Generally, the larger the sample (and therefore the larger the number of individual particles), the more closely will it be representative. A representative number of particles is the criterion for determining the requisite mass or volume of shredded material. The grate spacing of the shredder is a useful indicator of the particle size of the discharged product. In general, the wider the spacing, the larger the particle size of the discharged material, and hence the larger the mass of the sample that is required. The size distribution of the particles that make up the sample can be determined relatively precisely by manual screening, by mechanical screening, or by a combination of the two. The screening is preceded by a determination of the moisture content of the material.

To be meaningful, a determination of hammer wear must be preceded by a cleaning of the hammers. The cleaned hammers are weighed before and after a given amount of solid waste is shredded. The weight of material lost per unit weight of refuse shredded is the degree of wear.

Obviously, degree of size reduction accomplished is an essential consideration when making a comparison between two or more shredders with respect to nature, extent, and rate of hammer wear. Again, not unexpectedly, amount and rate of wear are functions of the spread between the particle size distribution of the input material and that of the product, inasmuch as the finer the particle size of the product, the longer has been the exposure time of the particles collectively to the hammers. Differences with respect to the particle size distributions of feed material and of the shredded product can be accounted for through the use of the parameter, "degree of size reduction" (Z_0) (see SECTION 4).

If a comparison is to be made between the wearing characteristics of two or more hardfacing alloys, the base hammer material and all of the alloys should be tested simultaneously in each run. Such a procedure ensures a uniformity of conditions of exposure for all materials.

COMPARISON BETWEEN SIZE REDUCTION ALTERNATIVES

Principles that may be applied in making a comparison between the respective advantages and disadvantages of two types of systems or shredders are illustrated by way of two examples. The first example is concerned with the relative effects of single-stage and of multi-stage shredding on energy consumption. The second example deals with the effect of shredder design on power consumption.

In the first example, single- vs multi-stage shredding, values for gross (P_g) and net (P_n) power consumption, for mass flow rate of refuse on a dry basis ($\dot{m}$), and for characteristic product size (X_0) are based upon actual operational data [29] reported for the single-stage Cockeysville plant and for the Ames two-stage plant.

The mass flow rate in the Cockeysville plant was 52.2 Mg/h; and in the Ames plant, 21.6 Mg/h. In the comparison, the product sizes from Cockeysville and Ames are regarded as being equal (i.e., X_0 value, 1.6 cm). Moreover, the moisture content (MC) of the products from the two plants is considered to average 20.5 percent.

According to Table 4, the appropriate relation for the Ames primary shredder is

$$P_n = 0.62\ \dot{m}^{1.20}(0.795)^{-7.04} \qquad (70)$$

and for the secondary shredder,

$$P_n = 0.28\ \dot{m}^{1.92}(0.795)^{-2.84} \qquad (71)$$

In both equations, $\dot{m}$ is 21.6 Mg/h. The average characteristic size of the secondary product at this throughput is 1.6 cm. The equation for net power for the Cockeysville shredder (Table 4, combined rotation) is

$$P_n = 21.85\ \dot{m}^{0.90}(0.795)^{2.25} \tag{72}$$

where $\dot{m}$ is 52.2 Mg/h. At this throughput, the characteristic particle size of the product is the same as that of the product from the Ames secondary shredder, viz. 1.6 cm.

By solving Equations 70, 71, and 72, it becomes apparent that the total net power required by the Ames plant to produce a particle size of 1.6 cm is 319.0 kW; and by the Cockeysville plant, 456.8 kW. Using the wet weight of the throughput material, the specific energy ($E_{OW} = P_n/\dot{m}_W$) for Ames becomes 14.8 kWh/ Mg; and for Cockeysville, 8.8 kWh/Mg. From these calculations one would be led to conclude that the specific energy required to produce a particle size of 1.6 cm at the Ames plant would be 1.6 times that at the Cockeysville plant.

As it stands thus far, the comparison is incomplete, because net energy represents only a part of the energy that is consumed. To complete the comparison, it is necessary to examine the gross power requirement. At the Ames two-stage shredding facility, the gross power consumption is 412.7 kW, 319.0 kW net power plus 53.2 kW freewheeling energy by the primary shredder and 40.5 kW by the secondary shredder. A 456.8 kW net power plus a 66.1 kW freewheeling power adds up to a gross power requirement at Cockeysville of 522.9 kW. Therefore, the production of a product having a particle size of 1.6 cm requires an energy input of 19.1 kWh/Mg at the Ames site (throughput, 21.6 Mg/h) and of 100 kWh/Mg at Cockeysville (throughput, 52.2 Mg/h). Apparently therefore, the energy consumption per Mg of refuse in the two-stage size reduction operation is more than twice that in the single-stage process.

When considering the preceding example, it must be kept in mind that data used in the example were collected at only two installations. They are not to be construed as being averages or medians of several observations. Moreover, findings based on the data pertain only to the two operations in the example, and hence cannot be validly extrapolated for purposes of generalization. This limitation is confirmed by results obtained by Savage et al [28]. In their studies, Savage et al observed that under certain conditions of grate opening and particle size, the total energy consumed in multiple-stage shredding was less than that consumed in single-stage shredding.

In the second example, the comparison is between the performances of two horizontal hammermills that had the design specifications listed in Table 15. Again, the values used in the examples were determined in an actual operation [29]. Characteristic product size is the basis of comparison. An examination of the data available on the performance of mill-2 (Table 15) revealed no statistically significant relation between product characteristic size and mass flow rate; whereas data pertaining to mill-1 indicated the existence of an inverse relationship between the two variables. The inverse relationship is best expressed as

TABLE 15. HAMMERMILL SPECIFICATIONS

Specification	Mill-1	Mill-2
Mill length	2.59 m	2.74 m
Motor:		
size	373 kW	746 kW
type	TIM, wound rotor	TIM, wound rotor
Grate:		
spacing	24.1x36.5 cm openings	20.3x35.6 cm openings
total opening	$3.79 m^2$	$3.54 m^2$
Number of hammers	14	24

$$X_o = -0.034 \, \dot{m} + 6.03 \qquad (73)$$

In the absence of a correlation between characteristic size and mass flow rate in the data from mill-2, a procedure was developed that can be followed in all similar situations. The procedure is as follows: Equation 73 and the data it describes are plotted as in Figure 21. The comparison between the data from mill-1 and those from mill-2 is made by drawing an auxiliary axis for the mill-2 flow rates below the flow rate axis for the mill-1 data. The mill-2 data are then plotted such that the average characteristic size of its product falls on the line that describes the mill-1 data, as is done in the figure. Since in the situation plotted in the figure, the average flow rate and characteristic size of the mill-2 product are 49.5 Mg/h and 2.1 cm, respectively, the flow rate through mill-1 to produce a product having an average characteristic size of 2.1 cm is 114.3 Mg/h. The basis of this conclusion is the similar flow rate size relation determined for the mill-1 data.

Assuming that the moisture content of the raw refuse processed in the two mills is 20 percent and with the use of Equation 27, Savage and Shiflett determined that the net power draw of mill-1 to reach a characteristic particle size of 2.1 cm would be 124.9 kW; and of mill-2, 441.7 kW. Such being the case, the specific energy requirement by mill-1 is 1.1 kWh/Mg; and by mill-2, 8.9 kWh/Mg. Provided, of course, that the characteristics of the refuse fed to mill-1 were roughly similar to those of the refuse fed to mill-2, the indicated conclusion would be that mill-2 significantly out performed mill-1.

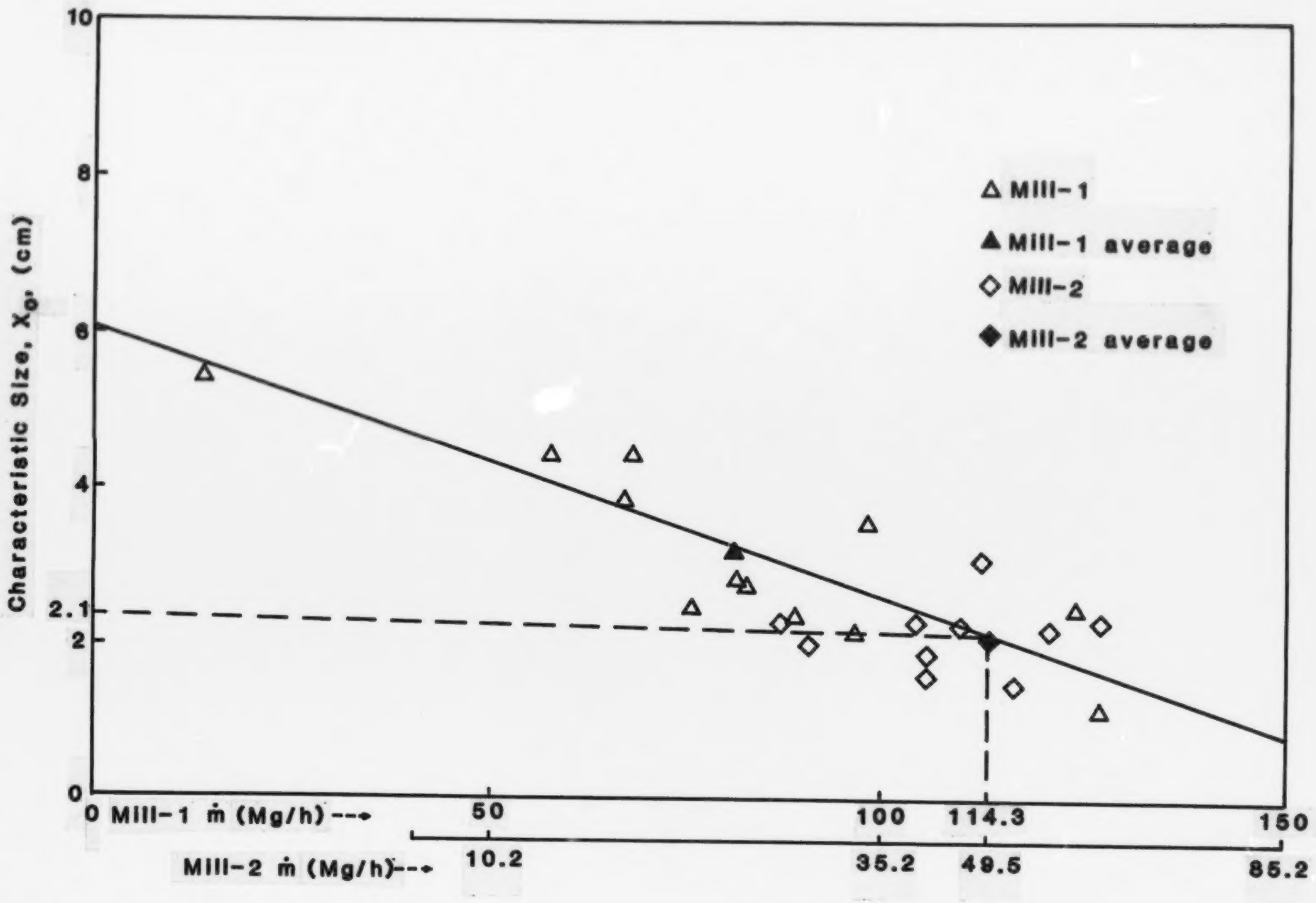

Figure 21. Observed and derived flow rate-size relationships.

TEST METHODS FOR SHREDDER PERFORMANCE EVALUATION

Two methods are presented for testing the performance of a shredder. Which of of the two is to be selected depends upon the objective being sought. The first method is appropriate for documenting the performance of a shredder pursuant to a set of written specifications that are to be met by the manufacturer. The second method would be appropriate if the objective were to define the performance of a shredder on the basis of variations in operating conditions, the principal variable being refuse throughput. The procedures in each of the two test methods differ slightly.

Method 1: Performance Documentation According to Manufacturer Specifications

Evaluation of the performance of a shredder in terms of the criteria specified by the manufacturer involves the specification of a nominal product size and power requirement for a given design throughput. Other performance parameters that may be specified as a function of design throughput are rate of hammer wear, time required for changing hammers or grates, and the specific gross (or net) energy consumption.

Judging from past experience, a sufficiently thorough evaluation would require the conduct of at least 20 tests in which the measured throughputs are within ±20 percent of the specified design throughput value. The flow diagram for such a program is shown in Figure 22. In each test, the throughput is measured, samples for determination of product size distribution are collected, and power levels are monitored. The processing of a representative sample of waste feedstock is assured by running each test over a period of one week. Details of procedures with respect to the determination of throughput, product size, power requirements, hammer wear rate, and hammer change time are given under the heading "Procedures," which directly follows the description of Method 2.

Method 2: Determination of the Effect of Changing Throughput on Shredder Performance

To adequately evaluate the effects had upon shredder performance as a result of changes in throughput, at least 24 tests would have to be conducted in which would be covered the expected range of throughputs. The test period should be one week. Selected increments of throughput should be such as to provide a uniform distribution throughout the entire operational range of the shredder. Product size distributions, mill holdup, and energy consumption are determined in each test according to the procedures described under the heading "Procedures." The flow diagram for Method 2 is given in Figure 23.

Procedures

Details of the procedures to be followed in the use of Methods 1 and 2 are as follows.

BEGIN FIRST LINE OF TEXT HERE
CENTER OF PAGE
TOP OF IMAGE AREA
DROPPED HEAD: BEGIN SECTIONS HERE

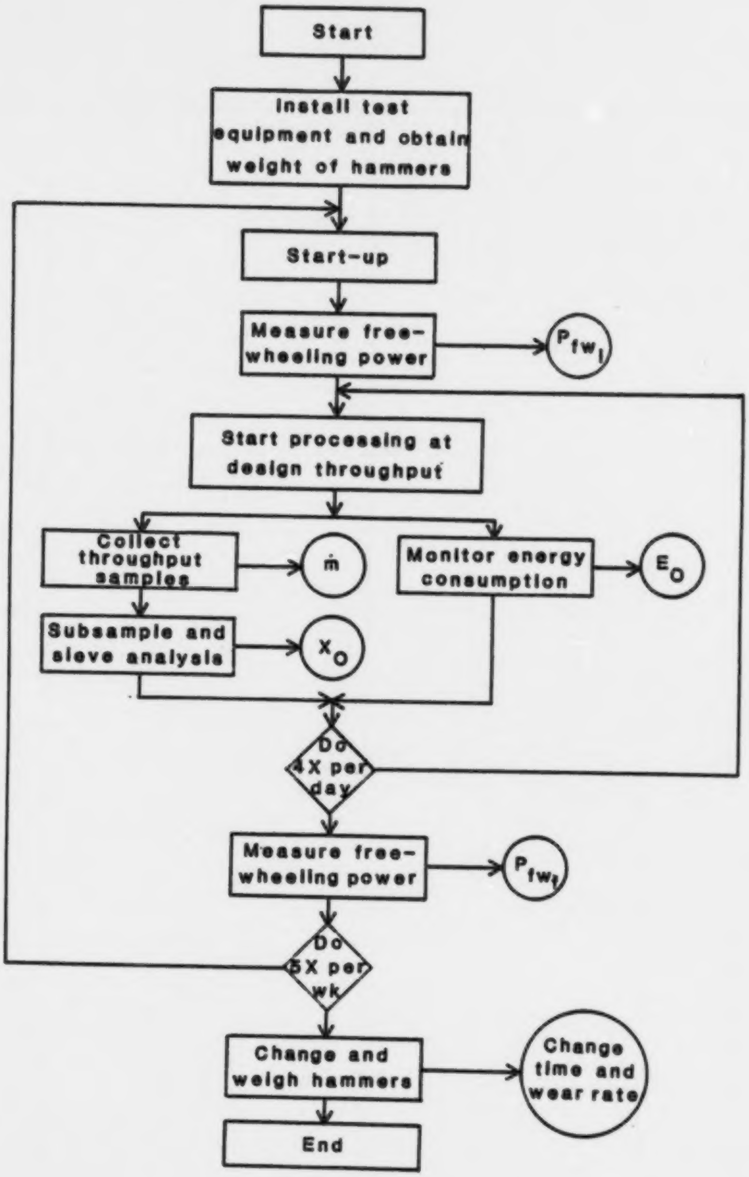
Start
Install test equipment and obtain weight of hammers
Start-up
Measure free-wheeling power
P_{fw_1}
Start processing at design throughput
Collect throughput samples
$\dot{m}$
Monitor energy consumption
E_0
Subsample and sieve analysis
X_0
Do 4X per day
Measure free-wheeling power
P_{fw_2}
Do 5X per wk
Change and weigh hammers
Change time and wear rate
End

Figure 22. Flow diagram for Method 1.

BEGIN LAST LINE OF TEXT
3/8"
BOTTOM OF IMAGE AREA OUTSIDE DIMENSION FOR TABLES AND ILLUSTRATIONS

EPA Form 2350-4 (4-80)
(PREVIOUSLY CIN. EPA FORM 227)
TYPING GUIDE SHEET

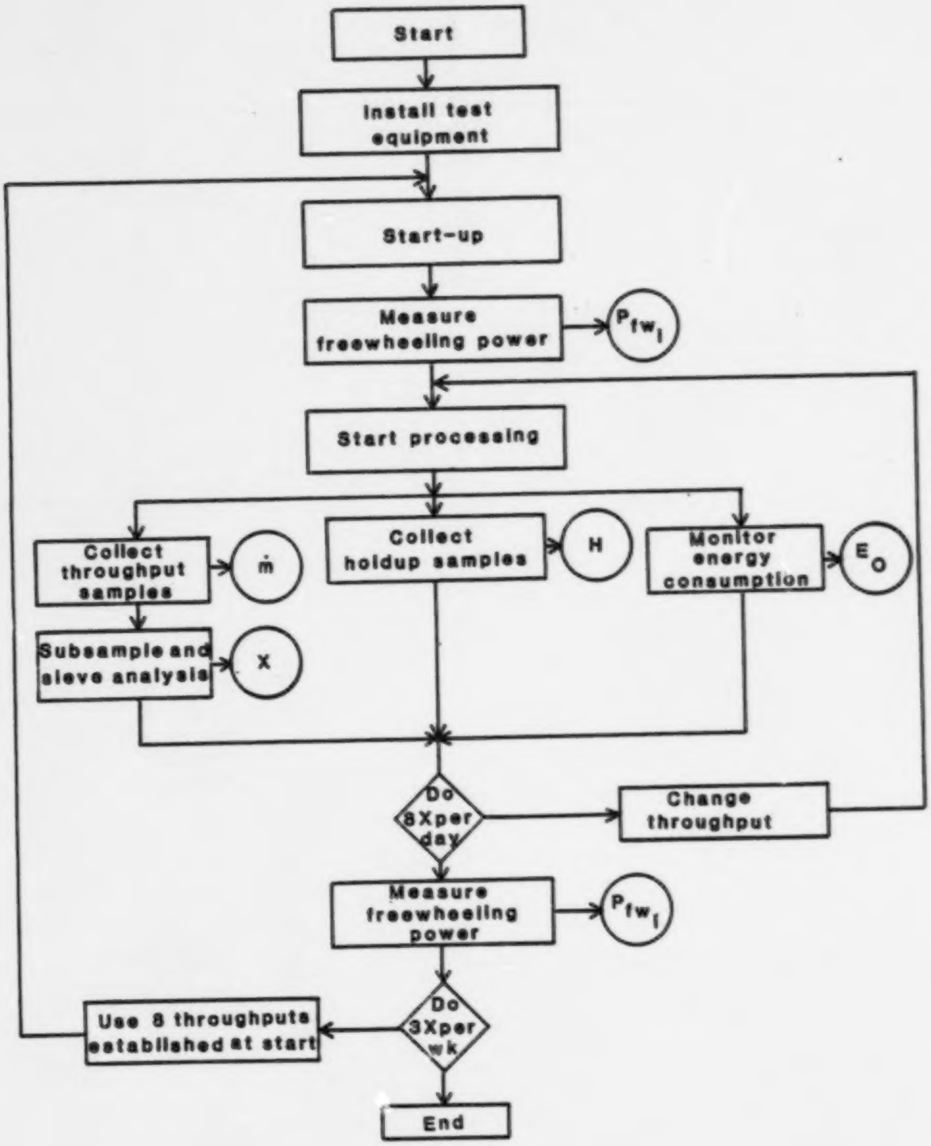
Start
Install test equipment
Start-up
Measure freewheeling power
P_{fw_i}
Start processing
Collect throughput samples
ṁ
Collect holdup samples
H
Monitor energy consumption
E_o
Subsample and sieve analysis
X
Do 8Xper day
Change throughput
Measure freewheeling power
P_{fw_f}
Do 3Xper wk
Use 8 throughputs established at start
End

Figure 23. Flow diagram for Method 2.

EPA Form 2350-4 (4-80)
(PREVIOUSLY CIN- EPA FORM 337)

TYPING GUIDE SHEET

I. Equipment Installation

1) Current transformers, potential transformers, and analog watt-hour meter are to be installed in accordance with the ASTM draft test standard, "Methods for Measuring Electrical Power and Energy Requirements of Processing Equipment" [46].

II. Start-Up

1) The shredder, conveyor belts, and all metering equipment must be in operation for 15 minutes before a test is begun.

2) The belt speed of the shredder discharge conveyor is measured after the 15-minute warm-up. This step involves a measurement of the time required for a fixed point on the conveyor belt to travel a measured distance.

III. Freewheeling Power Requirements

1) The initial freewheeling power (P_{fw_i}) is determined by measuring the difference in the analog watt-hour meter reading for a given time period under the no-load operating condition. The same procedure is used to determine the freewheeling power at the end of each day of testing (P_{fw_f}). The procedure for measuring freewheeling power is given in reference [46]. The average of P_{fw_i} and P_{fw_f} is used in all calculations involving freewheeling power.

IV. Throughput Measurements

1) Throughput is measured according to the draft test standard "Method of Measuring Throughput of Resource Recovery Unit Operations" [47], excepting for the allowable variation in throughput as noted below. The stopped-belt method is the preferred method. The stopped-belt method is as follows:

   a) The speed of the shredder discharge belt is measured.

   b) Three samples are taken by stopping both feed and output conveyors and removing material from three predetermined sections of the output conveyor. Sections of belt that are sampled must be long enough to negate instantaneous fluctuations in the throughput.

   c) Two of the three samples are selected, and throughput is calculated on the basis of each of the two samples by multiplying the discharge belt speed and the mass to sample length ratio. If the two calculated throughputs differ by more than 20 percent, the throughput is calculated on the basis of the third sample. If throughput on the basis of the third sample is in agreement (within ±20 percent) with either of the first two samples, the average of the two similar calculated throughputs is taken to be the actual throughput. If the throughput on the basis of the third sample is not in agreement with either of the first two calculated throughputs, all three samples are disregarded, and the test is repeated.

V. Subsampling

1) A subsample of the throughput sample is prepared according to the ASTM draft test standard "Standard Sampling Procedure for RDF-3 Collection and Division of a Gross Sample" [48]. The preferred method is coning and quartering. It is as follows.

   a) The throughput sample is piled in the form of a conical heap. The heap is then flattened to form a circular cake. The cake is divided into quarters. Two of the diagonally opposite quarters are taken as the sample, and the two remaining quarters are discarded. The two quarters taken as the sample are collected and the procedure of coning and quartering is repeated until the desired sample size is obtained.

   b) For shredded MSW with a bulk density in the range of 80 to 160 kg/m^3, the subsample weight should be in accordance with the following table:

Nominal size (mm)	20	100	180
Minimum wt (kg)	0.4	6.0	30.0

VI. Subsample Moisture Content

1) The subsample moisture content is determined according to the ASTM draft test standard "Standard Methods of Preparing RDF-3 Laboratory Samples for Analysis" [49]. The procedure is as follows:

   a) The entire subsample is weighed, and then is spread on a clean, dry, flat surface in a drying room. The thickness of the layer of sample must be no greater than 10 cm (4 in.). Clumps of material are to be broken.

   b) The sample is air-dried in an oven at 30° to 40°C until the weight loss is less than 0.1 percent of the sample weight per hour.

   c) At the end of the drying period, the sample is allowed to cool to room temperature (20°C) in a desiccator before it is weighed.

2) The wet weight, dry weight, and moisture content of the sample are recorded on a form of the type shown in Figure 24.

VII. Subsample Size Distribution

The size distribution of the subsample is to be determined according to the ASTM draft test standard "Standard Method of Designating the

BEGIN FIRST LINE OF TEXT HERE
CENTER OF PAGE
TOP OF IMAGE AREA

SIZE DISTRIBUTION DATA SHEET

Date: ____________
Site: ____________
Test No.: ____________
Grinder: ____________
Material: ____________

Sample Wet Weight: ____________
Sample Dry Weight: ____________
Water Content: ____________
Moisture Content: ____________
Screening Time: ____________

Screen Size	Bottom Screen Size ( )	Gross Wt. Retained by Bottom Screen ( )	Tare Wt. ( )	Net Wt. Retained by Bottom Screen ( )	% of Feed on Bottom Screen	Cumulative Wt.% Passing Bottom Screen
Pan						
		Total Sample Wt.:				

NOTES: ____
____
____
____
____
____

Figure 24. Example of a size distribution data sheet.

BEGIN LAST LINE OF TEXT
3/8"
PAGE NUMBER
BOTTOM OF IMAGE AREA; OUTSIDE DIMENSION FOR TABLES AND ILLUSTRATIONS
EPA Form 2350-4 (4-80)
(PREVIOUSLY CIN. EPA FORM 287)
TYPING GUIDE SHEET

Size of RDF-3 from its Sieve Analysis" [50]. The description is as follows:

1) Hand Sieving - An increment of sample is sieved through a series of screens, starting with the sieve that has the largest sized openings. The size of the increment should be such that individual particles are in direct contact with the screen surface after the completion of each shaking. Vertical as well as horizontal motion is applied during shaking to allow all small particles to pass through the openings. Hand fitting is not permitted.

2) Machine Sieving - The sieves are stacked progressively starting with the smallest aperture size at the bottom (on top of the pan) and finishing with the largest aperture size at the top. The sample is spread in the largest screen such that matting or blinding of the material does not occur and the increment is not more than one-third of the volume of the screen. The machine is turned on and the subsample agitated for 10 to 15 minutes. Material remaining in each screen is weighed. If the total weight after screening is more than 2 percent less than the pre-screened weight, the analysis is rejected and the test is repeated.

3) For complete particle size characterization, the sieves are selected such that no more than 25 percent of the gross sample weight is retained on any intermediate sieve, and less than 5 percent is retained on the top sieve and less than 15 percent in the pan.

4) Data are recorded as shown in Figure 24.

VIII. Specific Energy Requirement

1) The time-averaged specific energy requirement (kWh/Mg) is calculated from the following information: a) the gross energy used during the throughput interval (as measured using the procedures in reference [46]); b) the measured value of the throughput; c) the freewheeling power draw of the shredder; and d) the time duration of the test interval.

2) Specific energy requirement (E_0) is calculated with the use of the following equation:

$$E_0 = (E_g - P_{fw}t)/\dot{m}t$$

where E_g = gross energy consumed by shredder motor (kWh); P_{fw} = freewheeling power requirement (kW); t = duration of sampling (h); and $\dot{m}$ = throughput (Mg/h).

IX. Holdup: Feed and Discharge

1) The collection of holdup takes place only after material is no longer being fed to the shredder. Therefore, input conveyors

are stopped during the collection of the throughput sample. Material that continues to be discharged from the shredder after the input to the machine is stopped is collected, weighed, and recorded. Normally holdup is collected on a stationary shredder discharge conveyor.

a) The measurement of the holdup is corrected to account for the throughput material already on the belt below the shredder discharge when the infeed conveyor is stopped.

X. Rate of Hammer Wear

1) New hammers should be subjected to a "break-in" period prior to testing so as to avoid distortion of the results by the initial high rates of wear characteristic of new hammers. The wear rate is expressed as kilograms of hammer metal lost per metric ton of MSW processed. The break-in period must be long enough to result in a hammer weight loss of 2 percent. Typically, rates of hammer wear in MSW processing are 0.03 to 0.5 kg per Mg, for purposes of estimation.

2) Prior to the test period, the hammers are cleaned and weighed.

3) The MSW should be processed in a quantity sufficiently large as to bring about a hammer weight loss 40 times the precision of the weigh scale.

4) Because the rate of hammer wear depends upon throughput under a given set of operating conditions, throughput is not to deviate from the mean throughput during the test period by more than 20 percent over more than 10 percent of the test period.

5) At the close of the test period, the shredder hammers are cleaned and weighed, and the weight of each hammer is recorded. To determine the hammer wear rate, the total weight loss of all the hammers is divided by the total weight of MSW processed during the test period.

6) Data are be recorded on a data sheet of the type shown in Figure 25.

XI. Hammer Change Time

1) The manufacturer is expected to provide a manual for changing hammers.

2) The manufacturer and shredder operator should mutually agree on the type of labor required for changing the hammers.

3) Given conditions 1) and 2), the expected hammer change time is specified by the manufacturer.

4) The elapsed time is measured as follows:

BEGIN FIRST LINE OF TEXT HERE
CENTER OF PAGE
TOP OF IMAGE AREA
DROPPED HEAD; BEGIN SECTION HERE

WEAR MEASUREMENT DATA SHEET

Date: ____________________
Site: ____________________
Test No.: ________________
Grinder: _________________

Sheet ______ of ______
Tip Speed: ________________
Tonnage: __________________
Hammer Base Material: __________

Hammer	Hammer Location		Hardfacing Material	Initial Wt. ( )	Final Wt. ( )	Wt. Loss ( )
	Row	Position				
1.						
2.						
3.						
4.						
5.						
6.						
7.						
8.						
9.						
10.						
11.						
12.						
13.						
14.						
15.						
16.						
				Total Wt. Loss ( ):		

Total Tonnage: __________ Mg
Wear (kg/Mg): __________

NOTES: ____

Figure 25. Example of wear measurement data sheet.

BEGIN LAST LINE OF TEXT
BOTTOM OF IMAGE AREA OUTSIDE DIMENSION FOR TABLES AND ILLUSTRATIONS
3/8"

PAGE NUMBER
EPA Form 2350-4 (4-80)
(PREVIOUSLY CIN. EPA FORM 287)
TYPING GUIDE SHEET

a) Prior to beginning the test, the following should be checked:

   - o The motor circuit is de-energized.
   - o The motor is stationary.
   - o The work area is clean.
   - o All tools specified by the manufacturer are conveniently located in the work area.

b) Measurement of time commences at the instant an effort is made to open the shredder housing. Timing is stopped as soon as the shredder is operational, and the elapsed time is then recorded. The time required to clean-up the work area after closing the shredder housing, and time lost because of interruptions such as coffee and lunch breaks are subtracted from the total elapsed time.

5) Data are recorded on a form of the type shown in Figure 26.

DATA SHEET FOR HAMMER CHANGE TIME

Date: ____________________

Site: ____________________

Grinder: __________________

No. of Hammers: ____________

Personnel	Time In	Time Out	Net Working Time (hrs)
1.	1.		
	2.		
	3.		
	4.		
2.	1.		
	2.		
	3.		
	4.		
3.	1.		
	2.		
	3.		
	4.		
4.	1.		
	2.		
	3.		
	4.		

Total (man-hours) ____________________

Figure 26. Example of data sheet for hammer change time.

REFERENCES

1. Wiles, C.C. and G.E. Stone. Composting at Johnson City - Final Report. Volumes I and II. EPA Report No. 530/SW-31r.2, November 1975.

2. Ham, R.K. and J.J. Reinhardt. Final Report on a Demonstration Project at Madison Wisconsin to Investigate Milling of Solid Wastes Between 1966 and 1972. Volume I. U.S. Environmental Protection Aency, March 1973.

3. Significance of Size Reduction in Solid Waste Management. University of California (Berkeley), EPA Grant No. R804034, 1972.

4. Significance of Size Reduction in Solid Waste Management. University of California (Berkeley). EPA Grant No. R-805414-010, 1974.

5. Processing Equipment for Resource Recovery Systems. Midwest Research Institute and Cal Recovery Systems, Inc., EPA Contract No. 68-03-2589, 1978.

6. Solid Waste Shredding and Shredder Selection. EPA/530/SW-140, March 1975.

7. 1981 Shredder/Baler Index. Waste Age, 12(7):71-75, 1981.

8. Marshall, V.C. Crushing and Grinding - Critique of Existing Laws. Chem. and Process Eng. April 1966.

9. Austin, L.G. and R.R. Klimpel. Theory of Grinding Operations. I and EC Process, Design and Development. 56:19-29, 1964.

10. Snow, R.H. Annual Review of Size Reduction. Powder Techn. 5:351-364, 1971/72.

11. Fuerstenau, D.W. and P. Somasundaran. Cinetique de Ta Fragmentation. In: 6th Congres International de Ta Preparation des Minerals (Cannes), Edit. Saint-Etienne, 1963. pp. 39-48 (cf. also "Comminution Kinetics," in Mineral Processing, Edit. A. Roberts, Pergamon Press, Oxford, 1965. pp. 25-34).

12. Perov, V.A. and Y.A. Vasil'eva. Kinetics of Grinding of a Two-Component Mixture in a Ball Mill. Gornyi Zhurnal, 1961.

13. Kinasevich, S.R. Application of the Schumann Single Event Hypothesis to Comminution. M.S. Thesis, Univ. of California, 1962.

14. Von Rittinger, R.P. Lehrbuch der Aufbereitungskunde, Ernst und Korn, Berlin, 1857.

15. Kick, F. Das Gesetz der Proportionalem Widerstand und Seine Anwendung, Leipzig, 1885.

16. Bond, F.C. The Third Theory of Comminution. Trans. AIME, 193:484-494, 1952.

17. Stratton, F.E. and H. Alter. Application of Bond Theory to Solid Waste Shredding. Journal of the Environmental Engineering Division, pp. 93-107, February 1978.

18. Trezek, G.J. and G.M. Savage. Significance of Size Reduction in Solid Waste Management. EPA-600/2-77-131, Municipal Research Laboratory, Office of Research and Development, U.S. EPA, Cincinnati, Ohio 45268, July 1977.

19. Vesiland, P.A., A.E. Rimer, and W.A. Worrell. Performance Characteristics of a Vertical Hammermill Shredder. Proceedings 1980 National Waste Processing Conference, ASME, May 1980.

20. Charles, R.J. Energy-Size Reduction Relationships in Comminution. Trans. AIME, 208:80-88, 1957.

21. Holmes, J.A. Contribution to the Study of Comminution - Modified Kick's Law. Trans. Inst. Chem. Engrs., 35:125-141, 1957.

22. Schumann, R. Energy Input and Size Distribution in Comminution. Trans. AIME, 217:22-25, 1960.

23. Gaudin, A.M. An Investigation of Crushing Phenomena. Trans. AIME, 73:253, 1926.

24. Schumann, R. Principles of Comminution: 1.-Size Distribution and Surface Calculations. Tech. Publs. AIME, 1189:11, July 1940.

25. Rosin, P. and E. Rammler. Laws Governing the Fineness of Powdered Coal. Inst. of Fuel, 729-36, 1933.

26. Gaudin, A.M. and T.P. Meloy. Model and a Comminution Distribution Equation for Single Fracture. Trans. AIME, 223:40-43, 1962.

27. Bergstrom, B.H. Empirical Modification of the Gaudin-Meloy Equation. Trans AIME, 235.

28. Savage, G.M. and G.J. Trezek. Significance of Size Reduction in Solid Waste Management, Volume II, EPA-600/2-80-115, Municipal Environmental Research Laboratory, Office of Research and Development, U.S. EPA, Cincinnati, Ohio, 45268, August 1980.

29. Savage, G.M. and G.R. Shiflett. Processing Equipment for Resource Recovery Systems: III - Field Test Evaluation of Shredders, EPA Report No. 600/2-80-007c, July 1980.

30. Callcott, T.G. A Study of the Size Reduction Mechanisms of Swing Hammer Mills. J. Inst. Fuel, 33:529, 1960.

31. Obeng, D.M. Comminution of a Heterogeneous Mixture of Brittle and Non-Brittle Materials. Ph.D. Dissertation, University of California, Berkeley, 1973.

32. Broadbent, S.R. and T.G. Callcott. A Matrix Analysis of Processes Involving Particle Assemblies. Phil. Trans. Roy. Suc., 249, Series A:99. 1956.

33. Cal Recovery Systems. Field Test Evaluation of Shredders -- Additional Testing. EPA Contract No. 68-03-2866.

34. Savage, G.M., G.J. Trezek, and G.R Shiflett. Size Reduction in Solid Waste Processing - Fine Grinding. Progress Report 1976-1978. Report to the U.S. EPA, prepared under Grant No. EPA R803034.

35. Trezek, G.J. and G.M. Savage. Size Reduction in Solid Waste Processing. Progress Report 1973-1974. Report to U.S. EPA, prepared under Grant No. EPA R-80128, 1974.

36. Gawalpanchi, R.R., P.M. Berthovex, and R.K. Ham. Particle Size Distribution of Milled Refuse. Waste Age, 4(5):34-74, 1973.

37. Savage, G.M. and G.J. Trezek. On Grinder Wear in Refuse Comminution. Compost Science, 15(4), September 1974.

38. Shiflett, G.R. A Model for the Swing Hammermill Size Reduction of Residential Refuse, Ph.D. dissertation, University of California (Berkeley), 1977.

39. Shiflett, G.R. and G.J. Trezek. Parameters Governing Refuse Comminution. Resource Recovery and Conservation, 4:31-42, 1979.

40. Zalosh, R.G., et al. Factory Mutual Research Corporation - Assessment of Explosion Hazards in Refuse Shredders. Prepared for the U.S. Energy Research and Development Administration under Contract No. (49-1) -3737, April 1976.

41. Nollet, A.R. and E.T. Sherwin. An Approach to Energy Attenuation of Explosive Wastes in Processing Equipment. Proceedings of the Sixth Mineral Waste Utilization Symposium, May 1978.

42. Zalosh, R.G. and J.P. Coll. Explosion Venting Test Program for Municipal Solid Waste Shredders. Proceedings of the Seventh Annual EPA Research Symposium, March 1981.

43. Zalosh, R.G. and J.P. Coll. Explosion Venting Test Program for Municipal Solid Waste Shredders. Presented at the 1981 Annual Meeting of the Society of Fire Protection Engineers, May 1981.

44. NFPA 68. Explosion Venting 1978. National Fire Protection Association, Boston, Massachusetts, 1978.

45. Zalosh, R.G. and J.P. Coll. Determination of Explosion Venting Requirements for Municipal Solid Waste Shredders. Draft report submitted to the U.S. Environmental Protection Agency. EPA Contract No. 68-03-2880. September, 1981.

46. Method for Measuring Electrical Energy Requirements of Processing Equipment. Draft standard test method, prepared by Task Group 6, E38.08 Subcommittee, American Society of Testing and Materials, 1981.

47. Method of Measuring the Throughput of Resource Recovery Unit Operations. Draft standard test method, prepared by Task Group 6, E38.08 Subcommittee, American Society for Testing and Materials, 1981.

48. Standard Sampling Procedure for RDF-3 Collection and Division of a Gross Sample. Draft test standard, prepared by the E38.01 Subcommittee, American Society for Testing and Materials, 1981.

49. Standard Method of Preparing RDF-3 Laboratory Samples for Analysis. Draft test method, prepared by the E38.01 Subcommittee, American Society for Testing and Materials, 1981.

50. Standard Method of Designating the Size of RDF-3 from its Sieve Analysis. Draft test method, prepared by the E38.01 Subcommittee, American Society for Testing and Materials, 1981.

APPENDIX A

REFUSE SIZE REDUCTION LITERATURE REVIEWS

COMMINUTION PARAMETERS

Diaz, L.F., "Three Key Factors in Refuse Size Reduction," Resource Recovery and Conservation, 1 (1975) pp. 111-113.

> Experimental studies on parameters that affect the size reduction of MSW were conducted at Richmond Field Station, UC Berkeley. A 10-Mg/h Gruendler horizontal hammermill was used. Determinations were made of the effect of moisture content on product size distribution, grinder wear, and power consumption; and of feedrate on size distribution. The relation between hammer wear and hardfacing and non-hardfacing is described. A comparison is made between primary and secondary grinding.

"Field Test Evaluation of Shredders," Study of Processing Equipment for Resource Recovery Systems, Vol. III, EPA Contract No. 68-03-2589 (1979).

> Results are given of a study that involved field tests of nine large-scale shredders. The nine shredders included models of machines manufactured by Allis Chalmers, American Pulverizer, Tracor-Marksman, Heil, Carborundum, and Newell. From the data were developed analytical relationships between comminution parameters (moisture content, throughput, power draw) and performance levels (energy consumption, hammer wear). Shredder specifications and maintenance procedures are given for each site.

Ham, R.K., Reinhart, J.J., "Final Report on a Demonstration Project at Madison, Wisconsin, to Investigate Milling of Solid Wastes Between 1966-1972," Vol. I, EPA Grant No. 3-G06-EC-00000-0051.

> The study was conducted to determine the practicality of shredding MSW prior to landfill disposal. It involved the use of a Gondard horizontal hammermill and of a Tollemache vertical hammermill. Effects of hammer wear, moisture content, and mill design upon product size distributions were examined. The study describes first hand experiences with shredding problems (internal jamming, explosions, bearing failures, etc.). Seasonal variations of power consumption and production rate are thought to have a relationship to the moisture content of the air. Mill maintenance requirements and operating and capital cost data are also given.

Ruf, J.A., "Particle Size Spectrum and Compressibility of Raw and Shredded Municipal Refuse," University of Florida (1974).

Particle size distributions of each of the components of raw and shredded refuse were determined. Ruf found that hammermills reduce waste according to log-normal distributions. Methods of predicting size distributions for raw and processed MSW were developed. The variability of mean particle size as a function of grate opening was determined.

Savage, G., Trezek, G.J., "MSW Component Size Distributions Obtained from the Cal Resource Recovery System," Resource Recovery and Conservation, 2 (1976) pp. 67-77.

The effect of shredding on the size distributions of MSW component materials. A 10-Mg/h Gruendler horizontal hammermill was used. It is concluded that to obtain maximum efficiency on downstream separation processes, shredding should be as coarse as possible, but not too large for downstream equipment usage.

Trezek, G.J., Savage, G., "On Grinder Wear in Refuse Comminution," Compost Science, 15(4), (Sept.-Oct. 1974).

The relation between hammer and grate bar wear and hammermill speed in the size reduction of MSW was determined. A 10-Mg/h Gruendler hammermill was used. Operating speeds ranged from 790 to 1200 rpm. Austentic manganese steel was used for the hammer material (12.65 wt percent manganese). The hardfacing material was 10.5 percent manganese, 8.14 percent chromium, nickel, and molybdenum. Both materials were analyzed for their physical properties and resistance to wear.

Trezek, G.J., Shiflett, G.R., "Parameters Governing Refuse Comminution," Resource Recovery and Conservation, 4 (1979) pp. 31-42.

Experimental work was performed with the use of a 10-Mg/h Gruendler hammermill. The influence of residence time, moisture content, mill holdup, grate size, and flow rate on power requirements and product size distribution were identified and quantified. Quantitative relationships between the different parameters were determined.

Trezek, G.J., Savage, G., "Results of a Comprehensive Refuse Comminution Study," Waste Age, 6(8), (July 1975) pp. 49-55.

Experiments were conducted with the use of a Gruendler 10-Mg/h hammermill, the grate spacing of which was set at 2.5 inches. The effect of moisture content of the MSW and grinder speed on size distribution were determined. The moisture content ranged from 20 to 60 percent. The grinder speeds were 1200, 790, and 555 rpm. Relationships were found to exist between specific energy consumption and: (1) characteristic particle size, (2) moisture content, and (3) feed rate. A procedure for determining specific energy and the grate spacing required to attain particular particle size was identified.

Trezek, G.J., "Significance of Size Reduction in Solid Waste Management," EPA-600/2-77-131, (July 1977).

Data collected from MSW size-reduction experiments conducted with the use of a 10-Mg/h Gruendler hammermill were used to characterize relationships between comminution parameters (moisture content, grate spacing, shredder speed, energy consumption, hammer wear) and product size distributions. Grinder speed and hardfacing versus non-hardfacing were found to affect hammer wear and suitable hammer and hardfacing materials were identified. Quantitative relationships between parameters (power required, specific energy, characteristic particle size, grinder horsepower, feedrate, product size) are presented.

Trezek, G.J., Savage, G.M., "Significance of Size Reduction in Solid Waste Management," Vol. 2, EPA-600/2-80-115, (August 1980).

Experiments were conducted in which single and multiple stage size reduction were simulated. A 10-Mg/h Gruendler hammermill was used. Correlations were developed between: 1) single or multiple stage grinding versus energy consumption and characteristic particle size of product; 2) energy consumption versus grate size; and 3) hammer wear versus grate size, alloy hardness and type of waste (MSW or LSF). Quantitative relationships were determined between: 1) specific energy and degree of size reduction; 2) flow rate versus grate size, mill hold up, and mean residence time; and 3) power consumption versus flow rate and moisture content. A model is described for use in simulating size reduction. It incorporates variations in feed rate, mill holdup, residence time, moisture content, and energy consumption. Design considerations are presented for determining grate spacing and the need for single or double stage size reduction.

Trezek, George J., Size Reduction in Solid Waste Processing, "First Year Progress Report - 1971-1972," EPA Grant No. EC-00580-01.

It is a summarization of the "state of the art" knowledge involving size reduction of municipal refuse. It includes information on methods of measuring and characterizing size distributions, stress strain characteristics of aluminum and steel cans and light cardboard, and energy requirements for volume reduction of glass, steel, aluminum, and cardboard. Several resource recovery sites were visited, and during the visits information was obtained on hammer wear, power consumption, and incoming refuse compositions.

Trezek, G.H. Obeng, D.M., Savage, G., Size Reduction in Solid Waste Processing, "Second Year Progress Report - 1972-1973," EPA Grant No. R801218.

In experiments conducted with the use of a 10-Mg/h Gruendler hammermill, information was obtained on the combined effects of feed rate, moisture content, and feed composition on product size distribution. Relationships were determined between energy consumption and dry feed rate and moisture content; and between hammer and grate bar wear and moisture content, axial location, and face hardening, and lack of face hardening. Methods of describing and analyzing size distributions are presented. (Rosin-Rammler, matrix analysis methods).

Trezek, G.J., Savage, G., Size Reduction in Solid Waste Processing, "Progress Report - 1973-1974," EPA Grant No. R801218

Experiments involving the use of a 10-Mg/h Gruendler hammermill were conducted in which correlations were developed between: 1) energy consumption and characteristic size, multiple grinding, operating speed, moisture content, and feedrate; 2) product size distribution and operation speed and moisture content; 3) grinder wear and rotor speed and moisture content; and 4) grinder wear and rotor speed. A comparison was made between the energy consumption in the comminution of commercial and that of residential refuse.

Vesilind, P.A., Rimer, A.E., Worrell, W.A., "Performance Characteristics of a Vertical Hammermill Shredder," 1980 National Waste Processing Conference.

A vertical shaft hammermill at the Pompano Beach Solid Waste Reduction Facility was field-tested to determine whether or not output size specifications were being met. Wet and dry particle size distributions and power requirements were determined. Hammer wear was found to be linear with amount of refuse processed. Old and new hammers were found to wear at the almost identical rates. Bond's work index was calculated for the hammermill.

Vesilind, P. Aarne, Rimer, Alan E., Unit Operations in Resource Recovery, Prentice-Hall, Inc., New Jersey, 1981, pp. 93-133.

An overall view of MSW shredding is presented. The use of Rosin-Rammler and Gaudin-Meloy particle size distributions is explained. The particle breakage theory - Broadbent and Callcott matrix application are presented. Energy consumed in shredding is correlated with shredder speed, feed rate, particle size, and moisture content. A method of estimating energy requirements is described. Hammer wear is shown to be related to shredder speed and axial position of hammers. Explosion hazards and noise and dust levels around shredders are discussed. Guidelines are presented for the selection of the following shredder components: rotor inertia, motor hp, width/diameter ratio, and size of grate openings. Descriptions are given of wet pulping and roll crushing processes.

Jindal, V.K., Austin, L.G., "The Kinetics of Hammer Milling of Maize," Powder Technology, 14:35-39 (1976).

A small laboratory hammermill with a single hammer was used in a study on the kinetics of breakage of maize. First order breakage was observed, and breakage distribution functions were found to be independent of mill conditions and of the moisture content of the material. Results indicated that a sharp edged hammer accomplished more breakage than did a rounded edge. The authors determined that only the end inch of the hammer was effective in causing breakage, and that a significantly large amount of breakage occurred through the throwing of material against the mill wall. Increasing the hammer thickness brought about an increase in breakage.

ENVIRONMENTAL EFFECTS OF SHREDDING

"Evaluation of Shredding Facilities at Rock Cut Road Plant No. 1," EPA Grant No. G06-EC-00318 (1975).

In field test of a 40-Mg/h Eidal ring grinder, noise levels were found to exceed OSHA limits. Detailed cost figures are given for the shredding facility, as well as a description of operating problems, solutions, and maintenance requirements.

Study of Processing Equipment for Waste-to-Energy Systems, "Field Tests at Outgamie County, Wisconsin Waste Processing Plant," EPA Contract 68-03-2387.

Two Allis Chalmers 16 Mg/h shredders were thought to consume less energy after installation of water spray systems. Air emissions from the shredders were measured to determine their particle size and concentration, and the trace metal content. Hi Vol samplers were used. All trace metals were found to be below their threshold limit values.

EXPLOSIONS

Buckley, J.L., Wiener, S.A., Zalosh, R.G., "Assessment of Explosion Hazards in Refuse Shredders," ERDA Contract No. E(49-1)-3737 (1976).

An analysis is made of shredder explosion hazards. Design criteria are given for explosion venting, explosion protection systems, explosion suppression systems, dust collectors, and for a continuous waterspray in the shredder. Results of a survey of resource recovery facilities are presented. The survey was concerned with frequency and severity of explosions, and types and numbers of explosion protection methods in service.

Pyle, Forest B., "The Taming and Housebreaking of Refuse Shredders," 1978 National Waste Processing Conference, pp. 215-228.

Concepts and sources of shredder explosions are explained. A list is given in which shredder explosions are divided according to cause, shredder design, and frequency. Methods of explosion control and suppression are described, as are the economics involved.

MECHANISMS OF SIZE REDUCTION

Calcott, T.G., "A Study of the Size Reduction Mechanisms of Swing Hammer Mills," Journal of the Inst. of Fuel, 2:529-539 (1960).

High speed cine photography and experimentation were used to study the breakage of coal that took place in a 3 Mg/h vertical hammermill. The mill was divided into several size-reduction zones. Model equations were developed for the zones in which a significant amount of breakage occurred. Most of the size reduction was found to occur in the breaker bar zone. A critical feature was the gap between the tips of hammers and the breaker bar. Localized recirculation occurred in this area. Two approaches are presented that may be used to evaluate the overall mill matrix describing the size reduction process.

Drobney, N.L., Hull, H.E., Testin, R.F., "Recovery and Utilization of Municipal Solid Waste," U.S. EPA Contract No. PH 87-67-265 (1971) pp. 7-21.

The fundamentals of size reduction are described. The parts played by tension, compression, and shear mechanical forces are explained. Performance and cost data of twenty-one different shredders processing several types of waste are listed.

Savage, G., Size Reduction in Solid Waste Processing, "Aluminum Can Shredding Experiments," EPA Grant No. R801218.

Aluminum cans were shredded by acceleration down a tube into a plywood box and impacted on a variety of grates that included representatives of the following configurations: 1/4" flat bar, 1/8" flat bar, and 1/4" sharp bar. Mechanisms involved in shredding by high velocity impact were identified; and the velocities and impact energy required to shred cans were measured. The data was used to identify velocity zones in which certain types of mechanisms predominate and result in a characteristic shredding. The effects of grate bar thickness and sharpness on size distribution were determined.

Trezek, G.J., "Refuse Comminution," Compost Science, 13(4), July-August 1972).

A comparison is made between the product size distribution curves of two high speed hammermills and a low speed Eidal grinder. It was determined that machine-specific comminution mechanisms were responsible for the observed variances in the shape of the curves. As with brittle materials, it was concluded that the characteristic size distribution of shredded MSW was dependent upon the reduction mechanisms occurring.

MODELING OF COMMINUTION PROCESS

Obeng, D.M., Trezek, G.J., "Simulation of the Comminution of a Heterogeneous Mixture of Brittle and Nonbrittle Materials in a Swing Hammermill," I-EC Process Design and Development, 14(2), (1975).

Four matrix models, namely, π - Breakage Process; π, k - Breakage Process; π, k, w - Breakage Process; Repeated Breakage Cycles, were used to predict product size distributions from feed size distributions. Variations in feed rate, moisture content, and grinding stages (primary, secondary, tertiary) were simulated. The results obtained by semi-empirical analyses are compared to experimental data obtained with the use of a 10-Mg/h Gruendler hammermill. The π Breakage model gave the best results for all conditions.

Shiflett, G.R., Trezek, G.J. "The Use of Residence Time and Nonlinear Optimization in Predicting Comminution Parameters in the Swing Hammermilling of Refuse," I-EC Process Design and Development, 18(3), (1979) pp. 437-440.

> In order to develop a method of accurately predicting product size distribution for a given feed size distribution, non-linear optimization techniques were used to determine values for the selection and breakage functions. The functions were shown to be dependent upon the conditions of the operation of the shredder. The matrix approach to predicting size distributions was modified to include variances in residence time. Mean residence time was found to increase with increase in holdup and feed rate.

Stratton, F.E., Alter, H., "Application of Bond Theory to Solid Waste Shredding," J. Environ. Engr. Div., ASCE, 104 (EEI) (1978).

> The Bond relationship was applied to the shredding of solid waste to determine the energy required to reduce a particular feed distribution to a specific product size. Using field data and estimated power consumption, the Bond work index was calculated for eleven different shredders.

Shiflett, G.R., "A Model for the Swing-Hammermill Size Reduction of Residential Refuse", D. Eng. dissertation, University of California at Berkeley, 1978.

> A model is presented which can simulate the hammermill size reduction of refuse based on the actual parameters of a system. The π,K model is extended to include the residence time concept, and estimation of selection and breakage functions based on process operating conditions. Quantitative empirical relationships were found between feed rate versus holdup and power requirements versus feed rate.

Austin, L.G., Jindal, V.K., Gotis, C., "A Model For Continuous Grinding in a Laboratory Hammer Mill," Powder Technology, 22:199-204 (1979).

> An examination was made of steady-state continuous grinding of maize with the use of a small laboratory hammermill. Model equations were developed for grinding with non-rapid, ideal classification. The authors observed that during steady-state grinding, breakage rates of all sizes greater than that of the exit opening must exactly match the feed rate into the mill. This fact signifies the existence of a maximum stable production rate that could be obtained. Predicted product size distributions compared reasonably well with the experimental data.

PROTOTYPE SIZE REDUCTION SYSTEMS

Burke, J.A., "Municipal Solid Waste Comminution by Steam Explosion," Design and Management for Resource Recovery, Vol. I, Energy From Waste, Ann Arbor Science Publishers, Inc. 1980.

> A description is given of a pilot program sponsored by U.S. Department

of Energy to determine feasibility of MSW comminution by steam explosion. With the method of steam explosion tested in the study, most of the organics were reduced to small particles. The inorganics usually were not affected.

Ito, K., Hirayama, Y., "Semi-Wet Selective Pulverizing System," Resource Recovery and Conservation, Vol. I, (1975), pp. 45-53.

A prototype system is described which combines pulverizing and classification of MSW into a single operation. The system consists of two rotating screens, one of which contains internal scrapers. Refuse is separated into three fractions: (1) brittle materials and food waste; (2) paper; and (3), plastics, textiles, leather, metals and paper residue.

SHREDDER SELECTION AND INSTALLATION CONSIDERATIONS

Hitte, S.J., Rogers, H.W., Solid Waste Shredding and Shredder Selection," EPA/530/sw-140, (March 1975).

Available shredder technology and variables which determine shredder selection are described. Guidelines are given for the selection of a shredder motor and for the evaluation of a specific shredder. The relationship between operating considerations and shredder design is discussed.

Savage G., Trezek G., Size Reduction in Solid Waste Processing, "Refuse Size Reduction Facility," EPA Grant No. R801218.

Relying upon the experience gained in the studies at U.C. Berkeley's Richmond Field Station waste processing laboratory, quantitative guidelines are developed for the design of a size reduction facility. Parameters are given for the design of the following shredder system components: conveyors, shredder foundation, and drive system. Installation considerations and problems also are discussed.

APPENDIX B

SIZE REDUCTION DEVICES USED IN SOLID WASTE PROCESSING FACILITIES*

Plant Location	Start-up Date	Equipment Description	Rated Capacity (Mg/h)	Status
Alaska				
Sitka	1976	One vertical shaft shredder	15 each	Operational
Anchorage	1979	Two vertical shaft shredders	70 each	Not operational
Prudhoe Bay	1979	One vertical shaft shredder	15	Operational
Prudhoe Bay	1979	One shear-type shredder	45 each	Operational
California				
Los Angeles	1979	One vertical shaft shredder	15	Operational
Mountain View	1972	One vertical shredder	30	Not operational
Palomar	1978	Two vertical shaft shredders	45 each	Operational
Sacramento	1980	One shear-type shredder	6	Operational
San Diego	--	One horizontal shredder	30	Not operational
Colorado				
Pueblo	1975	Two vertical shaft shredders	20 each	Operational
Connecticut				
Ansonia	1974	One horizontal shredder	30	Not operational

---

*adapted from the 1981 Shredder/Baler Index, Waste Age; Vol. 12, No. 7.

SIZE REDUCTION DEVICES USED IN SOLID WASTE PROCESSING FACILITIES (cont.)

Plant Location	Start-up Date	Equipment Description	Rated Capacity (Mg/h)	Status
Bridgeport	1978	One horizontal shredder, one flail mill	70	Not operational
Delaware				
New Castle Co.	1972	Four horizontal shredders	45 each	Not operational
Pigeon Point Del. Reclamation Project	Under cons.	Two vertical shaft shredders	80 each	Under construction
District of Columbia				
Washington, DC	1974	One horizontal shredder	45	Operational
Washington, DC	1980	One shear-type shredder	4	Operational
Florida				
Brevard County	1976	Two horizontal shredders	45 each	Operational
Dade County	1981 (proj.)	One shear-type shredder	5	Under construction
Key West	1979	One horizontal shredder	20	Operational
Pompano Beach	1978	Vertical shredder	90	Operational
South Dade Co.	1981 (proj.)	Three horizontal shredders	50 each	Under construction
North Dade Co.	1981 (proj.)	Two horizontal shredders	35 each	Under construction
Lakeland	1981 (proj.)	One non-reversable shredder	35	Under construction
Georgia				
Atlanta	1976	One horizontal shredder	55	Operational
DeKalb County	1973	Three vertical-shaft shredders	15 each	Operational
Macon	1980	One shear-type shredder	5	Operational

SIZE REDUCTION DEVICES USED IN SOLID WASTE PROCESSING FACILITIES (cont.)

Plant Location	Start-up Date	Equipment Description	Rated Capacity (Mg/h)	Status
Illinois				
Chicago	1976	Two horizontal primary shredders	70 each	Not operational
Chicago	1970	One horizontal shredder	25	Operational
LaMont	1975	One vertical shredder	20	Operational
Springfield	1980	One shear-type shredder	55	Operational
Indiana				
East Chicago	1977	One horizontal shredder	25	Operational
Iowa				
Ames	1975	Two horizontal shredders	--	Operational
Kansas				
McPherson	1975	One vertical shredder	15	Operational
Kansas City	1981	One shear-type shredder	2	Under construction
Kentucky				
Louisville	1964	One horizontal shredder	20	Not operational
Louisville	1980	One shear-type shredder	5	Operational
Louisiana				
New Orleans	1976	One horizontal, one vertical shredder	55	Operational
New Orleans	1981	One shear-type shredder	3	Operational
St. Mary's Parish	1979	Two vertical shaft shredders	20 each	Operational

SIZE REDUCTION DEVICES USED IN SOLID WASTE PROCESSING FACILITIES (cont.)

Plant Location	Start-up Date	Equipment Description	Rated Capacity (Mg/h)	Status
Vermillion Parish	1978	Two horizontal shredders	35, 55	Operational
Maine				
Lewiston	1977	One vertical shredder	25	Operational
Maryland				
Cockeysville	1975	Two horizontal shredders	55 each	Operational
Cockeysville	1980	Horizontal secondary shredder	30	
Massachusetts				
East Bridgewater	1977	One horizontal shredder	35	Not operational
North Adams	--	One horizontal shredder	35	Operational
Haverhill	1984	None reported		Under construction
Holliston	1974	One non-reversable shredder	45	Operational
Michigan				
Mackinaw Is.	1981	One shear-type shredder	5	Operational
Minnesota				
St. Paul	1976	One shear-type shredder	30	Operational
St. Paul	1978	One vertical shredder	30	Operational
Duluth	1980	Two horizontal shredders	30 each	Shakedown, operational late 1981
Missouri				
St. Louis	1969	One horizontal shredder	30	Operational

SIZE REDUCTION DEVICES USED IN SOLID WASTE PROCESSING FACILITIES (cont.)

Plant Location	Start-up Date	Equipment Description	Rated Capacity (Mg/h)	Status
Nebraska				
Omaha	1976	One horizontal shredder	45	Operational
New Hampshire				
Nashua	1980	Two shear-type shredders	2	Operational
New York				
Albany	1979	Two horizontal shredders	--	Operational
Elmira	1973	Two horizontal shredders	35 each	Operational
Hempstead	1978	Four shredder-like devices, Hydrapulpers	140	Not operational
Jamestown	1975	Two vertical shredders	45 each	Operational
Niagara Falls	1980	Three non-reversable shredders	80 each	Shakedown
Rochester, Monroe County	1979	Seven horizontal shaft shredders	(2) 70 (4) 45 (1) 10	Shakedown
Ohio				
Akron	1980			Operational
Columbus	Under cons.	Two vertical shredders	90	Under construction
Columbus	1975	Three horizontal shredders	55 each	Operational
Lorain	1980	One shear-type shredder	15	Operational
Oklahoma				
Oklahoma City	1982 (proj.)	Two shear-type shredders	30, 3	Under construction

SIZE REDUCTION DEVICES USED IN SOLID WASTE PROCESSING FACILITIES (cont.)

Plant Location	Start-up Date	Equipment Description	Rated Capacity (Mg/h)	Status
Oregon				
LaGrande	1978	One vertical-shaft shredder	20	Operational
Lane County	1977	Two horizontal shredders	60, 40	Operational
Portland	1981	One portable shear-type shredder	30	Operational
Wilsonville	1972	One shear-type shredder	30	Operational
Pennsylvania				
Altoona	1965	One vertical shredder	15	Operational
Harrisburg	1970	One horizontal shredder	25	Operational
Reading	1981	One shear-type shredder	20	Operational
South Carolina				
Beaufort	1975	One horizontal shredder	70	Operational
Charleston	1974	Three horizontal shredders	30 each	Operational
Georgetown Co.	1974	One vertical shredder	20	Operational
Williamsburg	1973	One vertical shredder	20	Operational
South Dakota				
Aberdeen	1975	One vertical shredder	20	Not operational
Tennessee				
Clarksville	1981	One shear-type shredder	10	Operational
Crossville				Shakedown

SIZE REDUCTION DEVICES USED IN SOLID WASTE PROCESSING FACILITIES (cont.)

Plant Location	Start-up Date	Equipment Description	Rated Capacity (Mg/h)	Status
Texas				
Dallas	1981	One shear-type shredder	5	Under construction
Houston	1965	One horizontal shredder	35	Operational
Houston	1981	Two shear-type shredders	30	Operational
Odessa	1974	One horizontal shredder	45	Operational
Texarkana	1977	One horizontal shredder	20	Operational
Virginia				
Norfolk	1975	One horizontal shredder	30	Operational
Washington				
Cowlitz County	1976	One horizontal shredder	45	Operational
Longview	1978	One shear-type shredder	5	Operational
Tacoma	1971	One horizontal shredder	40	Operational
Wisconsin				
Appleton	1974	Two horizontal shredders	15 each	Operational
Madison	1967	Flail mill, one vertical shredder	30	Operational
Milwaukee	1976	Two horizontal primary shredders	70	Operational
		Two vertical secondary shredders	55	

APPENDIX C

PARTIAL LISTING OF MSW SHREDDER MANUFACTURERS

1. American Pulverizer Company
   5540 West Park
   St. Louis, Missouri 63110

2. Williams Patent Crusher and Pulverizer Company
   2707 N. Broadway
   St. Louis, Missouri 63102

3. Hammermills, Inc.
   800 First Avenue, N.W.
   Cedar Rapids, Iowa 52405

4. Saturn Shredders
   P.O. Box 386
   Dept. 1Z
   Wilsonville, Oregon 97070

5. The Heil Company
   Engineered Systems Division
   3000 W. Montana Street
   Milwaukee, Wisconsin 53201

6. Newell Manufacturing Company
   P.O. Box 9367
   San Antonio, Texas 78204

7. Tracor Shredders
   6500 Tracor Lane
   Austin, Texas 78721

8. Jeffrey Manufacturing Division
   Dresser Industries, Inc.
   P.O. Box 2252-S
   Columbus, Ohio 43216

9. Pennsylvania Crusher
   P.O. Box 100
   Broomall, PA 19008

10. Hazemag U.S.A., Inc.
P.O. Box 15515
Pittsburg, PA 15244

11. Gruendler Crusher and Pulverizer Company
2915 North Market Street
St. Louis, Missouri 63106

APPENDIX D

UTILIZATION OF SELECTION AND BREAKAGE FUNCTIONS IN SHREDDER ANALYSIS

BACKGROUND

One of the methods for analyzing size reduction processes involves the use of selection and breakage functions. With these functions an attempt is made to model the mechanisms that occur within a size reduction device (e.g., ball mill, rod mill, hammermill). They were first developed for use in the mineral processing industry. Several attempts have been made to apply the resulting models to the shredding of municipal solid waste (Obeng, 1974; Shiflett, 1977). However, the attempts were severely hampered by the fact that the analyses of MSW processes generally are substantially more complex than those of the relatively homogeneous and brittle materials encountered in mineral processing. Nevertheless, selection and breakage function modeling can serve as a valuable tool in the predicting of product size distribution on the basis of the feed size distribution of MSW entering a shredder.

The selection function represents the fractional amount of a given size material selected for breakage during an increment of grinding. The breakage function represents the proportion of particles initially in a given size class, that is redistributed to each of the other size classes after breakage. These functions may be expressed either on a continuous or on a discrete basis for the parameters particle size and time.

Inasmuch as the application of selection and breakage function modeling involves mathematical techniques such as matrix manipulation and nonlinear optimization, the calculational procedure can be quite complex. However, the emphasis in the presentation that follows is on a description of the conceptual nature of the models and on the development of a familiarity with the basic calculations. In keeping with this emphasis, only a simplified example is presented. Inasmuch as certain users of the models need only supply inputs to computer codes, it is not necessary that they understand all of the detailed mathematics involved in the development of the models.

BASIC MODELS

The operation of the selection and breakage functions in the size reduction calculations is illustrated in the general mass balance:

$$p_i = f_i - s_i f_i + \sum_{j=1}^{i-1} b_{i,j} s_j f_j \qquad (D.1)$$

where: p_i = mass fraction of product in size class i;
f_i = mass fraction of feed in size class i;
s_i = selection function, or mass fraction of material in size class i that is broken during an increment of grinding; and
$b_{i,j}$ = breakage functions, or mass fraction of the material which is broken out of size class j and which reports to size class i.

In other words, the amount of material in a given product size class is equal to the amount of feed material in that same size class, minus the material that broke out of that size class, plus the material that resulted in that size class after breakage of material in other (larger) size classes.

The size class indices (i,j) are ordered such that the largest particle size and the largest size class are indexed equal to 1. Thus, as the index increases, the particle size or the size class becomes smaller. It should be noted that under this scheme, size class i is bounded by particle size i at its upper limit and by particle size i + 1 at its lower limit.

Utilizing a matrix formulation, the feed and product size distributions can be described by one-dimensional column vectors $\underline{f}$ and $\underline{p}$, respectively, with elements f_i and p_i. Using the notation "*" to refer to an n x n matrix, if S* represents selection function, B* represents the breakage function, and I* represents the identity matrix, then $B^*S^*\underline{f}$ defines the proportions of materials that are broken, and $(I^* - S^*)\underline{f}$ defines the proportions of materials that are left unbroken. These relations can be used to re-express Equation D.1 as

$$\underline{p} = B^*S^*\underline{f} + (I^* - S^*)\underline{f} \tag{D.2}$$

Combining terms yields

$$\underline{p} = [B^*S^* + (I^* - S^*)]\underline{f} \tag{D.3}$$

or

$$\underline{p} = D^*\underline{f} \tag{D.4}$$

where

$$D^* = [B^*S^* + (I^* - S^*)] \tag{D.5}$$

Typically, the size classes of particles considered after a size reduction process are the same as the size classes considered in the feed. Under these conditions, $\underline{f}$ and $\underline{p}$ are both n x 1 column vectors, and S*, B*, and I* are n x n square matrices. Moreover, S* and I* are diagonal matrices, and B* is a lower triangular matrix.

On a time-continuous basis, a general mass balance would take the following form if constant holdup is assumed.

$$\frac{d}{dt} m_i(t) = -s_i m_i(t) + \sum_{j=1}^{i-1} b_{i,j} s_j m_j(t) \qquad (D.6)$$

where: m = mass fraction of material in a given size class at any point in time.

Thus, n simultaneous equations of the form given in Equation D.6 would be generated. This set of simultaneous equations can be expressed in a matrix formulation as

$$\frac{d}{dt} [\underline{m}(t)] = - (I^*-B^*)S^* \, \underline{m}(t) \qquad (D.7)$$

Due to the convenience resulting in the mathematics of the selection and breakage function modeling process, the difference between size classes is taken as a constant ratio, such that

$$x_i = r x_{i+1} \qquad (D.8)$$

where: x = the size limit of a size class (e.g., screen aperture size)
r = the ratio between the size limits of size classes (also referred to as the "sieve ratio")

Although some size classifying systems employ constant ratios between size limits (e.g., Tyler Series, U.S. Standard Series), it is not necessary to use such measurement systems in order to compare experimental results with the predictions of the selection and breakage function models. All that is required is a plot of both predicted and measured size distributions. The determination of selection and breakage function parametric values generally requires the use of data specified in terms of the same size classes as the models. An optimization technique is then employed to determine the "best fit" values for the selection and breakage functions.

EXAMPLE: CONSTANT SELECTION FUNCTION—EQUALLY DISTRIBUTED BREAKAGE FUNCTION

Assumptions

1. Feed Size Distribution

   The feed size distribution is assumed to be equally distributed among 4 size classes listed in Table D.1.

2. Selection Function

   A constant selection function is assumed that ensures that during a given increment of grinding, 75 percent of the material in each size class is broken.

3. Breakage Function

   The breakage function is assumed such that after breakage of material in a given size class, the broken material is equally distributed among

TABLE D.1. ASSUMED FEED SIZE DISTRIBUTION FOR SELECTION AND BREAKAGE FUNCTION ANALYSIS

Size Class	Mass Fraction	Cumulative Fraction
4.00> x >2.00	0.25	1.00
2.00> x >1.00	0.25	0.75
1.00> x >0.50	0.25	0.50
0.50> x >0.00	0.25	0.25

all of the smaller size classes. Thus, one-third of the material that breaks in the size class 4.00> x >2.00 is reduced to each of the three size classes smaller than itself, one half of the material that breaks in the size class 2.00> x >1.00 is reduced to each of the two size classes smaller than itself, and all of the material that breaks in the size class 1.0> x >0.5 enters the smallest size class.

Two solution approaches are now demonstrated, namely, an algebraic approach and a matrix approach.

A. Algebraic Approach

The product size distribution can be determined simply by applying Equation D.1 to each size class. The calculations are as follows:

$$\begin{aligned} p(4.00 > x > 2.00) &= 0.25 - (0.75)(0.25) + 0 \\ &= 0.063 \end{aligned}$$

$$\begin{aligned} p(2.00 > x > 1.00) &= 0.25 - (0.75)(0.25) + (0.33)(0.75)(0.25) \\ &= 0.125 \end{aligned}$$

$$\begin{aligned} p(1.00 > x > 0.50) &= 0.25 - (0.75)(0.25) + (0.33)(0.75)(0.25) \\ &\quad + (0.50)(0.75)(0.25) \\ &= 0.218 \end{aligned}$$

$$\begin{aligned} p(0.50 > x > 0.00) &= 0.25 - 0 + (0.33)(0.75)(0.25) \\ &\quad + (.050)(0.75)(0.25) \\ &\quad + (1.00)(0.75)(0.25) \\ &= 0.594 \end{aligned}$$

The product size distribution results are shown in Table D.2. The feed and product size distributions are graphically illustrated by way of the log-log plot shown in Figure D.1.

The algebraic approach is relatively straightforward in this example. However, as the number of size classes is increased, the algebraic approach rapidly becomes tedious. An alternative is a matrix approach that is well-suited to a computerized solution.

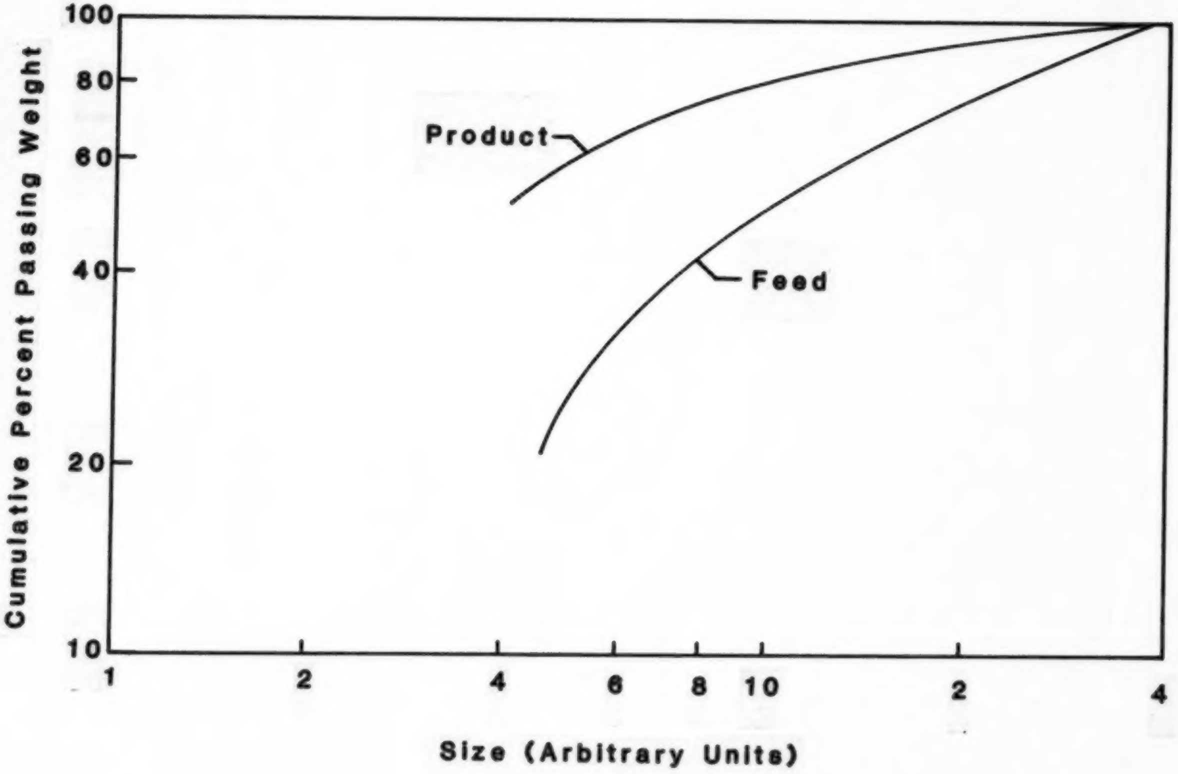

Figure D.1. The feed and product size distributions for selection and breakage function sample calculations.

EPA Form 2350-4 (4-80)
(PREVIOUSLY CIN. EPA FORM 337)
TYPING GUIDE SHEET

TABLE D.2. CALCULATED PRODUCT SIZE DISTRIBUTION FROM SELECTION AND BREAKAGE FUNCTION ANALYSIS

Size Class	Mass Fraction	Cumulative Fraction
4.00> x >2.00	0.063	1.000
2.00> x >1.00	0.125	0.937
1.00> x >0.50	0.218	0.812
0.50> x >0.00	0.594	0.594

B. Matrix Approach

Utilizing a matrix approach to the previous example, the following matrices are generated: The feed size distribution takes the form

$$\underline{f} = \begin{vmatrix} f_1 \\ f_2 \\ f_3 \\ f_4 \end{vmatrix} = \begin{vmatrix} 0.250 \\ 0.250 \\ 0.250 \\ 0.250 \end{vmatrix}$$

The selection function takes the form

$$S^{\star} = \begin{vmatrix} s_{11} & 0 & 0 & 0 \\ 0 & s_{22} & 0 & 0 \\ 0 & 0 & s_{33} & 0 \\ 0 & 0 & 0 & s_{44} \end{vmatrix} = \begin{vmatrix} 0.750 & 0 & 0 & 0 \\ 0 & 0.750 & 0 & 0 \\ 0 & 0 & 0.750 & 0 \\ 0 & 0 & 0 & 0 \end{vmatrix}$$

Inasmuch as no material is considered to break out of the smallest size fraction, s_{44} is set equal to zero in this case. The breakage function takes the form

$$B^{\star} = \begin{vmatrix} 0 & 0 & 0 & 0 \\ b_{21} & 0 & 0 & 0 \\ b_{31} & b_{32} & 0 & 0 \\ b_{41} & b_{42} & b_{43} & 0 \end{vmatrix} = \begin{vmatrix} 0 & 0 & 0 & 0 \\ 0.333 & 0 & 0 & 0 \\ 0.333 & 0.500 & 0 & 0 \\ 0.333 & 0.500 & 1.000 & 0 \end{vmatrix}$$

The identity matrix, by definition, is

$$I^* = \begin{vmatrix} 1 & 0 & 0 & 0 \\ 0 & 1 & 0 & 0 \\ 0 & 0 & 1 & 0 \\ 0 & 0 & 0 & 1 \end{vmatrix}$$

The step-by-step calculations for the solution of the product size distribution as given in Equation D.3 are as follows.

$$B^*S^* = \begin{vmatrix} 0 & 0 & 0 & 0 \\ 0.333 & 0 & 0 & 0 \\ 0.333 & 0.500 & 0 & 0 \\ 0.333 & 0.500 & 1.000 & 0 \end{vmatrix} \times \begin{vmatrix} 0.750 & 0 & 0 & 0 \\ 0 & 0.750 & 0 & 0 \\ 0 & 0 & 0.750 & 0 \\ 0 & 0 & 0 & 0 \end{vmatrix}$$

$$= \begin{vmatrix} 0 & 0 & 0 & 0 \\ 0.250 & 0 & 0 & 0 \\ 0.250 & 0.375 & 0 & 0 \\ 0.250 & 0.375 & 0.750 & 0 \end{vmatrix}$$

$$(I^*-S^*) = \begin{vmatrix} 1 & 0 & 0 & 0 \\ 0 & 1 & 0 & 0 \\ 0 & 0 & 1 & 0 \\ 0 & 0 & 0 & 1 \end{vmatrix} - \begin{vmatrix} 0.750 & 0 & 0 & 0 \\ 0 & 0.750 & 0 & 0 \\ 0 & 0 & 0.750 & 0 \\ 0 & 0 & 0 & 0 \end{vmatrix}$$

$$= \begin{vmatrix} 0.250 & 0 & 0 & 0 \\ 0 & 0.250 & 0 & 0 \\ 0 & 0 & 0.250 & 0 \\ 0 & 0 & 0 & 1.000 \end{vmatrix}$$

$$B^*S^* + (I^*-S^*) = \begin{vmatrix} 0 & 0 & 0 & 0 \\ 0.250 & 0 & 0 & 0 \\ 0.250 & 0.375 & 0 & 0 \\ 0.250 & 0.375 & 0.750 & 0 \end{vmatrix} + \begin{vmatrix} 0.250 & 0 & 0 & 0 \\ 0 & 0.250 & 0 & 0 \\ 0 & 0 & 0.250 & 0 \\ 0 & 0 & 0 & 1.000 \end{vmatrix}$$

$$= \begin{vmatrix} 0.250 & 0 & 0 & 0 \\ 0.250 & 0.250 & 0 & 0 \\ 0.250 & 0.3750 & 0.250 & 0 \\ 0.250 & 0.3750 & 0.750 & 1.000 \end{vmatrix}$$

From Equation D.3, the product size distribution is

$$\underline{p} = [B^*S^* + (I^*-S^*)]\underline{f}$$

Consequently, substitution of the matrices given above for B*S* and (I*-S*) yields,

$$\underline{p} = \begin{vmatrix} 0.250 & 0 & 0 & 0 \\ 0.250 & 0.250 & 0 & 0 \\ 0.250 & 0.375 & 0.250 & 0 \\ 0.250 & 0.375 & 0.750 & 1.000 \end{vmatrix} \times \begin{vmatrix} 0.250 \\ 0.250 \\ 0.250 \\ 0.250 \end{vmatrix}$$

and therefore,

$$\underline{p} = \begin{vmatrix} p_1 \\ p_2 \\ p_3 \\ p_4 \end{vmatrix} = \begin{vmatrix} 0.063 \\ 0.125 \\ 0.218 \\ 0.594 \end{vmatrix}$$

The product size distribution calculated by means of the preceding matrix approach is the same as those determined through the use of the algebraic approach (see Table D.2).

SELECTION AND BREAKAGE FUNCTIONS USED FOR SOLID WASTE ANALYSIS

The sophistication, and therefore the complexity, of the selection and breakage modeling method may be increased in order to improve the predictive capability of the method. For example, the selection and breakage process may be represented by functional relationships. Several such functional relationships have been developed. In general, they consist of analytical expressions that contain certain key fundamental variables where representation depends upon the developer of the theory.

Obeng (1974) and Obeng and Trezek (1975) examined the use of two different breakage functions for modeling the comminution of solid waste. The first one is based on a modified form of an equation proposed by Broadbent and Callcott, such that

$$B\,(x,X_0) = 1 - \exp[-(\tfrac{x}{X_0})^n]\,/[1 - \exp(-1)] \qquad \text{(D.9)}$$

where: B = breakage function;
x = a given size particle;
X_0 = the characteristic particle size; and
n = a positive index.

Equation D.9 represents a normalized form of the Rosin-Rammler equation. Experimental results reported by Obeng and Trezek indicate that values of n fall between 0.845 and unity. A second relation was based on the Gaudin-Meloy distribution equation

$$B\,(x,X_0) = 1 - (1-x/X_0)^r \qquad \text{(D.10)}$$

where: r = the size ratio.

Equation D.10 was found to better predict the size distribution after primary shredding; whereas Equation D.9 produced a better correlation for secondary and tertiary shredding.

Obeng and Trezek also examined the use of several selection functions. They found that either a constant selection function (as used in the preceding example) or a repeated breakage cycle based on a constant selection function could produce predicted distributions close to those measured after shredding.

Shiflett (1977) and Shiflett and Trezek (1979), following the approach of Herbst and Fuerstenau (1968), made use of discretized breakage and selection functions of the form

$$B_{ij} = \frac{K}{s_1}\left(\frac{x_i^{\,2}}{x_j\,x_{j+1}}\right)^{\alpha/2} \qquad \text{(D.11)}$$

and

$$s_i = s_1\left(\frac{x_j\,x_{i+1}}{x_1\,x_2}\right)^{\alpha/2} \qquad \text{(D.12)}$$

where: K, α = time invariant constants derived from zero-order production rate models; and

s_1 = the initial selection function.

Evaluation of the parameters K, α, and s_1 were determined through the use of an optimization technique to fit experimental data.

Further refinement of selection and breakage function models for use in solid waste analysis remains to be made, particularly for mixtures containing significant mass fractions of nonbrittle materials. Model parameters as yet must be correlated to shredder design and operating parameters. Nevertheless, the results of efforts made thus far indicate the existence of a promising potential for the use of selection and breakage function models in the analysis of solid waste shredding.

REFERENCES

1. Herbst, J.A. and Fuerstenau, D.W. 1968. "The Zero Order Production of Fine Sizes in Comminution and Its Implications in Simulation." Trans. AIME. 241:538.

2. Obeng, D.M. 1974. "Comminution of a Heterogeneous Mixture of Brittle and Non-Brittle Materials." Ph.D. Thesis. University of California, Berkeley.

3. Obeng, D.M. and Trezek, G.J. 1975. "Simulation of the Comminution of a Heterogenous Mixture of Brittle and Nonbrittle Materials in a Swing Hammermill." Ind. Eng. Chem. Process Des. Dev. 14(2).

4. Shiflett, G.R. 1977. "A Model for the Swing-Hammermill Size Reduction of Residential Refuse." Ph.D. Thesis. University of California, Berkeley.

5. Shiflett, G.R. and Trezek, G.J. 1979. "The Use of Residence Time and Nonlinear Optimization in Predicting Comminution Parameters in the Swing Hammermilling of Refuse." Ind. Eng. Chem. Process Des. Dev. 18(3).

APPENDIX E

SHREDDER ROTOR MASS MOMENT OF INERTIA

The mass moment of inertia (I) of a shredder rotor is an important machine parameter inasmuch as when the rotor is revolving it acts as an effective energy storage and delivery mechanism for meeting and overcoming transient loads placed on the shredder. Since potential energy is stored in a mass rotating at a constant speed, kinetic energy will be withdrawn from the system when the mass decelerates and will be added to the system when the mass is accelerated. The magnitude of the kinetic energy (KE) of a rotating mass is proportional to the product of the mass moment of inertia and the square of the rotational velocity (ω),

$$KE = \frac{1}{2} I \omega^2 \qquad (E.1)$$

Inasmuch as the work done by the system is proportional to the change in KE, a deceleration of a rotating mass results in a flow of energy into the system that is proportional to the difference in the squares of the rotational velocities. In the case of a size reduction system placed under a transient load, the rotating mass would respond by decelerating and thereby energy would be supplied for breakage of the material. After overcoming the transient load, the rotating mass would accelerate to a steady state value and stored energy again would be available to the system when needed.

From basic engineering mechanics, the mass moment of inertia (I) of a mass element about an axis is defined to be the product of the mass of the element (dm) and the square of the perpendicular distance (y) from the mass element to the axis. The limit of the sum of these products represents the value of I about the given axis for a solid body of mass m composed of an aggregate of mass elements:

$$I = \int y^2 dm \qquad (E.2)$$

Values of I about centroidal axes ($\bar{I}$) of solid bodies with common shapes such as cylinders, circular and rectangular plates, and spheres are listed in most texts on engineering mechanics.

If the value of I of a given body is required about an axis parallel to a centroidal axis (I^1) the parallel axis theorem may be used:

$$I^1 = \bar{I} + md^2 \qquad (E.3)$$

where m is the mass of the body and d is the perpendicular distance from its centroidal axis to the parallel axis about which the value of I is required. A body which is considered to be composed of a number of parts has a mass moment of inertia about a given axis equal to the sum of inertias of the parts about that axis.

$$I_T = \sum_{i=1}^{n} I_i \tag{E.4}$$

where I_T is the mass moment of inertia about the axis of the body composed of n parts and I_i is the mass moment of inertia of the $i^{\underline{th}}$ part about the same axis.

Typically, the elements of the MSW shredder rotor that compose the mass contributing to the inertia are the rotor shaft, the hammers, the hammer pins, and the disks that support the hammer pins and the hammers. Some rotor assemblies also have disk spacers and pin protectors -- the masses of which also will contribute to the inertia.

A method for determining the mass moment of inertia of the rotor assembly shown in Figure E.1 is as follows:

The axis of rotation of the shaft of the rotor assembly, the longitudinal axis of the rotor shaft (axis A-A), is that about which the moment of inertia (I) is evaluated. The rotor shaft, the hammer pins, the disks, and the hammers are the elements to be considered. The length (L) of the rotor assembly is taken to be the distance between the outside faces of the end disks. The value of I about axis A-A of each component is determined separately.

The mass moment of inertia of a circular cylinder about its longitudinal axis is given by:

$$\bar{I} = \frac{1}{2} mr^2 \tag{E.5}$$

where m is the mass of the cylinder and r is its radius. The bar above the I denotes that the value is being evaluated about the body's centroidal axis. Applying Equation E.5 the contribution to the rotor mass moment of inertia from the shaft is obtained:

$$I_s = \frac{1}{2} m_s r_s^2 \tag{E.6}$$

where the "s" subscripts signify shaft. It should be pointed out that the mass of an element may not be known. In such a case the volume of the element may be multiplied by the density (ρ) of the material in order to obtain the mass. The volume of the shaft (V_s) in the rotor assembly is given by:

$$V_s = \pi r_s^2 L \tag{E.7}$$

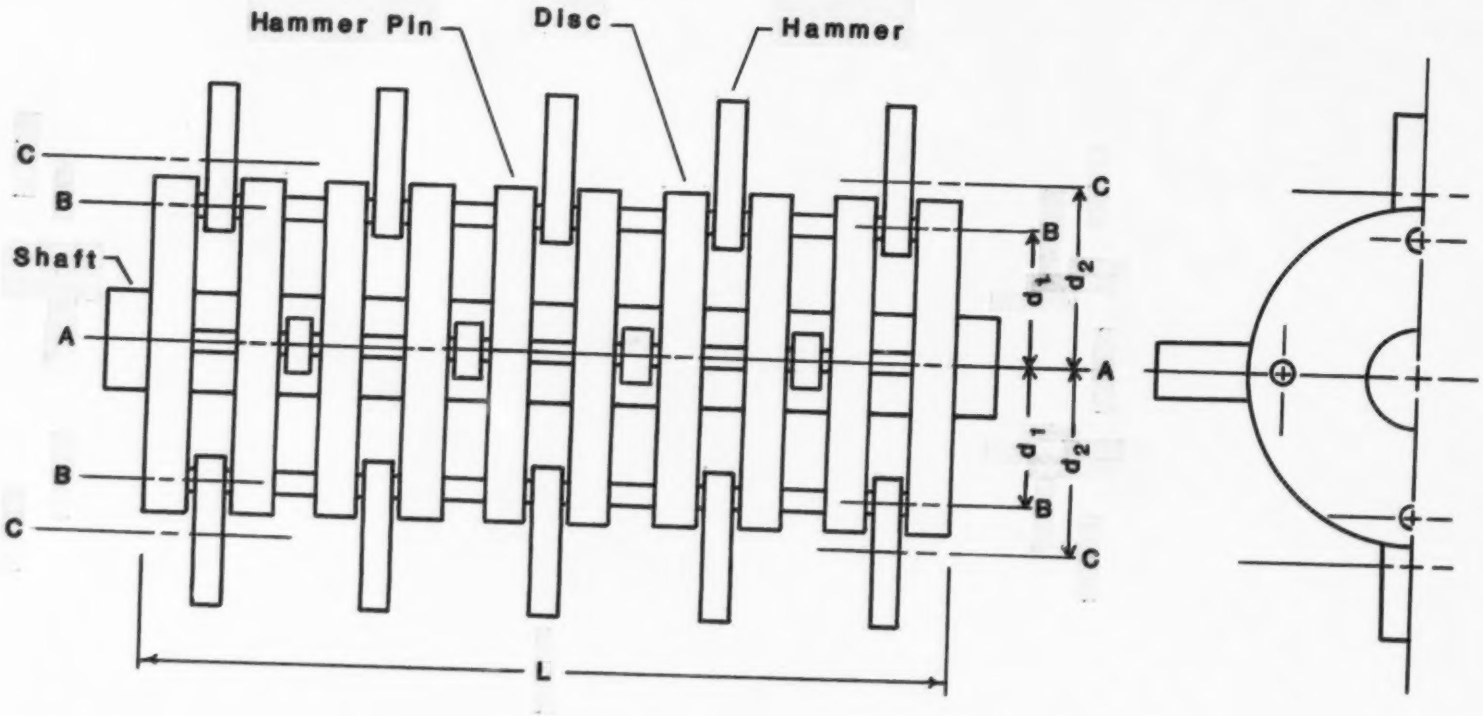

Figure E.1. Typical hammermill rotor assembly.

and

$$m_s = \pi r_s{}^2 L\rho \tag{E.8}$$

Equation E.6 can be rewritten in terms of density,

$$I_s = \frac{1}{2} \pi r_s{}^4 L\rho \tag{E.9}$$

The expression for the mass moment of inertia of a hammer pin about its own longitudinal axis, $\bar{I}_p$, (axis B-B in Figure E.1) is

$$\bar{I}_p = \frac{1}{2} \pi r_p{}^4 L\rho \tag{E.10}$$

where r_p is the radius of the hammer pin. The parallel axis theorem (Equation E.3) is needed for finding the value of the moment of inertia about axis A-A (I_p),

$$I_p = \bar{I}_p + m_p d_1{}^2 \tag{E.11}$$

where m_p is the mass of the hammer pin, and d_1 is the perpendicular distance from axis B-B to axis A-A in Figure E.1.

Making the appropriate substitution using Equation E.10 and expressing mass in terms of density and volume, the following equation is obtained:

$$I_p = \frac{1}{2} \pi r_p{}^4 L\rho + \pi r_p{}^2 L\rho\, d_1{}^2$$

$$= \pi r_p{}^2 L\rho \left(\frac{1}{2} r_p{}^2 + d_1{}^2\right) \tag{E.12}$$

Since the rotor shown in Figure E.1 has four identical hammer pins symmetrically spaced about the rotor shaft, the contribution to the mass moment of inertia of the rotor from the hammer pins is $4I_p$.

In evaluating I for a disc (I_d) shown in Figure E.1, an account must be made for the hole in the center of the disc through which the rotor shaft runs, as well as for the four holes around its perimeter through which the hammer pins run. The accounting is made by evaluating I for a solid disc (I_{sd}) and subtracting the values of I for the shaft hole (I_{sh}) and the pin holes (I_{ph}). Therefore, for a single disc:

$$I_d = I_{sd} - I_{sh} - 4I_{ph} \tag{E.13}$$

The centroidal axis about which I_s is evaluated is the same as axis A-A. The mass moment of inertia of a disc about the centroidal axis normal to its face can be obtained from Equation E.5, substituting in the values of m_d and r_d the mass and radius of the disc, respectively. The expression for the mass of the solid disc (m_{sd}) in terms of density is

$$m_{sd} = \pi r_d^2 t_d \rho \tag{E.14}$$

where t_d is the thickness of the disc.

Therefore,

$$I_{sd} = \frac{1}{2} \pi r_d^4 t_d \rho \tag{E.15}$$

The expression for I_{sh} is the same as that for I_s (Equation E.9) excepting that L is replaced by t_d.

$$I_{sh} = \frac{1}{2} \pi r_s^4 t_d \rho \tag{E.16}$$

Similarly, the equation for I_{ph} is the same as that for I_p (Equation E.10), excepting that t_d replaces L.

$$I_{ph} = \pi r_p^2 t_d \rho \left(\frac{1}{2} r_p^2 + d_1^2\right) \tag{E.17}$$

Substituting the expressions for I_{sd}, I_{sh}, and I_{ph} (obtained from Equations E.15, E.16, and E.17 respectively) into Equation E.13, the mass moment of inertia of a disc about the axis of rotation (I_d) results in

$$I_d = \frac{1}{2} \pi r_d^4 t_d \rho - \frac{1}{2} \pi r_s^4 t_p \rho$$

$$- 4 \pi r_p^2 t_d \rho \left(\frac{1}{2} r_p^2 + d_1^2\right) \tag{E.18}$$

The mass moment of inertia of all ten discs shown in Figure E.1 is $10I_d$.

In calculating the value of I for a hammer the contribution of the mass of the hole, through which the pin runs, must be subtracted from the hammer. The mass moment of inertia of a solid hammer (I_{sh}) minus that of the pin hole (I_o) yields the I value of hammer (I_h),

$$I_h = I_{sh} - I_o \tag{E.19}$$

The mass moment of inertia of a solid rectangular hammer about the centroidal axis normal to its face (axis C-C shown in Figure E.1), ($\bar{I}_{sh}$), is given by:

$$\bar{I}_{sh} = \frac{1}{12} m_{sh}(b^2 + h^2) \tag{E.20}$$

where the mass of the hammer (m_{sh}) is,

$$m_{sh} = bht_h\rho \qquad (E.21)$$

where t_h is the hammer thickness. Applying the parallel axis theorem (Equation E.3) the mass moment of inertia of the solid hammers about the axis of rotation (I_{sh}) can be obtained, if the perpendicular distance from between axes C-C and A-A in Figure E.1 is d_2. From Equation E.3,

$$\begin{aligned} I_{sh} &= \bar{I}_{sh} + m_{sh}{d_2}^2 \\ &= \frac{1}{12}\, bht_h\rho\, (b^2 + h^2) + bht_h\rho {d_2}^2 \\ &= bht_h\rho \left(\frac{b^2 + h^2}{12} + {d_2}^2\right) \end{aligned} \qquad (E.22)$$

The only difference between I_o and I_{ph} which is evaluated through the use of Equation E.17, is the use of thickness of a hammer (t_h) rather than of the thickness of a disc (t_d) in the evaluation of I_o.

$$I_o = \pi\, {r_p}^2 t_h\rho \left(\frac{1}{2}\, {r_p}^2 + {d_1}^2\right) \qquad (E.23)$$

I_h can now be obtained by substituting the expressions for I_{sh} (Equation E.22) and I_o (Equation E.23) into Equation E.19.

$$\begin{aligned} I_h &= bht_h\rho \left(\frac{b^2 + h^2}{12} + {d_2}^2\right) \\ &\quad - \pi\, {r_p}^2 t_h\rho \left(\frac{1}{2}\, {r_p}^2 + {d_1}^2\right) \end{aligned} \qquad (E.24)$$

Since there are 18 hammers spaced symmetrically about axis A-A shown in Figure E.1, the total mass moment of inertia contributed by the hammers is 18 I_h.

Given the expressions for the values of I of the components in Equations E.9, E.12, E.18, and E.24, Equation E.4 can be used to evaluate the mass moment of inertia of the shredder rotor about its axis of rotation (I_r), namely,

$$I_r = I_s + 4I_p + 10I_d + 18I_h \qquad (E.25)$$

Example

The mass moment of inertia of a shredder rotor can be calculated through the application of the equations developed in the previous paragraphs and the description of the rotor elements given in Table E.1. The detailed calculation of the mass moment of inertia of each element follows:

TABLE E.1. DESCRIPTION OF ROTOR ELEMENTS*

Item No.	Qty.	Item	Dimensions
1)	44	Hammers	Approximate as rectangular, 38.1 mm x 114.3 mm x 0.30 m W/1 pin hole 44.5 mm dia
2)	8	Pins	44.5 mm dia x 1.28 m long
3)	10	Inner Rotor Discs	0.56 m O.D., 0.22 m I.D., 25.4 mm thick W/8 pin holes 44.5 mm dia
4)	2	Outer Rotor Discs	0.58 m O.D., 0.22 mm I.D., 25.4 mm thick W/12.7 thick x 38.1 mm wide rim and 8 pin holes 44.5 mm dia
5)	1	Shaft	0.22 m dia x 1.28 m long
6)	2	Shaft	0.17 m dia x 0.42 m long
7)	2	Shaft	0.14 m dia x 0.33 m long
8)	1	Flywheel	0.89 m O.D., 0.14 m I.D., 0.10 m thick W/8 holes 50.8 mm dia
9)	1	Key Guard	0.28 m O.D., 0.14 m I.D., 0.10 m thick
10)	22	Disc Spacers	0.27 m O.D., 0.22 m I.D. 44.5 mm thick

* All elements are of steel.

Note: I^* = Mass moment of inertia of element about an axis parallel to axis of rotation through center of gravity (C.G.).

I = Mass moment of inertia about axis of rotation.

1) Hammers

$$I_h = I^*_{sh} - I^*_{ph} + m_1 d_1^2 - m_2 d_2^2$$

Where: H = hammer;

sh = solid hammer;

ph = pin hole;

d_1 = perpendicular distance from axis of rotation to C.G. of hammer (m);

d_2 = perpendicular distance from axis of rotation to C.G. of pin hole (m);

m_1 = mass of hammer (kg); and

m_2 = volume of pin hole (m^3) x density (ρ) of steel, kg/m^3.

$$I^*_{sh} = \frac{1}{12} m (b^2 + h^2) = \frac{1}{12} bht\rho\ (b^2 + h^2) = \frac{1}{12} (0.30\ m)(0.1143\ m)$$

$$(0.0381\ m) \times (7860\ kg/m^3)\ [(0.30\ m)^2 + (0.1143)^3]$$

$$= 881.9 \times 10^{-4}\ kg\text{-}m^2$$

$$I^*_{ph} = \frac{1}{2} mr^2 = \frac{1}{2} \pi r^2 t\rho r^2 = \frac{1}{2} \pi\ (0.0223\ m)^2(0.0381\ m)$$

$$(7860\ kg/m^3) \times (0.0223\ m)^2$$

$$= 1.16 \times 10^{-4}\ kg\text{-}m^2$$

$$m_1 d_1{}^2 = bht\rho d_1{}^2 = (0.30\ m)(0.1143\ m)(0.0381\ m)(7860\ kg/m^3)$$

$$\times\ (0.30\ m)^2 = 9241.8 \times 10^{-4}\ kg\text{-}m^2$$

$$m_2 d_2{}^2 = \pi r^2 t\rho_2{}^2 = \pi\ (0.0223\ m^2(0.0381\ m)(7860\ kg/m^2)(0.191\ m)$$

$$= 284.4 \times 10^{-4}\ kg\text{-}m^2$$

$$I_h = 881.9 \times 10^{-4}\ kg\text{-}m^2 - 1.2 \times 10^{-4}\ kg\text{-}m^2 + 9241.8 \times 10^{-4}\ kg\text{-}m^2$$

$= 9838.1 \times 10^{-4}\ kg\text{-}m^2$ per hammer x 44 hammers, $I_H = 43.29\ kg\text{-}m^2$

2) Pins

$$I_p = I^*_p + md^2$$

Where: p = pin;
d = perpendicular distance from axis of rotation to C.G. of pin (m); and
m = mass of pin (kg).

$$I^*_p = \frac{1}{2} mr^2 = \frac{1}{2} \pi r^2 l\rho r^2 = \frac{1}{2} \pi\ (0.0223\ m)^2(1.28\ m)(7860\ kg/m^3)$$

$$(0.0223\ m)^2 = 39.1 \times 10^{-4}\ kg\text{-}m^2$$

$$md^2 = \pi r^2 l\rho d^2 = \pi(0.0223\ m)^2(1.28\ m)(7860\ kg/m^3)(0.191\ m)$$

$$= 30021.0 \times 10^{-4}\ kg\text{-}m^2$$

$$I_p = 39.1 \times 10^{-4}\ kg\text{-}m^2 + 30021.0 \times 10^{-4}\ kg\text{-}m^2 = 30060.1 \times kg\text{-}m^2$$

per pin x 8 pins = $I_p = 24.05\ kg\text{-}m^2$

3) Inner Rotor Disc

$$I_{di} = I_{sd} - I_{sh} - 8I^*_{ph} - 8m_1d_1{}^2$$

Where: di = inner rotor disc;
sd = solid disc;
sh = shaft hole;
ph = pin hole;
d_1 = perpendicular distance from axis of rotation to C.G. of pin hole (m); and
m_1 = volume of pin hole x density of steel.

$$I_{sd} = \frac{1}{2}mr^2 = \frac{1}{2}\pi r^4\rho t = \frac{1}{2}\pi\ (0.28\ m)^4(0.0254\ m)(7860\ kg/m^3)$$

$$= 19275.6 \times 10^{-4}\ kg\text{-}m^2$$

$$I_{sh} = \frac{1}{2}mr_1{}^2 = \frac{1}{2}\pi r_1{}^4t\rho = \frac{1}{2}\ (0.11\ m)^4(0.0254\ m)(7860\ kg/m^3)$$

$$= 459.1 \times 10^{-4}\ kg\text{-}m^2$$

$$8I^*_{ph} = 8\ (\frac{1}{2}mr_2{}^2) = 4\pi r_2{}^4t\rho = 4\pi\ (0.0223\ m)^4(0.0254\ m)(7860\ kg/m^3)$$

$$= 6.2 \times 10^{-4}\ kg\text{-}m^2$$

$$8m_1d_1{}^2 = 8\ (\pi r_2{}^2t\rho d_1{}^2) = 8\pi\ (0.0223\ m)^2(0.0254)(7860\ kg/m^3)(0.191)^2$$

$$= 910.3 \times 10^{-4}\ kg\text{-}m^2$$

$I_{di} = 19275.6 \times 10^{-4}\ kg\text{-}m^2 - 459.1 \times 10^{-4}\ kg\text{-}m^2 - 6.2 \times 10^{-4}\ kg\text{-}m^2 - 910.3 \times 10^{-4}\ kg\text{-}m^2$ per inner rotor disc x 10 inner rotor discs = $I_{di} = 17.90\ kg\text{-}m^2$

4) Outer Rotor Disc

$$I_{do} = I_{ds} - I_{sh} - 8I^{*}_{ph} - 8m_1d_1^2 + m_2d_2^2$$

Where: do = outer rotor disc;

ds = solid disc;

$I_{sh} = 459.1 \times 10^{-4}$ kg-m^2 (from item No. 3);

$8I^{*}_{ph} = 6.2 \times 10^{-4}$ kg-m^2 (from item No. 3);

$8m_1{d_1}^2 = 910.3 \times 10^{-4}$ kg-m^2 (from item No. 3); and

$m_2{d_2}^2$ = moment of inertia of rim.

$$I_{ds} = \frac{1}{2} mr^2 = \frac{1}{2} \pi r^4 t\rho = \frac{1}{2} \pi \ (0.29)^4(0.0254 \text{ m})(7860 \text{ kg/m}^3)$$

$$= 22180.3 \times 10^{-4} \text{ kg-m}^2$$

$$m_2{d_2}^2 = \pi({r_o}^2 - {r_1}^2)t)\rho {d_2}^2 = \pi \ [(0.303 \text{ m})^2 - (0.290 \text{ m})^2](0.0381 \text{ m})$$

$$(7860 \text{ kg/m}) \times (0.298 \text{ m})^2 = 21612.8 \times 10^{-4} \text{ kg-m}^2$$

$$I_{do} = 22180.3 \times 10^{-4} \text{ kg-m}^2 - 459.1 \times 10^{-4} \text{ kg-m}^2 - 910.3_{m} \times 10^{-4} \text{ kg-m}^2$$

$$+ 21612.8 \times 10^{-4} \text{ kg-m}^2 = 42417.5 \times 10^{-4} \text{ kg-m}^2 \text{ per outer rotor}$$

$$\text{disc} \times 2 \text{ outer rotor discs} = I_{DO} = 8.48 \text{ kg-m}^2$$

5) Shaft

$$I_{s1} = I^{*}_{sI} = \frac{1}{2} mr^2 = \frac{1}{2} \pi r^4 l\rho = \frac{1}{2} \pi \ (0.11 \text{ m})^4(1.28 \text{ m})(7860 \text{ kg/m}^3)$$

$$= 2.31 \text{ kg-m}^2$$

6) Shaft

$$I_{s2} = I^{*}_{S2} = \frac{1}{2} mr^2 = \frac{1}{2} \pi r^4 l\rho = \frac{1}{2} \pi \ (0.085 \text{ m})^4(0.42 \text{ m})(7860 \text{ kg/m}^3)$$

$$= 0.27 \text{ kg-m}^2 \text{ per shaft} \times 2 \text{ shafts} = I_{S2} = 0.54 \text{ kg-m}^2$$

7) Shafts

$$I_{s3} = I^{*}_{S3} = \frac{1}{2} mr^{2} = \frac{1}{2} \pi \ (0.33 \text{ m})(7860 \text{ kg/m}^{3})$$

$$= 0.098 \text{ kg-m}^{2} \text{ per shaft x 2 shafts} = I_{S3} = 0.20 \text{ kg-m}^{2}$$

8) Flywheel

$$I_{f} = I^{*}_{sf} - 8I^{*}_{h} - I_{sh} - 8m_{1}d_{1}^{2}$$

Where: f = flywheel;
sf = solid flywheel;
h = hole;
sh = shaft hole;
d_1 = perpendicular distance from axis of rotation to C.G. of hole (m); and
m_1 = volume of hole x density of steel.

$$I_{sf} = \frac{1}{2} mr^{2} = \frac{1}{2} \pi r_{1}^{4} t\rho = \frac{1}{2} (\pi)(0.445 \text{ m})^{4}(0.10 \text{ m})(7860 \text{ kg/m}^{3})$$

$$= 48.42 \text{ kg-m}^{2}$$

$$8I^{*}_{h} = 8 \left(\frac{1}{2} mr_{1}^{2}\right) = 4\pi r_{2}^{4} t\rho = 4\pi \ (.025 \text{ m})^{4}(0.10 \text{ m})(7860 \text{ kg/m}^{3}$$

$$= 0.03 \text{ kg-m}^{2}$$

$$8m_{1}d_{1}^{2} = 8 \ \pi r_{2}^{2} t\rho d_{1}^{2} = 8\pi \ (0.025 \text{ m})(0.10 \text{ m})(7860 \text{ kg/m}^{3})(.203 \text{ m})^{2}$$

$$= 0.51 \text{ kg-m}^{2}$$

$$I_{f} = 48.42 \text{ kg-m}^{2} - 0.044 \text{ kg-m}^{2} - 0.03 \text{ kg-m}^{2} - 0.51 \text{ kg-m}^{2}$$

$$= 47.88 \text{ kg-m}^{2}$$

9) Key Guard

$$I_{kg} = I_{skg} - I_{sh}$$

Where: kg = key guard;
skg = solid key guard; and
sh = shaft hole.

$$I_{skg} = \frac{1}{2}\,mr^2 = \frac{1}{2}\,\pi r_1{}^4 t\rho = \frac{1}{2}\,\pi\ (0.14\ \text{m})^4(0.10\ \text{m})(7860\ \text{kg/m}^3)$$

$$= 0.47\ \text{kg-m}^2$$

$$I_{sh} = \frac{1}{2}\,mr_2{}^4 t\rho = \frac{1}{2}\,\pi\ (0.07\ \text{m})^4(0.10\ \text{m})(7860\ \text{kg/m}^2)$$

$$= 0.03\ \text{kg-m}^2$$

$$I_{kg} = 0.47\ \text{kg-m}^2 - 0.03\ \text{kg-m}^2 = I_{kg} = 0.44\ \text{kg-m}^2$$

10) Disc Spacers

$$I_{ds} = I^{*}_{sds} - I_{sh}$$

Where: ds = disc spacer;
sds = solid disc spacer; and
dh = shaft hole.

$$I_{sds} = \frac{1}{2}\,mr^2 = \frac{1}{2}\,\pi r^2 t\rho = \frac{1}{2}\,\pi\ (0.135\ \text{m})^4(0.0445\ \text{m})(7860\ \text{kg/m}^3)$$

$$= 0.182\ \text{kg-m}^2$$

$$I_{sh} = \frac{1}{2}\,\pi r^4 t\rho = \frac{1}{2}\,\pi\ (0.11\ \text{m})^4(0.0445\ \text{m})(7860\ \text{kg/m}^3)$$

$$= 0.080\ \text{kg-m}^2$$

$$I_{ds} = 0.182\ \text{kg-m}^2 - 0.080\ \text{kg-m}^2 = 0.102\ \text{kg-m}^2 \text{ per disc spacer}$$

$$\times\ 22 \text{ spacers} = I_{ds} = 2.24\ \text{kg-m}^2$$

Total Mass Moment of Inertia of Rotor (I_T)

$$I_T = \sum_{i=1}^{10} I_i = 147.33\ \text{kg-m}^2$$

A summary of the contribution of each of the rotor elements to the mass moment of inertia shows the total to be 147.33 kg/m^2, with the hammers and flywheel contributing approximately thirty percent each to the total. A complete breakdown by rotor element is given in Table E.2.

TABLE E.2. CONTRIBUTION OF ROTOR ELEMENTS TO MASS MOMENT OF INERTIA

Item No.	Quantity	Description	I (kg-m^2)	Percent of Total I
1	44	Hammers	43.29	29.4
2	8	Pins	24.05	16.3
3	10	Inner Rotor Discs	17.90	12.1
4	2	Outer Rotor Discs	8.48	5.8
5	1	Shaft	2.31	1.6
6	2	Shafts	0.54	0.4
7	2	Shafts	0.20	0.1
8	1	Flywheel	47.88	32.5
9	1	Key Guard	0.44	0.3
10	22	Disc Spacers	2.24	1.5
		TOTAL	147.33	100.0

APPENDIX F

DERIVATION OF GOVERNING EXPRESSIONS FOR MOTOR POWER IN TERMS OF MOTOR CHARACTERISTICS

Nomenclature

I_1 = Stator current (amperes/phase)
I_2 = Rotor current (amperes/phase)
I_m = Magnetizing current (amperes/phase)
I_e = Exciting current (amperes/phase)
I_{fe} = Current induced in iron core (amperes/phase)
V_o = Voltage applied to one phase of stator (volts)
V = Line to line voltage
E_z = Voltage across rotor (volts)
r_1 = Stator resistance (ohms/phase)
r_{fe} = Iron core resistance (ohms/phase)
r_2 = Rotor resistance (ohms/phase)
x_1 = Stator leakage reactance (ohms/phase)
x_m = Magnetizing reactance (ohms/phase)
P_{in} = Real power into motor (watts)
P_r = Real power into rotor (watts)
P_{nl} = Real power into motor at no-load (watts)
P_{em} = Mechanical power developed by rotor (watts)
P_m = Mechanical power delivered to load (watts)
S = Slip
$(Pf)_{nl}$ = Power factor at no load
m = Number of phases

The equivalent circuit of one phase of an induction motor is shown in Figure F.1. In the circuit, the load is represented by $[(I-S)/S]r_2$.

So the power developed by the rotor is,

$$P_{em} = m \frac{I-S}{S} I_2^2 r_2 \qquad (F.1)$$

For the case of no-load operation, the slip equals zero. Therefore the equivalent circuit is reduced to that shown in Figure F.2 and the real power consumed during no-load operation becomes,

$$P_{nl} = m I_m^2 (r_1 + r_{fe}) \qquad (F.2)$$

Because r_{fe} is much larger than r_1, the no-load power draw may be approximated as a loss that is independent of slip.

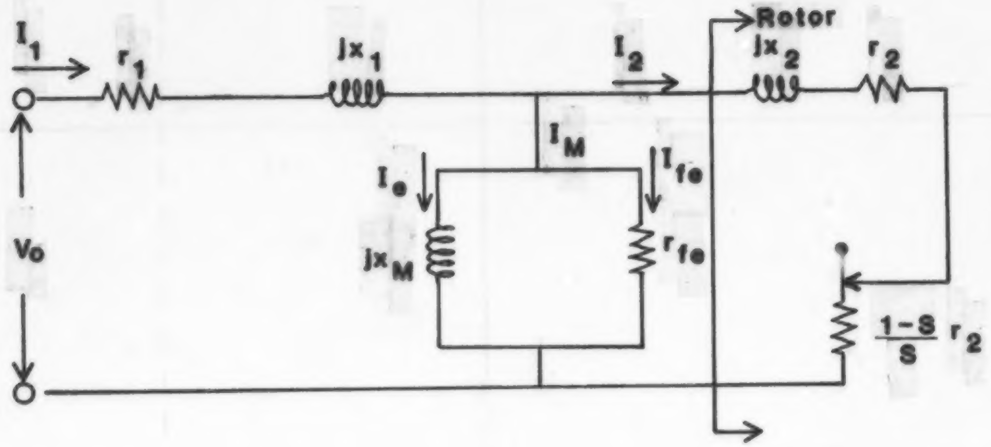

Figure F.1. Equivalent circuit of one phase of a polyphase induction motor.

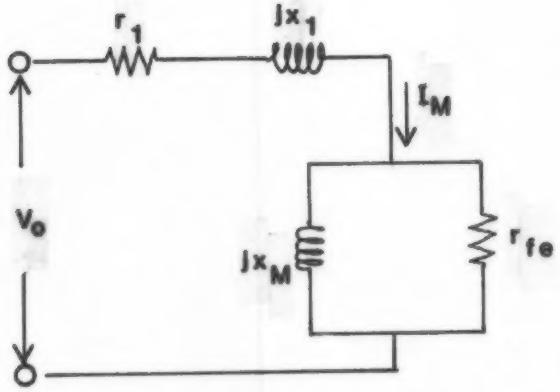

Figure F.2. Equivalent circuit of one phase of a polyphase induction motor with no load.

EPA Form 2350-4 (4-80)
TYPING GUIDE SHEET

To establish the real no-load power draw, it can be measured directly using a wattmeter, or alternatively it can be calculated from measured values of I_1, V, and the power factor:

$$P_{nl} = m\ I_m\ V_o (Pf)_{nl} \qquad (F.3)$$

Denoting the voltage across one phase of a three phase electrical service as,

$$V_o = \frac{V}{\sqrt{3}} \qquad (F.4)$$

Equation F.3 may be rewritten in the form,

$$P_{nl} = \frac{m}{\sqrt{3}}\ m\ V\ I_m\ (Pf)_{nl} \qquad (F.5)$$

As an illustration, the three phase, 187 kW motor driving the shredder at the University of California solid waste processing facility operates on a 3-phase line-to-line voltage of 480 volts. The manufacturer has specified that at no-load, the current draw of the motor (I_m) is 73 amps per phase and the power factor at no-load is 4 percent. Hence, for the 187 kW motor it follows from Equation F.5 that,

$$P_{nl} = \frac{3}{\sqrt{3}}\ (73)(480)(0.04)$$

$$P_{nl} = 2400 \text{ watts}$$

Consequently, the power lost in the stator is 2.4 kW.

The real power into the rotor is equal to the power into the stator minus the losses in the stator,

$$P_r = P_{in} - P_{nl} \qquad (F.6)$$

where

$$P_r = m\ I_2{}^2\ \frac{r_2}{S} \qquad (F.7)$$

Combining Equation F.7 with Equation F.1 yields the efficiency of the rotor,

$$\frac{P_{em}}{P_r} = \eta_r = 1-S \qquad (F.8)$$

From Equations F.5, F.6, and F.8, it follows that the mechanical power developed by the rotor is

$$P_{em} = (P_{in} - \frac{1}{\sqrt{3}}\ m\ I_m V\ (Pf)_{nl})\ (1-S) \qquad (F.9)$$

In the case of the 187 kW motor (where P_{nl} = 2400 W), the equation for P_{em} becomes,

$$P_{em} = (P_{in} - 2400)\ (1-S) \tag{F.10}$$

In a size reduction system, the mechanical power which is delivered to the load (P_m) is less than the power developed by the rotor (P_{em}) because there are friction and windage losses occurring (P_{fw}). Consequently,

$$P_m = P_{em} - P_{fw} \tag{F.11}$$

The friction and windage losses are determined by operating the shredder system under no-load conditions. Therefore by measuring P_{in}, equating P_m to zero, and calculating P_{em} from Equation F.9, a value of P_{fw} may be calculated which is independent of the rotational speed. The agreement of course, becomes progressively worse as the rpm declines due to the contribution of aerodynamic drag to the windage losses.